

Catalytic Solvent Regeneration for Energy-Efficient CO₂ Capture

Masood S. Alivand, Omid Mazaheri, Yue Wu, Geoffrey W. Stevens, Colin A. Scholes, and Kathryn A. Mumford*



Cite This: <https://dx.doi.org/10.1021/acssuschemeng.0c07066>



Read Online

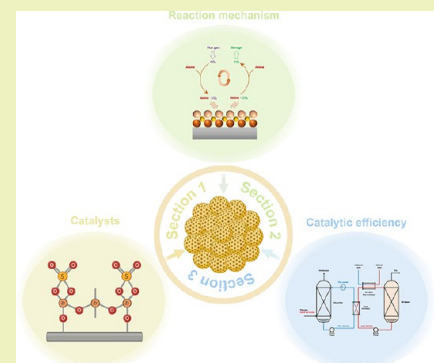
ACCESS |

Metrics & More

Article Recommendations

ABSTRACT: CO₂ emissions from industrial processes and their adverse implications on the climate is of major concern. Carbon capture and storage (CCS), especially using chemical-absorption-based processes, has been regarded as one of the most realistic pathways to curtail global warming and climate change. However, the energy-intensive nature of CO₂ capture and therefore its expensive cost of operation has been regarded as the main barrier halting its widespread implementation among the portfolio of low-carbon energy technologies currently available. Recently, catalytic solvent regeneration has drawn significant attention as a new class of technology for energy-efficient CO₂ capture with great potential for large-scale implementation. In this review, recent progress and developments associated with catalyst-aided solvent regeneration for low-temperature energy-efficient CO₂ desorption is presented. A detailed discussion of heterogeneous acid–base catalyst is undertaken and the specific privileges, drawbacks, and challenges of each catalyst identified and commented upon. In keeping with the latest investigations, the promotion mechanism of catalytic CO₂ desorption and the role of Lewis acids, Brønsted acids, and basic active sites are scrutinized. The performance of solid acid–base catalysts in different primary and blended amine solutions associated with their physicochemical properties is also reviewed. Finally, the status of catalytic solvent regeneration for post-combustion CO₂ capture is comprehensively analyzed and a clear pathway for future research investigations is provided.

KEYWORDS: Energy reduction, CO₂ capture, Heterogeneous catalysts, Acidic and basic sites, Catalytic solvent regeneration, Enhanced CO₂ desorption



INTRODUCTION

Throughout the last century, global warming (and its adverse impacts) has been one of the major environmental challenges threatening lives, the environment, and human health and well-being.^{1,2} In the previous century, fossil fuels (i.e., coal, crude oil, and natural gas) came to dominance as the main source of energy for human society, in both developed and developing countries.^{3–5} Due to the release of carbon dioxide (CO₂) from fossil fuels when combusted, anthropogenic CO₂ emission has consistently increased year on year for decades, resulting in the atmospheric CO₂ concentration rising from 280 ppm in 1750 to 412 ppm in 2020.^{6,7} The global warming potential of this CO₂ buildup in the atmosphere has correspondingly resulted in a 0.8 °C increase in the average atmospheric temperature.⁸ In response to this growing environmental emergency, around 200 countries signed the Paris Agreement in 2015 and agreed to keep the global temperature rise to less than 2 °C by controlled CO₂ emission.^{9,10}

Considering the low price of crude oil compared to the price of other green and renewable energy sources (e.g., solar energy and wind power), especially its noticeable drop in 2020 due to the Russia–Saudi Arabia oil price war, fossil fuels are expected to remain the predominant resources for energy production into the foreseeable future.^{11,12} A significant source of emitted CO₂

also comes from the industrial sector (e.g., cement kilns, iron and steel manufacturing, ammonia, and fertilizer production). This sector's emissions are being targeted for mitigation strategies, in part because of their growing demand as well as lack of renewable alternatives. For example, there are no methods available to produce cement, ammonia, and fertilizers on the scale needed that do not also emit significant amounts of CO₂. Hence, carbon capture strategies are required to prevent emissions from these industrial processes being released. Hence, post-combustion CO₂ capture seems the only viable strategy to control CO₂ emission from these sectors and achieve the committed goals of the Paris Agreement. Among the different CO₂ separation and purification technologies available (e.g., absorption,^{13,14} adsorption,^{15,16} membrane separation,^{17,18} and cryogenic distillation^{19,20}), chemical absorption using aqueous solvents has been the most reliable and therefore promising

Received: September 23, 2020

Revised: November 7, 2020

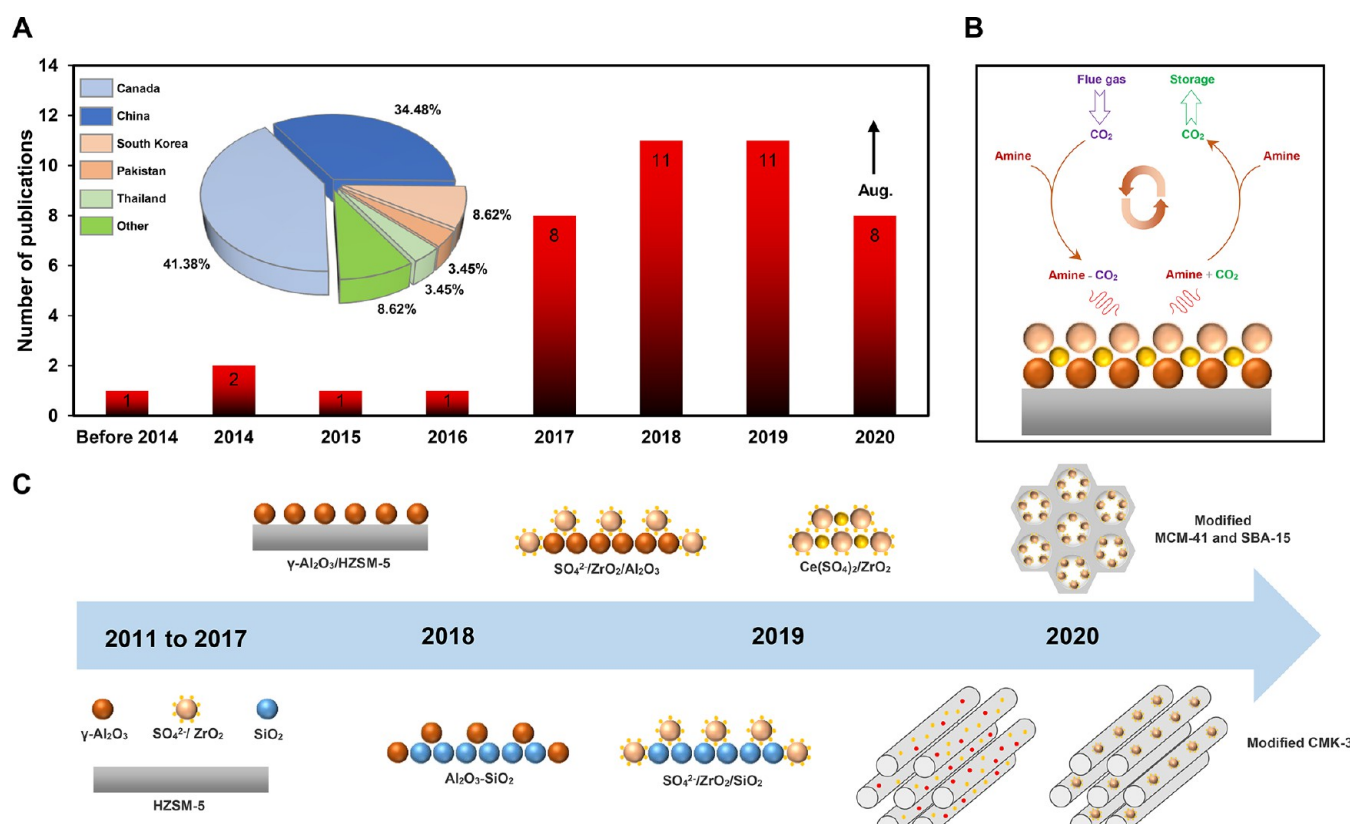


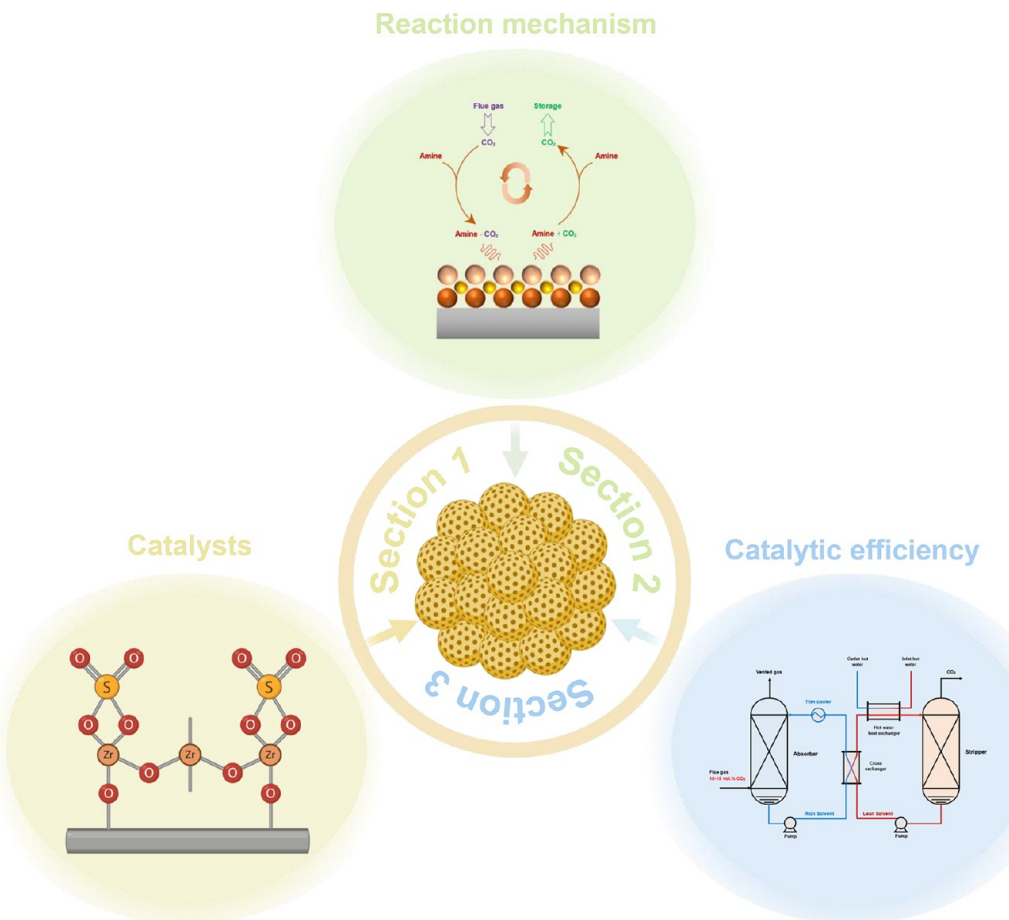
Figure 1. (A) Number of catalytic solvent regeneration publications from 2011 to August 2020 (using Web of Science) and the share of different countries. (B) Schematic diagram of the catalytic solvent regeneration. (C) Timeline of the heterogeneous catalyst employment in low-temperature solvent regeneration.

technology for large-scale post-combustion CO₂ capture (PCC). This is because the flexibility of chemical absorption processes in dealing with various CO₂ concentrations and feed rates make them favorable options for large-scale CO₂ capture from a range of point-sources. There are two key limitations to this technology, the energy demand of the process as well as the reaction kinetics to capture CO₂. The energy demand of solvent absorption is widely discussed in the literature with various strategies presented to generate significant reductions. The kinetics of CO₂ absorption–desorption are less explored, though they strongly control the efficiency of the process and are intrinsically linked with the energy requirement.^{21,22}

The slow kinetics of CO₂ absorption are particularly apparent in solvents based on potassium carbonate,²³ tertiary amines,²⁴ and some amino acids²⁵ which has counteracted their advantages and prevented their widespread employment for industrial CO₂ capture. To overcome this challenge, a series of rate promoters have been successfully developed, including weak acids (e.g., boric acid²⁶), amines (e.g., monoethanolamine (MEA), piperazine, and polyamines^{27–29}), amino acids (e.g., proline and glycine³⁰), metal compounds (e.g., Zn(II)³¹), enzymes (e.g., carbonic anhydrase³²), metal oxides (e.g., CuO, Fe₂O₃, SiO₂, and Al₂O₃^{33,34}), and carbon-based (e.g., graphene oxide³⁵) nanoparticles. Conversely, limited attention has been devoted to understanding the CO₂ desorption process rate, even though this is strongly linked with the solvent's required regeneration temperature and hence the economics of the overall process. Hence, there is much scope in chemical absorption processes to optimize the desorption process kinetics to improve the overall viability of the technology. At constant

temperature, the kinetics of CO₂ desorption is much slower than that of CO₂ absorption, and hence, the solvent is typically regenerated at high temperatures (above 100 °C) to partially compensate for the lower CO₂ desorption rate.³⁶ This requires intensive energy consumption and results in a high carbon capture cost. As the U.S. Department of Energy has reported, the installation of a PCC plant using typical aqueous MEA solutions—the most widespread chemical solvent for CO₂ capture industrially—can increase the cost of electricity generation up to 81–85% in a coal-fired power plant station.³⁷ Evidently, the main cause of this increase can be attributed to the energy-intensive nature of CO₂ desorption processes imposing huge challenges on the development of economically acceptable CO₂ capture packages at a large scale.

During the past decades, various research efforts have focused on solving the issues surrounding the high energy consumption of solvent regeneration processes. One successful strategy to reduce the intensive regeneration energy has been phase-change solvents.^{38–42} These solvents are non-aqueous or aqueous-based solutions of amines, amino acids, or ionic liquids that can form two immiscible CO₂-rich and CO₂-lean phases after CO₂ absorption. As there is a significant difference in the concentration of absorbed CO₂ in the two phases (i.e., CO₂-rich phase with a high concentration of CO₂ and CO₂-lean with a comparatively low concentration of CO₂), the CO₂-lean phase is typically recycled to the absorption column without any thermal degasification and the remaining CO₂-rich phase is sent for solvent regeneration.^{43,44} The regeneration of the CO₂-rich phase ensures the process consumes significantly less energy compared to typical CO₂ absorption–desorption systems, due

Scheme 1. Outline of This Catalytic Solvent Regeneration Review Paper

to the lower flow rate, higher CO_2 loading, and partial pressure of the CO_2 -rich stream. However, according to the recent literature review published by Lu et al., phase change solvents that can be split into liquid–liquid and liquid–solid phases suffer from a number of disadvantages.⁴⁵ Systems that recycle the CO_2 -lean phase to the absorption column have a higher initial CO_2 loading and the cyclic loading capacity and rate of CO_2 absorption is reduced. Recently, the next generation of aqueous-based phase-change solvent with liquid–liquid–solid phase separation has been developed. In these solvents, the upper liquid phase is CO_2 -free which enables an extremely high CO_2 loading in the lower liquid phase leaving the absorption column.⁴⁶ Nevertheless, the potential of this next generation phase-change solvent requires more research to prove its viability for large-scale CO_2 capture.

A recently emerged viable technique for energy-efficient solvent regeneration is using novel solid acid–base catalysts during CO_2 stripping (Figure 1A). In catalyst-aided solvent regeneration processes, catalysts can enhance the desorption efficiency, promote the CO_2 desorption rate, and decrease the CO_2 stripping time and total energy consumption during solvent regeneration (Figure 1B). Apart from these benefits, catalyst addition also enables the solvent to achieve a regeneration temperature below 100 °C. Reducing the regeneration temperature from 120 to 140 °C to the 70–95 °C range can be regarded as the main benefit of catalytic solvent regeneration and has highlighted its feasibility as an energy-efficient method for large-scale CO_2 capture.^{47,48} In general, metal oxides, zeolites, and mesoporous silica materials have been the most employed

heterogeneous catalysts for energy-efficient solvent regeneration. A schematic of the chronology of the heterogeneous catalysts is given in Figure 1C.

Although a handful of review papers have been published regarding the use of phase-change solvents as an energy-efficient method for cyclic CO_2 absorption–desorption processes,^{45,49,50} from the beginning of 2011, when the first use of heterogeneous catalysis for energy-efficient solvent regeneration was introduced, there has not yet been an overview of catalytic solvent regeneration published. This paper comprehensively reviews the current status of various catalytic approaches to achieve energy-efficient CO_2 capture in detail and focuses on recent advances in solid acid catalysts for catalytic solvent regeneration and CO_2 desorption enhancement. For a better comprehension, this review is divided into three sections (Scheme 1). In the first section, different heterogeneous nanocatalysts used for catalytic solvent regeneration are presented and discussed. In the second section, the catalytic CO_2 desorption mechanism of different heterogeneous catalysts is analyzed and the effect of different influential parameters on the catalytic CO_2 desorption enhancement and energy reduction is reviewed. In the third section, the role of different physical, chemical, and physicochemical properties of solid acid–base catalyst in single and blended amine solutions is systematically summarized and discussed. Eventually, conclusion, current status, and future prospects toward the ideal energy-efficient CO_2 absorption–desorption process are presented, providing guidance for the research field.

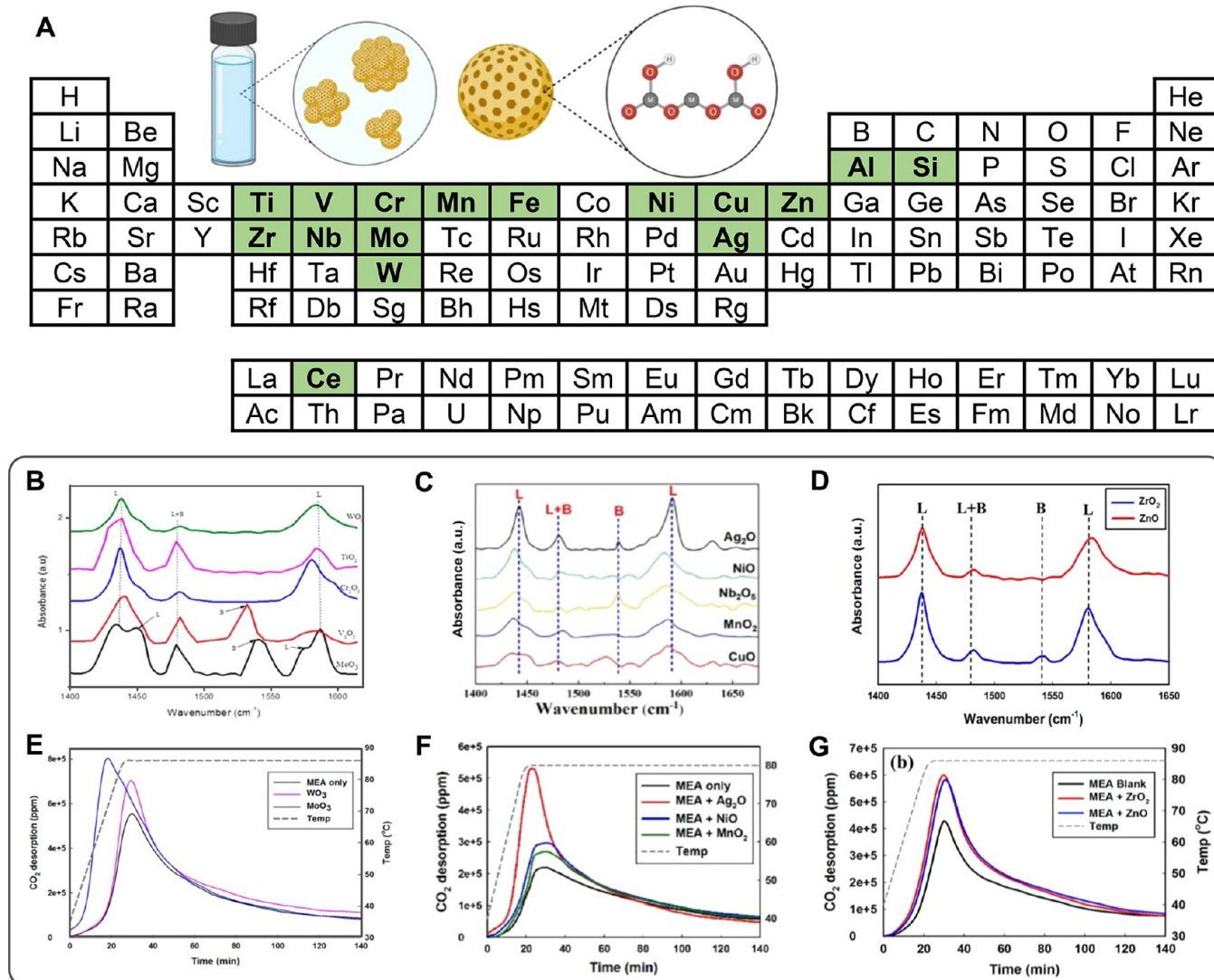


Figure 2. (A) Periodic table: highlighted metals in green have been used for the synthesis of different metal oxide nanocatalysts. Pyridine FTIR spectra of (B) MoO_3 , V_2O_5 , Cr_2O_3 , TiO_2 , and WO_3 ,⁵⁵ (C) Ag_2O , NiO , Nb_2O_5 , MnO_2 , and CuO ,⁴⁸ and (D) ZrO_2 and ZnO ⁵⁶ nanocatalysts. L and B denote Lewis and Brønsted acids, respectively. CO_2 desorption profile of blank MEA solution and (E) WO_3 and MoO_3 ,⁵⁵ (F) Ag_2O , NiO , and MnO_2 ,⁴⁸ and (G) ZrO_2 and ZnO ⁵⁶ nanocatalysts. Copyright ACS 2017–2018 and Elsevier 2018.

HETEROGENEOUS NANOCATALYSTS APPLIED FOR ENHANCED SOLVENT REGENERATION

Metal Oxides. Metal oxides or metal oxide nanoparticles have been widely used as a viable solid acid catalyst on a commercial scale. Metal oxide nanoparticles benefit from both physical and chemical promotion mechanisms. The physical enhancement mechanism is focused around Brownian motion of nanoparticles in the solution that break down gas bubbles, increase mass transfer surface area, and decrease mass transfer resistance at gas–liquid interfaces. This results in a large increase in the CO_2 desorption rate. Metal oxide nanoparticles also exhibit advantages associated with catalytic enhancements. The catalytic behavior of metal oxides is attributed to their active acidic sites available through surface defects which are primarily categorized into two types, Lewis and Brønsted acidity. The Lewis acidic property is characterized by unsaturated metal atoms accepting one pair of electrons, while Brønsted acidic behavior is demonstrated by the dissociation of water molecules and the production of active hydroxyl groups on the surface of the metal oxide with a great proton donation capability.

In 2011, Idem et al. at the University of Regina for the first time succeeded in introducing $\gamma\text{-Al}_2\text{O}_3$ as a suitable solid acid catalyst for CO_2 stripping.⁵¹ They reported that adding $\gamma\text{-Al}_2\text{O}_3$ into the mixture can decrease the regeneration temperature of aqueous 5 M MEA solution from 120–140 to 90–95 °C and decrease the regeneration energy requirement by 27%. Since $\gamma\text{-Al}_2\text{O}_3$ was a commercially available solid acid catalyst, it became the benchmark for further investigations.^{52,53} In a similar trend, other research studies tried to employ different commercial metal oxide nanoparticles with different accessible Lewis acidity, Brønsted acidity, and surface defects to find the optimum metal oxide catalyst, with the lowest level of energy consumption, during catalyst-aided solvent regeneration in CO_2 capture systems (Figure 2A). Wang et al.⁵⁴ studied the role of TiO_2 and SiO_2 as two new metal oxide nanoparticles during CO_2 desorption, compared the results with the typical $\gamma\text{-Al}_2\text{O}_3$ catalyst, and found both TiO_2 and SiO_2 nanoparticles are more efficient than $\gamma\text{-Al}_2\text{O}_3$ ($\text{TiO}_2 > \text{SiO}_2 > \gamma\text{-Al}_2\text{O}_3$). They reported that TiO_2 was able to decrease the regeneration time by up to 42% in aqueous 5 M MEA solutions. However, the CO_2

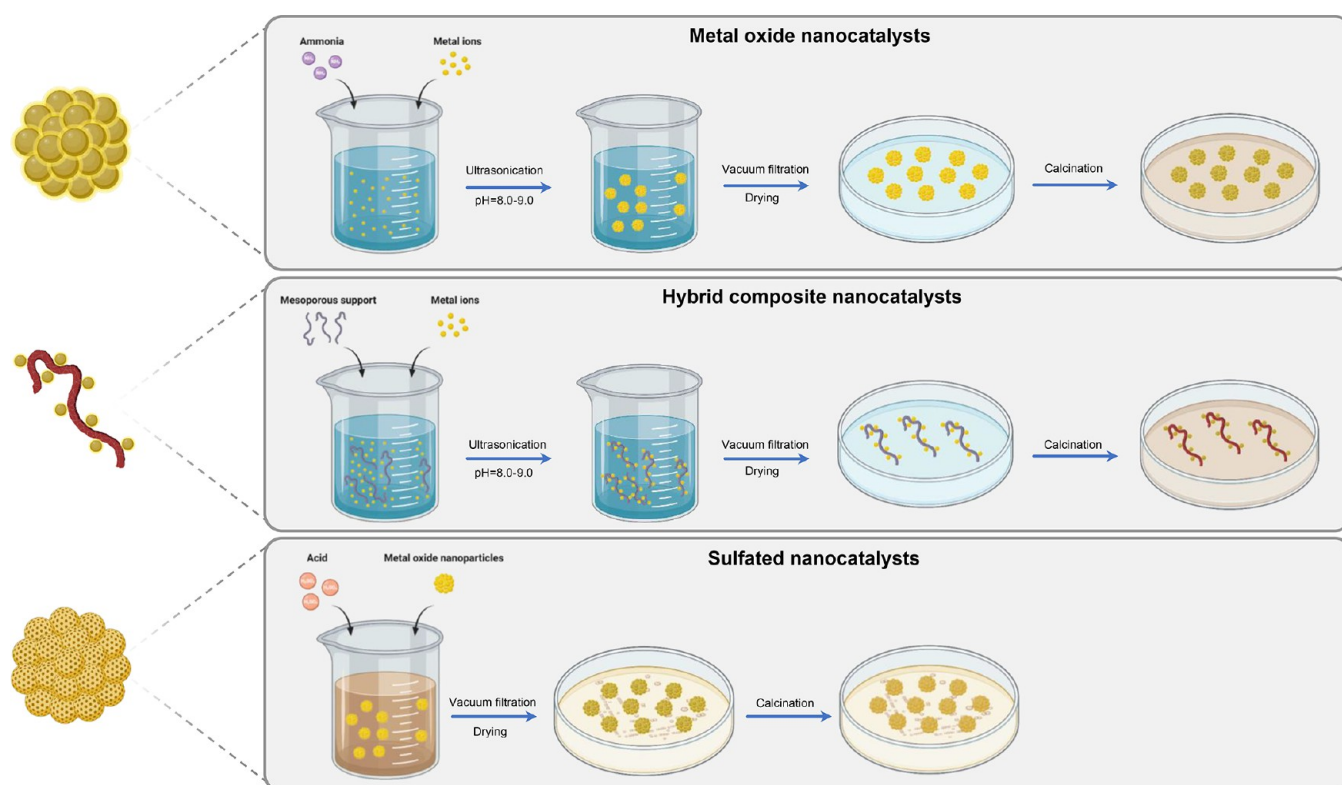


Figure 3. Schematic process for the preparation of metal oxide nanocatalysts, hybrid composite nanocatalysts, and sulfated nanocatalysts.

desorption rate enhancement was only ascribed to the physical promotion mechanism and they failed to take the catalytic role of metal oxides into account.

After the first introduction of metal oxides in catalytic solvent regeneration by Idem and his colleagues in 2011, Bhatti and his research group at the Korean Institute of Energy Research have extensively investigated metal oxide nanocatalysts for energy-efficient solvent regeneration since 2017. To scrutinize the role of active Lewis and Brønsted acidic sites on the CO₂ desorption rate of saturated MEA solutions, Bhatti and co-workers used two different groups of novel metal oxide nanoparticles: (i) TiO₂, Cr₂O₃, and WO₃ with predominantly Lewis acid sites and (ii) V₂O₅ and MoO₃ with a combination of both Lewis and Brønsted acid sites on the surface (Figure 2B).⁵⁵ Interestingly, they observed that the performance of Lewis acid catalysts was lower than those with active Brønsted acid sites (Figure 2E). TiO₂, Cr₂O₃, and WO₃ nanoparticles reduced the energy consumption between 25 and 30% at 86 °C, while using V₂O₅ and MoO₃ further reduced the amount of required energy and saved 44–48% at the same regeneration temperature. In a later study, they attempted to broaden their investigation and introduced five new metal oxide nanoparticles, namely, Ag₂O, Nb₂O₅, NiO, CuO, and MnO₂.⁴⁸ Both Ag₂O and Nb₂O₅ metal oxides improved the rate of CO₂ desorption by 2.53 and 2.19 times, respectively, while NiO, CuO, and MnO₂ displayed a poorer performance between 1.26 and 1.57 times. Similarly, they used the types of active acidic sites on the surface of the metal oxides as a proven tool to interpret their experimental findings and justify the superiority of Ag₂O and Nb₂O₅ (Figure 2F). They pointed out that the high performance of Ag₂O and Nb₂O₅ can be attributed to the presence of Brønsted acid sites, as well as abundant Lewis acid sites, on the surface while all NiO, CuO, and MnO₂ are predominantly Lewis acid catalysts with a very

low amount of Brønsted acidity (Figure 2C). In a recent study in 2018, they focused on ZrO₂ and ZnO metal oxides and found nearly the same CO₂ desorption rate enhancement, up to 54% for both, which was ascribed to their similar acidic characteristics (Figure 2D and G).⁵⁶ Based on the promising performance of the Ag₂O metal oxide, they continued their detailed examinations on Ag₂O metal oxide and noticed Ag₂CO₃ had a more pronounced activity.⁵⁷ The CO₂ desorption experiments of saturated MEA solution at 80 °C revealed that the Ag₂CO₃ catalyst improved the rate of CO₂ desorption by up to approximately 1000% and greatly minimized energy consumption. However, they failed to quantitatively measure the relative heat duty of the catalytic Ag₂CO₃ solution to compare its energy efficiency with other metal oxides.

Although metal oxide nanocatalysts are typically commercially available, they are generally synthesized in the literature using a simple precipitation method (Figure 3). First, an amount of metal salt is dissolved in water and the pH of the solution set within a range of 9–10 using an ammonia solution to induce precipitation. Afterward, the solid particles are separated, dried in the oven, and calcinated at a high temperature. Different metal oxide nanocatalysts are typically synthesized using different metal salts in the synthesis procedure.

In 2018, Lai et al.⁵⁸ at University of Wyoming reported using TiO(OH)₂ nanocatalyst as a fundamentally different metal oxide catalyst. Their inspiring work confirmed that catalytic TiO(OH)₂ can drastically improve the CO₂ desorption rate of a CO₂-saturated 5 M MEA solution by up to 4500% at a low temperature of 88 °C which was much higher than the previous catalysts investigated (Figure 4A–C). They used Raman spectroscopy to qualitatively measure the concentration of carbamate, carbonate, and bicarbonate in the solution at different times during the absorption and desorption processes

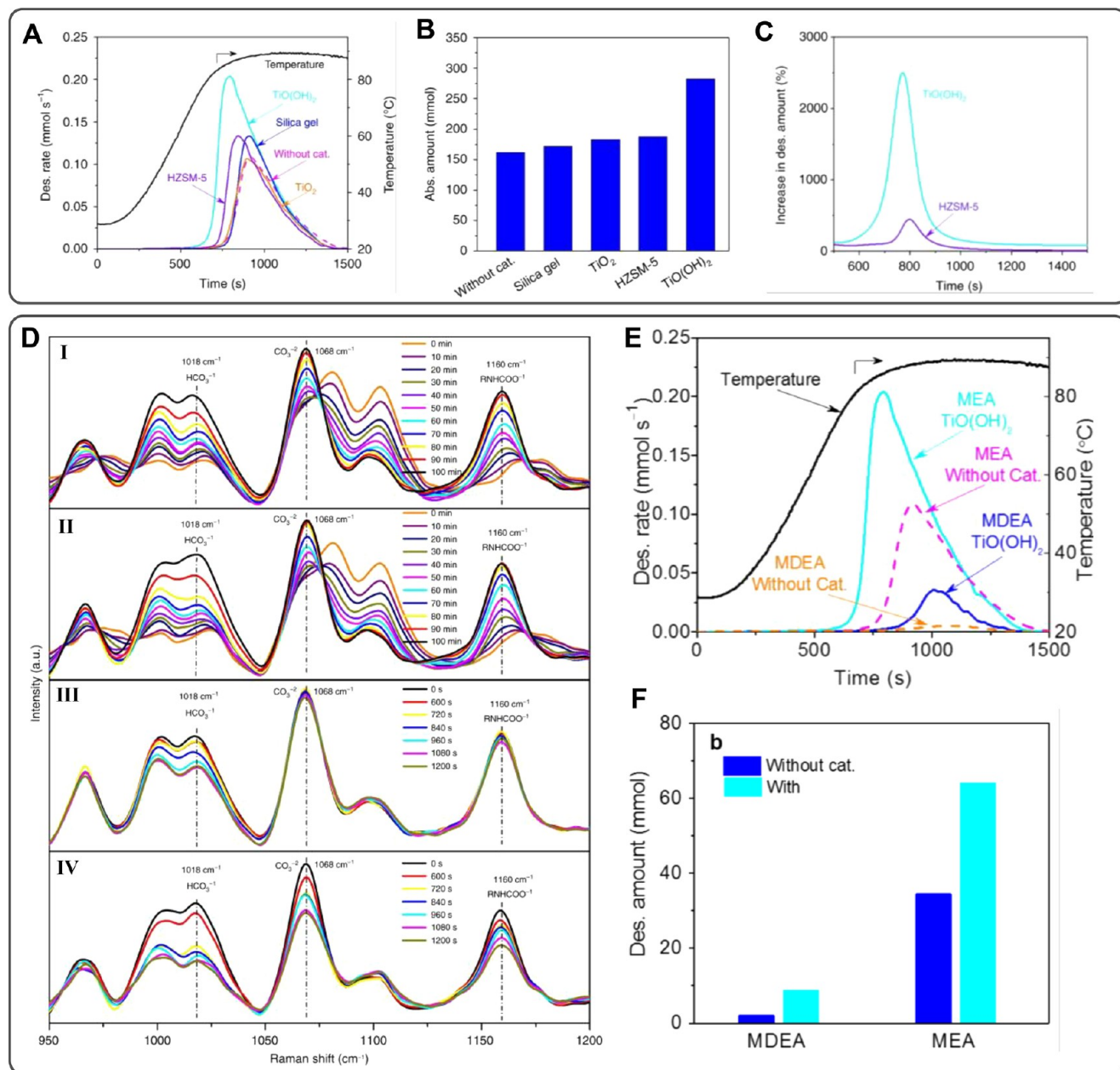


Figure 4. (A) CO₂ desorption rate from spent MEA solution with and without uses of catalysts. (B) The amount of absorbed CO₂ in a constant operation time (>90% CO₂ capture). (C) The percentage of increase in the CO₂ desorption amount with HZSM-5 and TiO(OH)₂. (D) Raman spectra of MEA solution at different time intervals during (I) CO₂ absorption without TiO(OH)₂, (II) CO₂ absorption with TiO(OH)₂, (III) CO₂ desorption without TiO(OH)₂, and (IV) CO₂ desorption with TiO(OH)₂ catalyst. The effect of TiO(OH)₂ catalyst on (E) the CO₂ desorption rate and (F) the amount of desorbed CO₂ from the MEA and MDEA solutions.⁵⁸ Copyright Nature 2018.

to determine the mechanism of catalytic solvent regeneration (Figure 4D). In addition to the aqueous MEA solution, they also reported promising results for the catalytic effect of TiO(OH)₂ in MDEA solutions (Figure 4E,F). This development not only could be a determining step in the establishment of highly energy-efficient CO₂ capture systems but also could pave the way for employing solar hot water as the main energy source for regeneration.

Zeolites. Synthetic Zeolites. Zeolites are aluminosilicates with a three-dimensional crystalline structure composed primarily of silicon, aluminum, and oxygen atoms.^{59,60} The Al—O—Si linkages within the zeolite structure provide accessible pores, cavities, and channels with a regular size and arrangement.⁶¹ The combination of these properties has made zeolites a

unique material for catalytic applications. However, the disadvantages of natural zeolites (e.g., mordenite and clinoptilolite), including typically high impurity contents, low surface areas, and pore volumes, have resulted in researchers extensively investigating the synthesis and catalytic applications of synthetic zeolites. Zeolite Socony Mobil-5 (ZSM-5) is one of the most common synthetic zeolites (Figure 5A). It is characterized by a high crystallinity and surface area, low impurity content, and tunable Si/Al ratio in the structure.^{62,63} The H-type of ZSM-5 (HZSM-5) has been one of the most efficient commercial solid acid catalysts from its first introduction in industry. The hydroxyl groups in the Si—(OH)—Al unit of the HZSM-5 catalyst are able to act as Brønsted acid sites while also improving the textural properties

Pristine and metal-modified catalysts

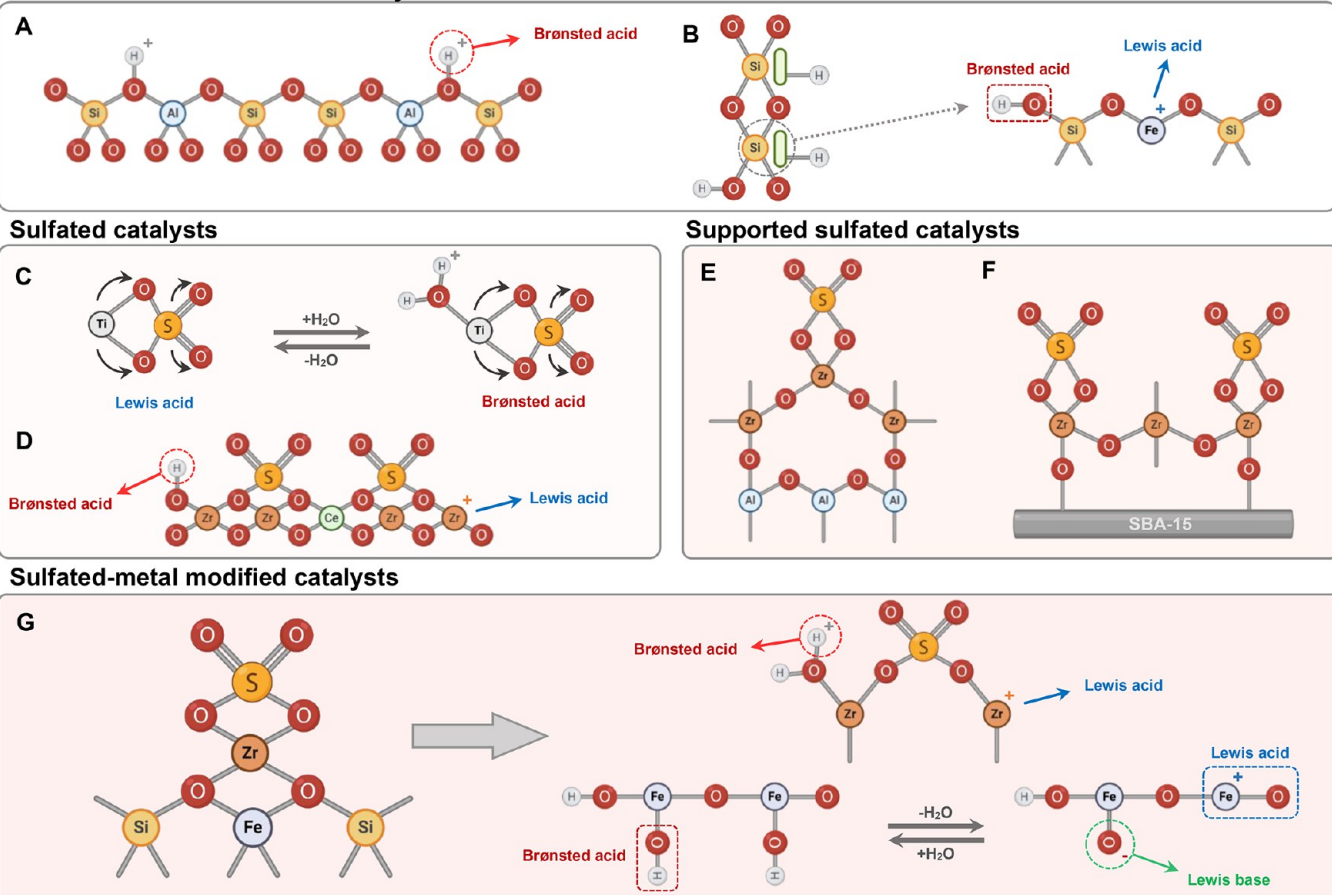


Figure 5. Schematic of the pristine catalysts, including (A) HZSM-5, (B) sulfated catalysts, including (C) $\text{SO}_4^{2-}/\text{TiO}_2$ and (D) $\text{Ce}(\text{SO}_4)_2/\text{ZrO}_2$, supported sulfated catalysts, including (E) $\text{SO}_4^{2-}/\text{ZrO}_2/\text{Al}_2\text{O}_3$ and (F) $\text{SO}_4^{2-}/\text{ZrO}_2/\text{SBA}-15$, and sulfated-doped catalysts, including (G) Fe promoted $\text{SO}_4^{2-}/\text{ZrO}_2/\text{MCM}-41$.

and molecule selectivity compared to the ZSM-5.^{64,65} Therefore, the HZSM-5 zeolite has widely been considered as a predominantly Brønsted acid catalyst for many different research areas.⁶⁶

Idem et al. first tested HZSM-5 as a commercial Brønsted acid catalyst for energy-efficient CO_2 stripping in 2011.^{51,52} The results clearly demonstrated that HZSM-5 was superior to that of the $\gamma\text{-Al}_2\text{O}_3$ metal oxide catalyst. In a simple comparison, the HZSM-5 decreased the relative heat duty to 62.7%, while the $\gamma\text{-Al}_2\text{O}_3$ metal oxide catalyst only reached 72.5% relative heat duty for the regeneration of CO_2 saturated MEA solution at 90 °C. This difference in the catalytic performance of $\gamma\text{-Al}_2\text{O}_3$ and HZSM-5 is attributed to their accessible acid sites. $\gamma\text{-Al}_2\text{O}_3$ is predominantly a Lewis acid catalyst with a very low surface area restricting access of the CO_2 laden species to the active acidic sites. Alternatively, HZSM-5 is predominantly a Brønsted acid catalyst with a large surface area enabling a notable increase in the total accessible acid sites and catalytic efficiency. It has also been revealed that the superiority of the HZSM-5 over the $\gamma\text{-Al}_2\text{O}_3$ catalyst is limited to high concentrations of CO_2 in the amine solution and $\gamma\text{-Al}_2\text{O}_3$ has a better performance at low concentrations of CO_2 .

However, as the majority of CO_2 is desorbed from aqueous solutions at high concentrations of CO_2 , Brønsted acid catalysts like HZSM-5 have been regarded as the premier choice of catalyst for promoted CO_2 desorption. Hence, improving both chemical and physical properties of HZSM-5 catalyst seems a

viable technique to enhance its performance for low-temperature CO_2 stripping. For example, as HZSM-5 has a micro-porous structure with a narrow pore size distribution, there is a high mass transfer resistance for the CO_2 -containing species to diffuse through the micropores and reach the active acid sites. Although the commercial grade of HZSM-5 has been broadly used from 2011, recently, Bhatti and his colleagues⁶⁷ synthesized a series of HZSM-5 nanocatalysts with differing physicochemical properties using an alkaline desilication and surfactant induced reassembly technique and tested the samples using an in-house-made apparatus (Figure 6A and B). The results clearly suggest that increasing the mesoporosity in hierarchical HZSM-5 plays a key role in their catalytic performance, since more acid sites (both Lewis and Brønsted acidity) become available for catalytic reaction (Figure 6F and G). They reported that for the best tuned HZSM-5 the relative heat duty reduced to 62.7%, while for a typical HZSM-5 catalyst they recorded 70.8% relative heat duty (Figure 6C–E).

In addition to the prevalent employment of hierarchical HZSM-5 catalyst as a benchmark, H-type zeolite Y (HY) has barely been used for catalyst-aided solvent regeneration. Idem et al.⁶⁸ reported the first use of HY catalyst for catalytic solvent regeneration in 2016 and compared their results with the HZSM-5 catalyst. One of the main characteristics of the HY catalyst is its large number of Brønsted acid sites and high surface area which can make it a perfect candidate for catalytic solvent regeneration. However, they experimentally confirmed that the

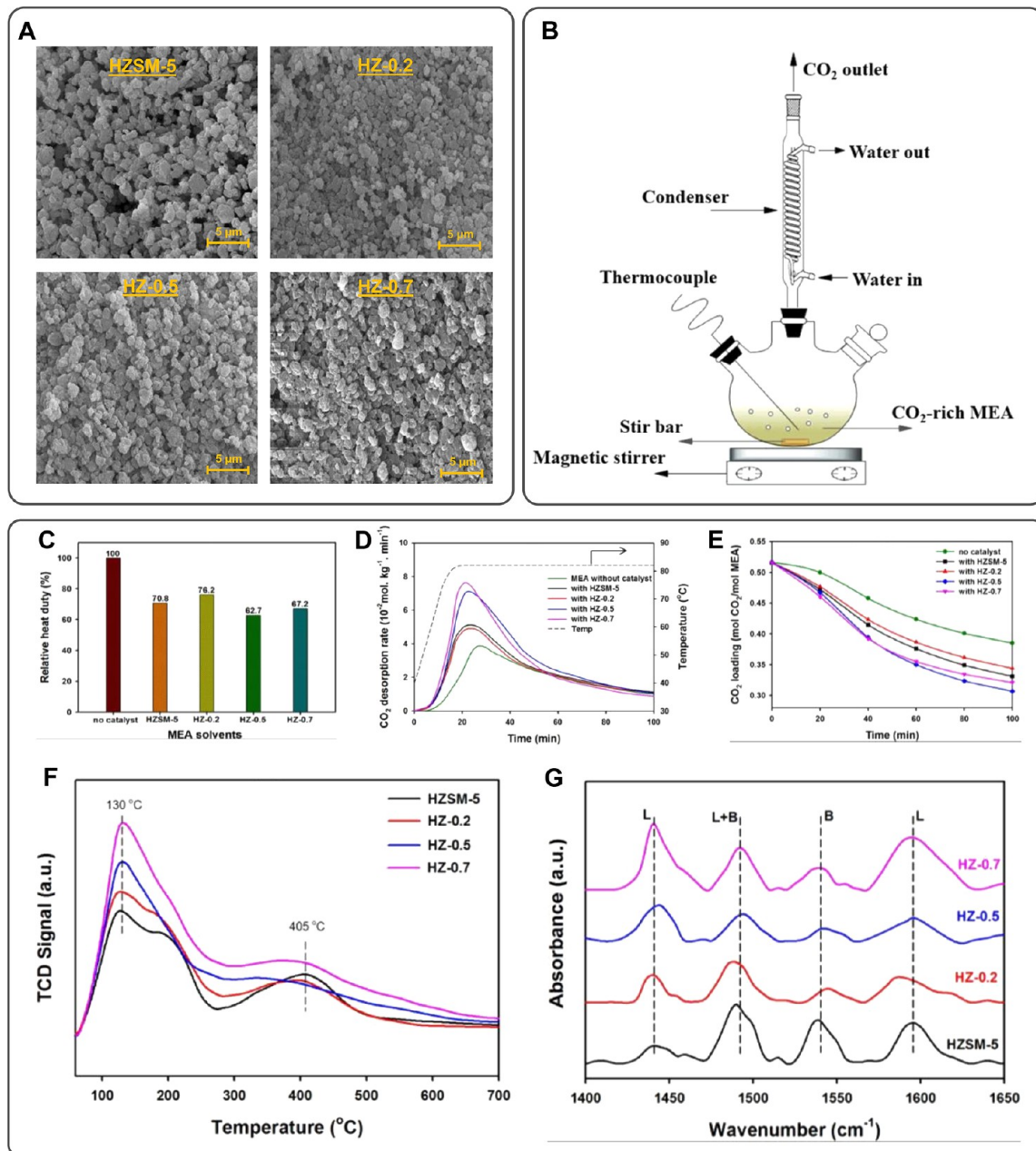


Figure 6. SEM images of (A) pristine HZSM-5, HZ-0.2, HZ-0.5, and HZ-0.7. (B) Schematic diagram of the CO_2 desorption rig. The effect of HZSM-5, HZ-0.2, HZ-0.5, and HZ-0.7 catalysts on the (C) relative heat duty, (D) CO_2 desorption rate, and (E) CO_2 loading of MEA solution during the regeneration experiment. (F) NH_3 -TPD and (G) pyridine FTIR characterization of HZSM-5, HZ-0.2, HZ-0.5, and HZ-0.7 catalysts.⁶⁷ Copyright Elsevier 2020. It should be noted that L and B represent Lewis and Bronsted acid sites, respectively.

catalytic performance of HY is significantly inferior to that of HZSM-5. A reasonable explanation is the exceptionally high microporosity of the HY structure provides a very low mass transfer coefficient for all CO_2 -containing species and, subsequently, a low catalytic efficiency. This is likely the main reason HY has not been a favorable solid acid catalyst for energy-efficient solvent regeneration during the past decade. Since the first report of HY solid acid catalyst by the Idem research group in 2016, it again used the HY catalyst in 2017 to demonstrate the superiority of the HZSM-5 zeolite for catalytic CO_2 desorption.⁶⁹ No further research has been reported for the use of HY catalyst to the best knowledge of the authors.

A recent study by Liang et al.⁷⁰ at Hunan University has reported the exceptionally high catalytic performance of H-beta

(HB) zeolite. Their experimental measurements demonstrated that the HB is able to elevate the CO_2 desorption factor up to 131.43% and decrease the relative heat duty to 70.5% for the regeneration of aqueous MEA solution at 98 °C, while they recorded 76.22 and 79.4% for the commercial HZSM-5 catalyst. Based on the previous works on the HZSM-5 and HY catalysts, they interpreted their findings and attributed the prosperity of HB to its large mesoporous surface area, high average pore diameter, abundant Brønsted acid sites, and total acid strength (both Brønsted and Lewis acid sites) which all are much higher than those of commercial HZSM-5.

The microporous molecular sieve SAPO-34 has been another promising synthesized zeolite used for catalytic solvent regeneration in CO_2 capture systems. In addition to its high

surface area, SAPO-34 has a unique pore size (0.43–0.5 nm) and acidic properties due to the presence of phosphorus in its structure ($\text{SiO}_2/\text{P}_2\text{O}_5/\text{Al}_2\text{O}_3$).⁷¹ Hence, SAPO-34 has been the most favored catalyst in methanol-to-olefin (MTO) reactions with an extremely high selectivity for ethylene and propylene.⁷² Relying on the reputation of SAPO-34, Liang et al.⁷³ tested the catalytic efficiency of commercial grade SAPO-34 during the thermal regeneration of CO_2 -saturated MEA solution at 96 °C and showed the optimum amount of SAPO-34 catalyst can reach a minimum relative heat duty of 75.7%. A similar observation was also reported by Hu et al.⁷⁴ in Xiangtan University of China and SAPO-34 was mentioned as a strong candidate for catalytic solvent regeneration, though a comparison by Liang et al.⁷⁵ revealed that SAPO-34 had a lower catalytic efficiency than HZSM-5 for CO_2 desorption. Although the material characterization showed a similar surface area, average pore width, and Brønsted to Lewis acid ratio in both commercial SAPO-34 and HZSM-5 samples, HZSM-5 has a greater number of total acid sites—both Lewis and Brønsted—than SAPO-34 which makes it a superior solid acid catalyst for enhanced CO_2 desorption.

Natural Zeolites. Natural zeolites are an economically viable type of hydrated aluminosilicate materials with different physicochemical properties and a wide range of applications. Among more than 40 different types of natural zeolite, clinoptilolite, mordenite, chabazite, and phillipsite are the most common. The low cost and availability of natural zeolites have made them one of the practical options for catalytic applications, such as cumene disproportionation,⁷⁶ 1-butene skeletal isomerization,⁷⁷ methanol to dimethyl ether conversion,⁷⁸ and water purification.⁷⁹ Nevertheless, only one literature source has reported the catalytic performance of natural zeolite for low-temperature CO_2 desorption to date. In 2019, Liang et al.⁷⁰ evaluated the H-mordenite zeolite as a superior solid acid catalyst with both Lewis and Brønsted acid sites. Although the catalytic performance of H-mordenite was less than that of HZSM-5, the results were comparable. As was reported, H-mordenite and HZSM-5 displayed 82.6 and 79.4% relative heat duty for the regeneration of aqueous MEA solution at 98 °C, respectively. Considering the low cost of H-mordenite as a natural zeolite, its abundant active sites, facile molecular diffusion due to the large pore structure, and good potential for further acid–base modifications, natural zeolites can be employed as a promising heterogeneous catalyst for further investigations. Based on the performance of H-mordenite, other natural zeolites—particularly clinoptilolite as the abundant natural zeolite—are a good candidate for future investigations.

Mesoporous Silica. Mesoporous silica is an inorganic material with regular mesoporous structure and an average pore diameter in the 2.0–6.5 nm range.⁸⁰ During the past several decades, a series of mesoporous silica nanomaterials with different properties have been developed in which MCM-41 and SBA-15 are the most common with wide-ranging applications in drug delivery and catalysis.⁸¹ The use of MCM-41 mesoporous silica for catalyst-aided solvent regeneration in CO_2 capture was initially reported by both Idem et al.⁸² and Liang et al.⁸³ in 2017. The recorded values by Idem et al.⁸² show that MCM-41 reduces energy consumption from 20.7 to 16.9 MJ/kg of CO_2 (i.e., 81.64% relative heat duty) for thermal regeneration of 5 M MEA at 98 °C. Additionally, they reported a lower value of 15.6 MJ/kg of CO_2 for HZSM-5 under the same conditions and concluded that, in spite of the advantages of MCM-41, it is not a good substitute for the HZSM-5 catalyst. A similar conclusion was made by Hu et al.⁷⁴ whom recorded a lower catalytic

efficiency for MCM-41 compared to SAPO-34. The poorer catalytic performance of MCM-41 can be attributed to its smaller number of available acidic sites, particularly Brønsted acid sites.

Based on the positive catalytic use of MCM-41 mesoporous silica in the solvent regeneration, Gao and his group⁸⁴ (Joint International Center for CO_2 Capture and Storage (iCCS) of China) recently reported the successful use of SBA-15 as the second most prevalent mesoporous silica for catalytic energy-efficient CO_2 absorption–desorption processes. Based on the published data for the catalytic regeneration of 5 M MEA solution at 97 °C, they claimed that SBA-15 dropped the relative heat duty to 81.05% (from 2710.19 to 2196.61 kJ/mol of CO_2) which was lower than ZSM-5 with 84.30% (from 2710.19 to 2284.60 kJ/mol of CO_2) relative heat duty. Even though they failed to justify the better performance of SBA-15 over the HZSM-5 catalyst, the material characterization indicated that the higher surface area and mesopore volume as well as a larger number of active acid sites with predominant Brønsted acids may be the main reason for this superiority.

Sulfated Metal Oxides. It is known that metal oxides can be used as an effective solid acid catalyst in energy-efficient CO_2 capture processes. Since metal oxides are predominantly Lewis acid catalysts, their efficiency is less than those solid acid catalysts with both Lewis and Brønsted acid sites. Therefore, modification of metal oxides with a source of sulfur compound (e.g., H_2SO_4) at high temperatures has gained great attention. The characterization of sulfated metal oxides shows the acid strength of these heterogeneous solid acid catalysts can be even greater than pure H_2SO_4 , which has caused its extensive employment in industrial reactions from 1979.^{85–87}

In 2017, the Liang research group in Hunan University measured the catalytic effect of sulfated zirconia ($\text{SO}_4^{2-}/\text{ZrO}_2$) as a super strong solid acid catalyst in single and blended amine solutions. The $\text{SO}_4^{2-}/\text{ZrO}_2$ catalyst was synthesized using a wet impregnation method followed by high-temperature calcination at 600 °C for 3 h (Figure 3).^{82,83} The characterization results revealed that, although the synthesized $\text{SO}_4^{2-}/\text{ZrO}_2$ catalyst has strong acidic sites, its Lewis and Brønsted acid sites as well as its mesoporosity are much less than those of HZSM-5 and MCM-41, which explains the relatively poor catalytic performance of $\text{SO}_4^{2-}/\text{ZrO}_2$. They reported 90.2% relative heat duty for $\text{SO}_4^{2-}/\text{ZrO}_2$ in 5 M MEA at 98 °C, whereas HZSM-5 and MCM-41 showed a better performance at 75.2 and 81.6%, respectively. Several months later, they synthesized sulfated TiO_2 ($\text{SO}_4^{2-}/\text{TiO}_2$) by a wet impregnation method and high-temperature calcination at 500 °C for 4 h.^{73,75} Nevertheless, the number of Lewis and Brønsted acid sites of $\text{SO}_4^{2-}/\text{TiO}_2$ was not significantly higher than that of $\text{SO}_4^{2-}/\text{ZrO}_2$. A simple comparison between the desorption rate and heat duty of aqueous MEA–AMP–PZ (3.0–2.5–0.5 M) solution in the presence of $\text{SO}_4^{2-}/\text{TiO}_2$ (7.04×10^{-2} mol/min and 602.2 kJ/mol of CO_2), SAPO-34 (7.63×10^{-2} mol/min and 577.2 kJ/mol of CO_2), $\gamma\text{-Al}_2\text{O}_3$ (7.83×10^{-2} mol/min and 566.5 kJ/mol of CO_2), and HZSM-5 (7.94×10^{-2} mol/min and 540.9 kJ/mol of CO_2) as the prevalent solid acid catalysts depicted the inferior catalytic performance of sulfated metal oxides. In a recent research study, Zhang et al.⁷⁴ tested the catalytic performance of $\text{SO}_4^{2-}/\text{TiO}_2$ in the aqueous DEAPA solution and reconfirmed the experimental findings of the previous reports. The measured heat duty of DEAPA– $\text{SO}_4^{2-}/\text{TiO}_2$ was 1092.6 kJ/mol of CO_2 displaying 91.1% relative heat duty with less efficiency than those of MCM-41 (84.8%) and SAPO-34 (78.7%).

Against the low catalytic performance of sulfated metal oxides, this type of heterogeneous solid acid catalysts is appealing due to their facile synthesis procedure and cheap cost. Accordingly, decreasing the production cost and finding the optimum synthesis condition has been widely investigated. Yue et al.⁸⁸ working at the Low-Carbon Technology and Chemical Reaction Engineering Laboratory of Sichuan University succeeded to synthesize $\text{SO}_4^{2-}/\text{TiO}_2$ nanocatalyst (see Figure 5C) by direct calcination of industrial rough metatitanic acid at high temperatures (400–600 °C) and succeeded to promote the CO_2 desorption rate up to 28.9% in the aqueous MEA solutions.

Unfortunately, the low efficiency of sulfated metal oxides has excluded this potential group of heterogeneous catalysts from the recent research investigations on the modification of solid acid catalysts. Recently, Idem et al.⁸⁹ nominated cerium sulfate on zirconia ($\text{Ce}(\text{SO}_4)_2/\text{ZrO}_2$) as a new category of super solid acid catalyst for low-temperature CO_2 desorption (Figure 5D). In the synthesis of $\text{Ce}(\text{SO}_4)_2/\text{ZrO}_2$ catalyst, aqueous solutions of $\text{Ce}(\text{SO}_4)_2$ were used as a source of Ce and SO_4 acidic groups, instead of typical H_2SO_4 . The obtained catalyst was calcinated at 600 °C for 4 h to dope Ce into the structure. Unlike previously synthesized $\text{SO}_4^{2-}/\text{ZrO}_2$ and $\text{SO}_4^{2-}/\text{TiO}_2$ super acid catalysts, $\text{Ce}(\text{SO}_4)_2/\text{ZrO}_2$ possessed a significant number of Brønsted acid sites, even more than the HZSM-5 catalyst. The addition of $\text{Ce}(\text{SO}_4)_2/\text{ZrO}_2$ resulted in 56.4% relative heat duty (110 to 62 kJ/mol of CO_2) for the regeneration of binary BEA–AMP amine solution at 85 °C. Though $\text{Ce}(\text{SO}_4)_2/\text{ZrO}_2$ has a low mesoporosity, it has the advantage of having a large pore volume which can highly facilitate the accessibility of carbamate molecules to the acidic sites. In a different research study, Idem and co-workers⁹⁰ studied the catalytic effect of $\text{Ce}(\text{SO}_4)_2/\text{ZrO}_2$ on the regeneration of BEA–AMP amine solution in a bench-scale CO_2 capture pilot plant. Their reported heat duty value for noncatalytic solvent regeneration was 7.77 GJ/tonne which was reduced to 6.08 and 7.27 GJ/tonne after utilizing $\text{Ce}(\text{SO}_4)_2/\text{ZrO}_2$ and HZSM-5 with 78.25 and 93.56% relative heat duty, respectively. This promising finding strongly supports the capability of sulfated solid acid catalyst for a low temperature of CO_2 regeneration which can pave the way for further research studies in this area.

Hybrid Composite and Metal Modified Materials.

Despite the common belief that heterogeneous catalysts with predominantly Brønsted acid sites can more significantly facilitate CO_2 desorption, both Lewis and Brønsted acid sites in solid acid catalysts play an indispensable role. Thus, the development of new Brønsted solid acid catalysts has not significantly reduced the minimum theoretical heat duty for amine regeneration and, subsequently, significant operating cost reduction in CO_2 stripping. On the other hand, promising materials with both Lewis and Brønsted acid sites typically suffer from low porosity and surface area, high microporosity, low kinetics of molecular diffusion, and aggregation. Based on these scenarios, using hybrid catalysts can be an approach to enhance the efficiency of solid acid catalysts and further reduce energy consumption in catalytic solvent regeneration. Hybrid composite catalysts are typically a mixture of two different materials with different characteristics which take the advantages of each material. During the past two decades, the combination of different metal oxides with synthetic zeolites (e.g., $\text{Ni}-\text{HZSM-5}$,⁹¹ $\text{Fe}_3\text{O}_4-\text{HZSM-5}$,⁹² and $\text{In}_2\text{O}_3-\text{HZSM-5}$ ⁹³) and carbon-based materials (e.g., $\text{Fe}_3\text{O}_4-\text{C}$ ⁹⁴ and $\text{MgO}-\text{C}$ ⁹⁵) has been gaining attention as promising hybrid catalysts.

There are very limited efforts for using hybrid composite materials in the area of energy-efficient CO_2 desorption. Hybrid solid acid catalyst was first reported in 2015 where Idem et al.⁶⁸ mixed commercial $\gamma\text{-Al}_2\text{O}_3$ and HZSM-5 single solid acid catalysts to exploit the advantages of each (Figure 3). They found that $\gamma\text{-Al}_2\text{O}_3/\text{HZSM-5}$ catalyst exhibited a better catalytic efficiency than either $\gamma\text{-Al}_2\text{O}_3$ or HZSM-5 catalyst alone in the regeneration of aqueous 5 M MEA solution at 105 °C. This superiority can be ascribed to the fact that $\gamma\text{-Al}_2\text{O}_3/\text{HZSM-5}$ hybrid composite catalyst benefits from the abundant Lewis acid sites of $\gamma\text{-Al}_2\text{O}_3$, Brønsted acid sites and high surface area of HZSM-5, and synergistic effect between $\gamma\text{-Al}_2\text{O}_3$ and HZSM-5. In a different research study in 2018, they synthesized a series of $\gamma\text{-Al}_2\text{O}_3/\text{HZSM-5}$ hybrid catalysts using a combined precipitation ultrasound method to scrutinize the role of different effective characteristics in the catalytic performance of $\gamma\text{-Al}_2\text{O}_3/\text{HZSM-5}$ hybrid catalyst.⁹⁶ Interestingly, the characterization of the synthesized materials demonstrated that $\gamma\text{-Al}_2\text{O}_3/\text{HZSM-5}$ has a higher surface area, mesoporosity, average pore diameter, and, more importantly, number of Brønsted acid sites than both $\gamma\text{-Al}_2\text{O}_3$ and HZSM-5. As a result, $\gamma\text{-Al}_2\text{O}_3/\text{HZSM-5}$ was able to reduce the relative heat duty to 65.8% of the aqueous 5 M MEA solution at 96 °C, while $\gamma\text{-Al}_2\text{O}_3$ and HZSM-5 reached 79.1 and 80.9%, respectively.

Choosing the appropriate type of catalytic components in the hybrid solid acid catalyst is one of the most important parameters and has a great impact on the total performance of hybrid composite nanocatalyst. For instance, $\text{SiO}_2/\text{Al}_2\text{O}_3$ composite was tested in 2017 as a hybrid solid acid catalyst for the catalytic regeneration of MEA solvent. It exhibited a very poor catalytic performance due to the similar Lewis acid sites of both SiO_2 and Al_2O_3 metal oxides.⁶⁹

Even with research progression into the development of hybrid $\gamma\text{-Al}_2\text{O}_3/\text{HZSM-5}$ solid acid catalysts, the amount of energy reduction is still far from the theoretical required energy for amine regeneration. This lack of success is related to two factors. On one hand, the microporous structure of HZSM-5 is easily blocked due to its ultranarrow pore diameter. This vulnerability has made $\gamma\text{-Al}_2\text{O}_3/\text{HZSM-5}$ hybrid composite prone to a remarkable increase in mass transfer resistance through the pores, resulting in a decrease in its catalytic performance, and rapid inactivation. On the other hand, both $\gamma\text{-Al}_2\text{O}_3$ and HZSM-5 solid acid catalysts provide fewer Lewis and Brønsted acid sites compared to the novel catalysts such as sulfated metal oxides, especially those with super acidic properties. To address this, sulfated ZrO_2 superacid catalysts supported on a mesoporous structure are being investigated. Liang et al.⁹⁷ chose $\gamma\text{-Al}_2\text{O}_3$ as a mesoporous catalyst support with Lewis acid sites and used a precipitation–impregnation method to synthesize $\text{SO}_4^{2-}/\text{ZrO}_2/\gamma\text{-Al}_2\text{O}_3$ composite catalyst with different $\text{SO}_4^{2-}/\text{ZrO}_2$ loadings (Figure 5E). They claimed the synthesized $\text{SO}_4^{2-}/\text{ZrO}_2/\gamma\text{-Al}_2\text{O}_3$ not only can benefit from the Lewis acid sites of $\gamma\text{-Al}_2\text{O}_3$ and Brønsted acid sites of $\text{SO}_4^{2-}/\text{ZrO}_2$ but also can provide a large accessible area for superacid $\text{SO}_4^{2-}/\text{ZrO}_2$ metal oxides. The recorded energy values confirmed the claim of authors and displayed that $\text{SO}_4^{2-}/\text{ZrO}_2/\gamma\text{-Al}_2\text{O}_3$ reduced the relative heat duty of MEA solution to 63.1% (1582.2 to 998.9 kJ/mol of CO_2), which was the best recorded value at the time. As expected, both $\text{SO}_4^{2-}/\text{ZrO}_2$ (79.5%, 1257.8 kJ/mol of CO_2) and $\gamma\text{-Al}_2\text{O}_3$ (82.7%, 1307.9 kJ/mol of CO_2) exhibited much less catalytic performance under the same regeneration conditions, reconfirming the benefits of hybrid composite catalysts with a mesoporous support. In a

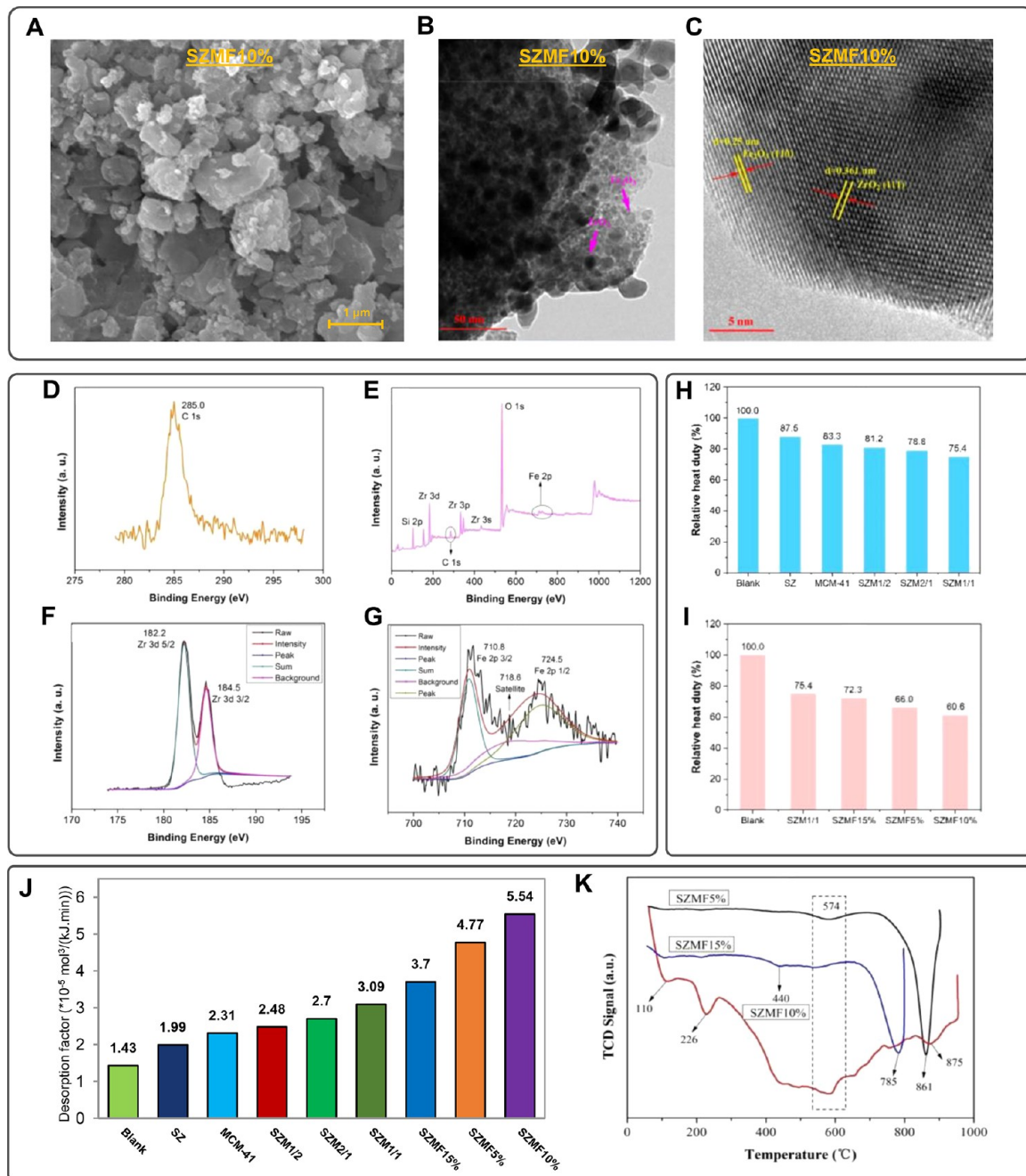


Figure 7. (A) SEM, (B) TEM, and (C) HRTEM images of SZMF10% sample. The XPS results of the SZMF10% sample. (D) XPS C 1s spectrum, (E) full survey spectrum, (F) high-resolution Zr 3d spectrum, and (G) high-resolution Fe 2p spectrum. Relative heat duty of MEA solution with (H) SZM and (I) SZMF catalysts. (J) Desorption factor of blank MEA solution and SZ, SZM, and SZMF catalysts. (K) NH₃-TPD characterization of SZMF5%, SZMF10%, and SZMF15%.⁹⁹ Copyright ACS 2019.

similar research study, Ali Saleh Bairq and co-workers⁹⁸ selected SiO₂ as a mesoporous acidic support and employed a modified impregnation method to load superacid SO₄²⁻/ZrO₂ catalyst. The investigations revealed that the SO₄²⁻/ZrO₂ to SiO₂ ratio plays an indispensable role in the synthesis of a hybrid SO₄²⁻/ZrO₂/SiO₂ catalyst to optimize catalytic activity. Despite replacing γ-Al₂O₃ with SiO₂ as a more suitable acidic support, they reported 63.53% as the minimum achieved heat duty for MEA solution at 97–98 °C, which was so close to that of SO₄²⁻/ZrO₂/γ-Al₂O₃ with 63.1% relative heat duty.

Recently, Gao et al.⁸⁴ reported the catalytic performance of SO₄²⁻/ZrO₂ supported on SBA-15 mesoporous silica for

energy-efficient solvent regeneration (Figure 5F). The main reason behind the selection of mesoporous SBA-15—instead of γ-Al₂O₃ and SiO₂ supports—was its predominant Brønsted acidity. The recorded value for the relative heat duty of the best SO₄²⁻/ZrO₂/SBA-15 sample was 73.5% for thermal regeneration of the MEA solution. This value is higher than those of SO₄²⁻/ZrO₂/γ-Al₂O₃ and SO₄²⁻/ZrO₂/SiO₂ catalysts with 63.1 and 63.53% relative heat duty, respectively, demonstrating the inferiority of SBA-15 as a catalyst support. It might be due to the low acid strength or the concentration of active acid sites on the surface of SO₄²⁻/ZrO₂/SBA-15. This point was highlighted again by Liang et al.⁹⁹ for the interpretation of Fe promoted

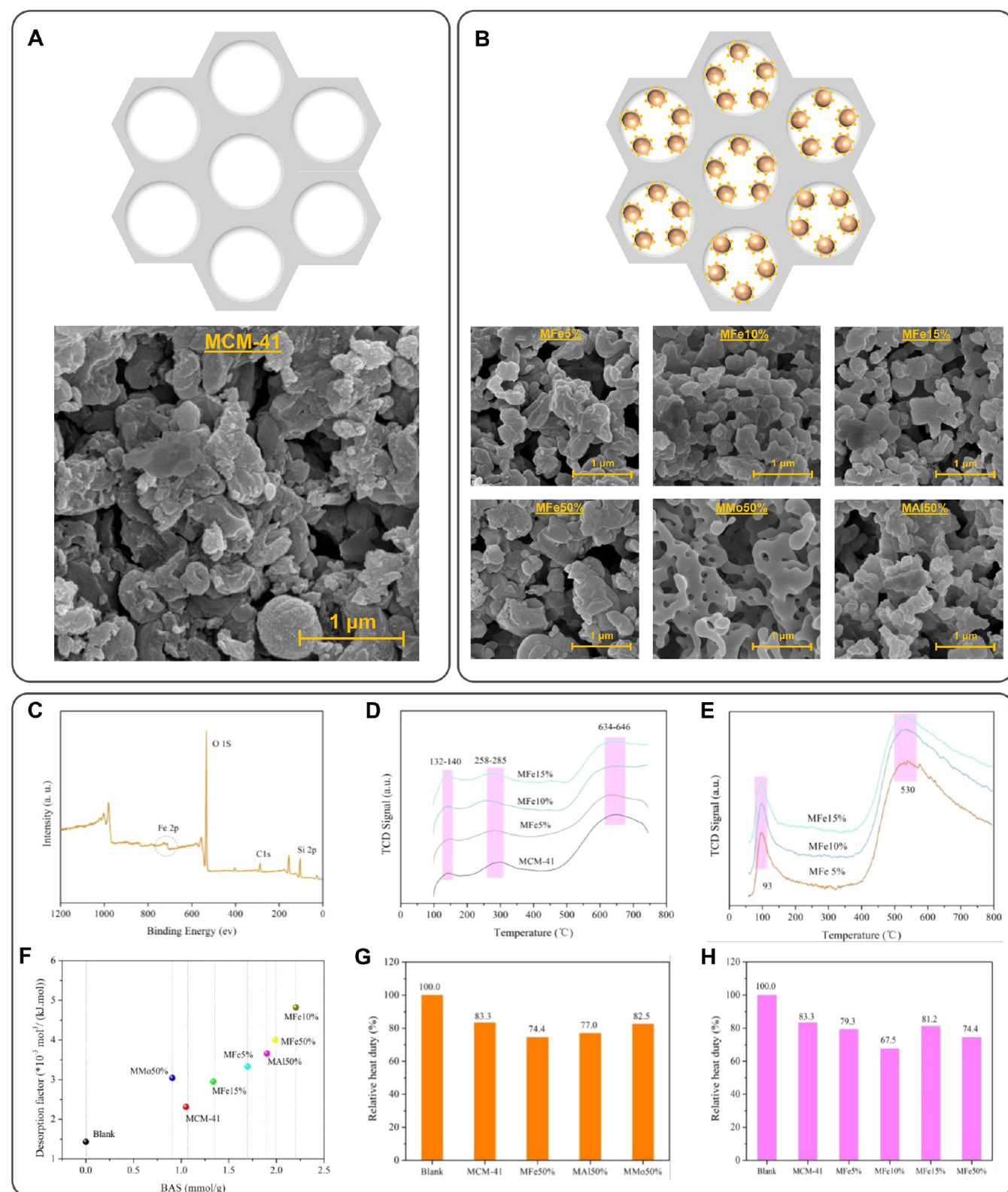


Figure 8. SEM images of (A) MCM-41, (B) MFe5%, MFe10%, MFe15%, MFe50% MMo50%, and MA150%. (C) Total XPS survey spectrum of the MFe10% sample. The results of (D) NH₃-TPD and (E) CO₂-TPD characterization for the MCM-41, MFe5%, MFe10%, and MFe15% samples. (F) The relationship between Bronsted acid sites (BAS) and catalytic activity. (G) The relative heat duty of MCM-41 and its metal doped (i.e., Fe, Mo, and Al) derivative catalysts. (H) The relative heat duty of MCM-41 and its Fe doped derivative catalysts with different weight percentages.¹⁰⁰ Copyright Elsevier 2020.

SO₄²⁻/ZrO₂/MCM-41 performance in catalyst-aided solvent regeneration (Figure 7A–C). They believed the poor catalytic performance of MCM-41 is due to its weak acid strength which

can substantially hinder its widespread application. Since SO₄²⁻/ZrO₂ is considered a solid acid catalyst with strong acidic strength, SO₄²⁻/ZrO₂ loading on MCM-41 support can

cover its drawbacks (see Figure 5G). To improve the catalytic performance, they used the wet impregnation method and promoted the $\text{SO}_4^{2-}/\text{ZrO}_2/\text{MCM-41}$ structure with Fe^{3+} species mainly in its Fe_2O_3 metal oxide form (Figure 7D–G). They proved the introduction of Fe not only can notably increase the concentration of weak acid sites (Figure 7K) but also can promote the basicity of hybrid $\text{SO}_4^{2-}/\text{ZrO}_2/\text{MCM-41}$ catalysts. Accordingly, they reported the minimum recorded relative heat duty of 60.6% to date for 5 M MEA solution at 98 °C (Figure 7H–J).

The main characteristic property of metal atoms which can distinguish them from other catalytic modifiers is that their incorporation into the structure can result in the formation of basic sites on the surface, as well as both Lewis and Brønsted acid sites. The introduced basic sites have a positive influence on the CO_2 desorption performance and can complement the catalytic effect of acid sites. Thus, metal modified structures like Fe promoted $\text{SO}_4^{2-}/\text{ZrO}_2/\text{MCM-41}$ can be considered as a bifunctional catalyst having both acidic and basic active sites on the surface. In their latest research, Liang et al.¹⁰⁰ utilized the promising results of Fe modification on catalytic solvent regeneration and specifically investigated the role of different metals (i.e., Fe, Al, and Mo) on the catalytic efficiency of corresponding bifunctional metal promoted MCM-41 (Figure 5B and Figure 8A–F). Among Fe, Al, and Mo metals, it was observed that Fe, Al, and Mo displayed the best, medium, and worst catalytic performance with 67.5% (1013.3 kJ/mol of CO_2), 77.0% (1155.6 kJ/mol of CO_2), and 82.5% (1237.5 kJ/mol of CO_2) relative heat duty, respectively (Figure 8G,H).

In a later study, Liang et al.¹⁰¹ used modified mesoporous carbon CMK-3 for the first time with three different templates (i.e., SBA-15, MCM-41, and SiO_2). The results showed that using CMK-3–SBA-15, CMK-3–MCM-41, and CMK-3– SiO_2 , drastically reduced the relative heat duty of MEA solvent regeneration to 78.51, 69.71, and 62.59%, respectively. The superiority of CMK-3– SiO_2 compared to the other structures was attributed to the strong interaction between SiO_2 and the carbon surface in the presence of SO_4^{2-} . These findings clearly reveal that the use of carbon-based heterogeneous catalysts can open a new promising approach for catalyst-aided solvent regeneration for energy-efficient CO_2 desorption and other carbon-based materials should be considered in the future research investigations.

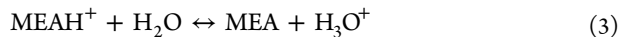
PROMOTION MECHANISM OF CATALYTIC CO_2 DESORPTION

Nocatalytic Solvent Regeneration. As discussed in the literature, CO_2 desorption during the regeneration process involves a series of complex reactions.^{68,89} However, it is widely accepted that the chemical absorption–desorption of CO_2 into the primary amine solutions, like MEA, follows the zwitterion mechanism, introduced by Caplow¹⁰² in 1968 and reproposed by Danckwerts¹⁰³ in 1979. According to reaction 1, carbamate (MEACOO^-) and protonated amine (MEAH^+) are formed as the main products of CO_2 absorption. Additionally, a part of generated MEACOO^- can further react with water and produce bicarbonate (HCO_3^-) in the solution (reaction 2).^{75,90,104}



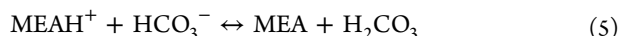
In the regeneration process of CO_2 saturated amine solution, two main steps are followed: protonated amine deprotonation

(reaction 3) and carbamate breakdown (reaction 4). It should be noted that both amine deprotonation and carbamate breakdown reactions are strongly endothermic with 73.4 and 15.5 kJ/mol heats of reactions, respectively.⁷⁰ Although CO_2 molecules are released by the carbamate breakdown reaction, the yield of this reaction is highly dependent on the number of released protons from the deprotonation reaction.⁷⁴ Regardless of the energy requirement, CO_2 desorption reactions require a high temperature, in the range 120–140 °C for spontaneous proton transfer (reaction 3) and bond cleavage (reaction 4).^{67,105}

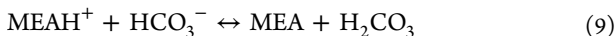
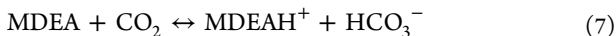


A simple comparison between the amine deprotonation (reaction 3) and carbamate breakdown (reaction 4) reactions as the main steps of the CO_2 desorption mechanism shows that as the amine deprotonation reaction is highly energy-intensive (78.2 kJ/mol) it may be considered as one of the main barricades to low-temperature solvent regeneration. The difficulty of H^+ transfer from MEAH^+ to H_2O in the amine solution is attributed to the high alkalinity of MEA and the neutral nature of H_2O .^{90,106} On the other hand, the carbamate breakdown reaction requires a lower energy (14.7 kJ/mol) than that of amine deprotonation but is complicated and highly dependent on the number of available protons in the solution released by the amine deprotonation reaction.¹⁰⁷

The Role of HCO_3^- . In addition to H_2O molecules acting as proton acceptors in solution, the HCO_3^- species generated can play a similar essential role for carrying a proton from MEAH^+ (as the main proton donor) to MEACOO^- .^{82,90} Since HCO_3^- is a stronger base than H_2O , the presence of free HCO_3^- in solution can act as a catalyst and reduce the required energy of amine deprotonation from 78.2 up to 21.2 kJ/mol (reactions 5 and 6).^{52,70} According to the findings of Barzaghi et al.,¹⁰⁸ HCO_3^- requires much less energy and a lower temperature than MEACOO^- for regeneration, which leads to the decomposition of HCO_3^- species before MEACOO^- species during solvent regeneration. Hence, it can be concluded that the energy consumption for the regeneration of CO_2 -lean solvents is more than that for CO_2 -rich solvents.⁴²

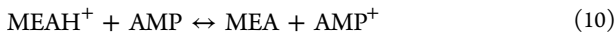


Generally, the carbamate formation reaction is the main absorption mechanism in primary amine solutions (reaction 1) and bicarbonates are formed only at high concentrations of carbamate in CO_2 -rich solvents.^{53,97} Consequently, a considerable amount of energy is required for the decomposition of carbamate during the regeneration of primary amine solutions. Conversely, tertiary amines—unlike primary and secondary amines—can indirectly react with CO_2 molecules and produce bicarbonate instead of carbamate. Regarding the CO_2 absorption mechanism of MDEA as the most common tertiary amine for CO_2 capture, HCO_3^- is the main CO_2 -containing species produced by the chemical reaction of MDEA– CO_2 with less required energy than carbamate species (reactions 7–9).¹⁰⁹ As a consequence, the required energy for the regeneration of tertiary amine solution is much less than those of primary amine solution, since HCO_3^- is a much better proton acceptor than H_2O .⁸²



One of the well-developed techniques to reduce intensive energy consumption in primary amine solutions is via using a tertiary amine as an additive into the primary amine solution. The significance of tertiary amines in the MEA solution can be well explained by increasing the number of proton acceptors, accelerating HCO_3^- formation and, subsequently, reducing the activation energy of proton transfer from MEA^+ to H_2O through multiple proton transfer routes. This agrees well with the HCO_3^- concentration in the single MEA and blended MEA–MDEA solutions. As reported by Liang et al.,⁷⁰ the HCO_3^- species in the MEA, MDEA, and MEA–MDEA–PZ solutions are formed when the concentration of CO_2 passes 0.4, 0.05, and 0.32 mol of CO_2 /mol of amine, respectively, confirming facilitated HCO_3^- formation in the primary–tertiary amine mixtures compared to the aqueous primary amine solutions.

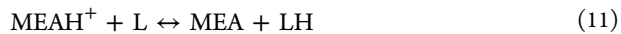
In MEA–MDEA or MEA–DEAB binary mixtures, the beneficial role of tertiary amines in aqueous MEA solutions (strong base) is twofold. First, the introduced MDEA,¹⁰⁹ DEAB,¹⁰⁹ or DEAPA⁷⁴ (medium base) are good proton acceptors with a high potential to aid in receiving H^+ from MEA^+ and pass it to H_2O . In some cases, sterically hindered amines like AMP have also been used as proton carriers in MEA solutions (reaction 10).⁷⁵ Second, the generated species HCO_3^- can be decomposed at a lower temperature with much less energy.



In general, increasing the number of available free protons in the primary–tertiary solution can accelerate stepwise proton transfer, change the reaction pathway, and substantially reduce regeneration energy consumption.^{52,110} More importantly, the additional HCO_3^- species (weak base) produced by the tertiary amine mechanism can strikingly increase the concentration of this proton acceptor even at low CO_2 loadings.^{53,82}

The Role of Lewis and Brønsted Acid Sites in Carbamate Decomposition. As is known, catalysts can improve the energy efficiency and diminish the overall energy penalty of the CO_2 desorption reaction. It is worth mentioning that catalysts cannot change the theoretical level of thermodynamic energy required. It is generally accepted that the energy consumption required for CO_2 desorption is related to the difficulty of proton transfer from MEA^+ to H_2O in the deprotonation reaction (reaction 3), the limited number of available protons for carbamate decomposition (reaction 4), and the endothermic nature of these reactions.^{75,98} These conditions cause the CO_2 liberation process to barely occur at low temperatures. The importance of Lewis and Brønsted acid sites on the surface of solid acid catalysts at low-temperature CO_2 desorption has been extensively investigated since 2011.^{51,52,58,74}

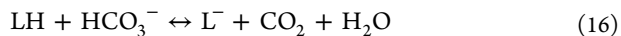
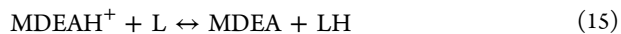
Lewis acidity (L) is one of the main acidic types on the heterogeneous acid surface. Lewis acids are typically provided by unsaturated metal atoms, which makes them able to accept a lone pair of electrons.⁵⁵ The catalytic role of Lewis acid sites in the amine deprotonation mechanism is demonstrated in reactions 11 and 12.^{96–98}



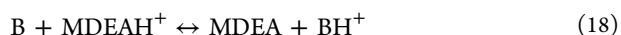
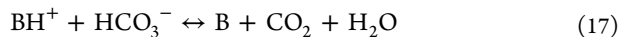
The second category of acid sites on the surface of solid acid catalysts is Brønsted acidity (B) which can donate a proton (H^+) to a base.¹¹¹ The catalytic role of Brønsted acid sites in the carbamate breakdown mechanism is illustrated in reactions 13 and 14.^{96–98}



Besides primary amine solutions, solid acid catalysts can effectively contribute to the CO_2 desorption mechanism of tertiary amines. The reaction mechanism of Lewis acid sites is presented as follows:



Similarly, the reaction mechanism of Brønsted acid sites is presented as follows:¹⁰⁵



According to reactions 15 and 16, Lewis acid needs to follow two consecutive steps to play its role in the reaction mechanism. Initially, Lewis acid needs to accept a proton from MDEAH^+ , since it has no proton in its structure. Subsequently, it can donate its proton to HCO_3^- ion and speed up the solvent regeneration and CO_2 desorption process with significantly lower energy consumption. On the other hand, Brønsted acids have an active proton which makes it capable of donating its proton first and then receiving a proton from MDEAH^+ (reactions 17 and 18). Therefore, Brønsted acids can directly supply the required number of protons for HCO_3^- decomposition.¹¹² This difference in the reaction mechanism may be the main reason that HZSM-5 (predominantly Brønsted acid) displays a superior CO_2 desorption performance to $\gamma\text{-Al}_2\text{O}_3$ (predominantly Lewis acid) catalyst in 1DMA2P and DEEA solutions.¹¹²

It has been widely accepted that metal oxides are able to indirectly generate Brønsted acidity in the aqueous solutions. According to reactions 19 and 20, the strong interaction between O atoms in water molecules and metal atoms (e.g., Al, Si, Fe, Zr, and Mo) can chemically adsorb and split water molecules on the surface of metal oxides, forming a hydroxyl group (i.e., surface-bound OH group), and behave as the Brønsted acid site.^{48,55,99,100} Therefore, the Lewis acid sites of metal oxides can be converted to the Brønsted acid sites in aqueous solutions. Although metal oxides have the advantages of both Lewis and Brønsted acids, they are known as predominantly as Lewis acid catalysts.



The carbamate breakdown reaction in the presence of solid acid catalyst was first studied by Idem and his colleagues⁵¹ in 2011. Following this, more publications have suggested a similar reaction mechanism for catalytic carbamate breakdown, especially between 2017 and 2020. The decomposition of carbamate formed in the CO_2 -saturated amine solution needs

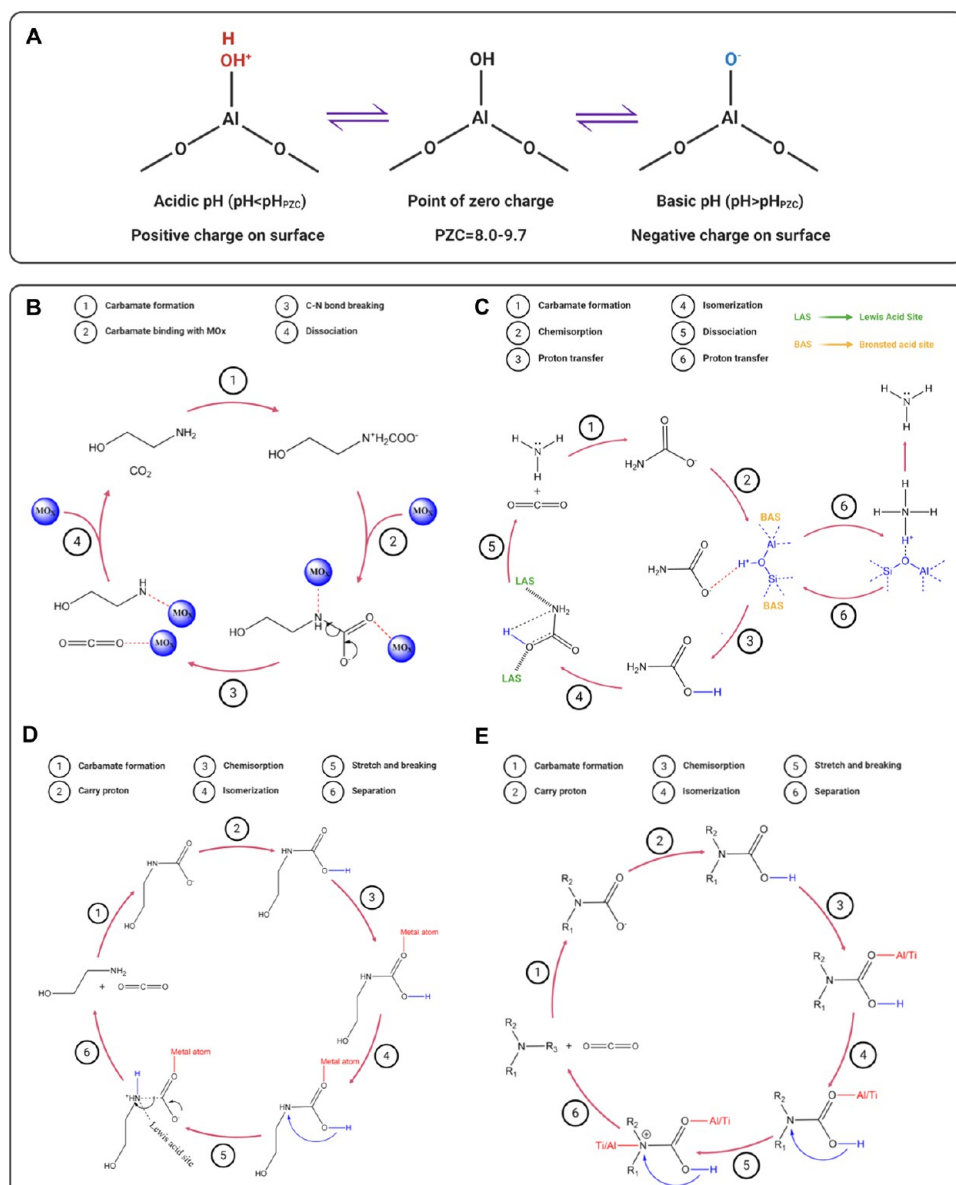


Figure 9. (A) Surface charge properties of Al_2O_3 at different pH values.⁷⁰ Copyright Elsevier 2019. The proposed CO₂ desorption mechanism from (B) MEA solution in the presence of metal oxide catalysts, (C) ammonia solution over HZSM-5, TiO₂, and γ -Al₂O₃ solid acid catalysts, (D) MEA solution in the presence of $\text{SO}_4^{2-}/\text{ZrO}_2/\gamma\text{-Al}_2\text{O}_3$, and (E) 3 M MEA–2.5 M AMP–0.5 M PZ solution over H-ZSM-5, γ -Al₂O₃, SAPO-34, and $\text{SO}_4^{2-}/\text{TiO}_2$ solid acid catalysts.

two principal factors: heat and protons.^{100,113} While the required heat is usually provided by superheated steam, most of the protons are tightly bound to the protonated amines, decreasing the number of available protons for carbamate decomposition. As a result, the lack of free protons in the solution is the main limiting factor for the regeneration of carbamate.

Oxygen (O) and nitrogen (N) atoms have a critical position in the MEACOO[−] structure. First, the O anion (O[−]) is an essential part of the carbamate species with excellent potential for obtaining protons from either the deprotonation reaction or the Brønsted acid.^{73,97} Second, the N atom is the main connection between the MEA molecule and CO₂ through the N–C bond.^{98,100} Based on the presented catalytic mechanism of metal oxides (Figure 9B,C), both Lewis and Brønsted acids can directly attack the N atom of carbamate molecules. Moreover, both metals (Lewis acid) and free protons (Brønsted acid) can facilitate the carbamate breakdown by decreasing the activation

energy of the desorption reactions.^{55,57,105,114} The attached acidic sites rob the lone pair electrons of the N and change its configuration from sp² to sp³. Consequently, the acidic sites of the catalyst can stretch the C–N bond of the carbamate, weaken its bond strength, delocalize the N–COO[−] conjunction, and break up the carbamate with a faster CO₂ desorption rate using much less energy.^{48,51,55,73}

The thorough investigation of HZSM-5 discloses that, although HZSM-5 is an eminent Brønsted acid catalyst, the presence of both Lewis and Brønsted acid on its active surface can strikingly boost the catalytic effect of HZSM-5 and its key role in changing the reaction pathway.^{69,89} As mentioned, the Brønsted acids of HZSM-5 directly supply plenty of free protons (H⁺) for the transformation of MEACOO[−] to MEACOOH. Due to the presence of Lewis acids on the surface of the HZSM-5 catalyst with electron acceptor behavior, the lone pair electron in the O atom of MEACOOH is potentially attracted and

chemisorbed by the empty orbital of Al atoms ($\text{Al}-\text{O}$). Then, the MEACOOH becomes a zwitterion by the relocation of the attached H atom to its adjacent N atom with an isomerization reaction on the surface of the acidic catalyst, which makes it positively charged (N^+) and shifts the hybridization orbital from sp^2 to sp^3 (see Figure 9C). Moreover, another Al^{3+} (Lewis acid) atom can attack the free lone pair of electrons on the N atom, accelerate its chemisorption, and further promote the proton transfer of N and its positive charge. Subsequently, the transferred proton weakens the delocalized conjunction of the N atom, stretches the N–C bond, and, eventually, breaks this bond. This results in the division of the zwitterion into the amine and CO_2 in the solution. At high regeneration temperatures, CO_2 has a low solubility in the aqueous solution and leaves the solution as gaseous CO_2 molecules.^{69,70,105,114}

Recently, Liang et al.⁹⁸ synthesized $\text{SO}_4^{2-}/\text{ZrO}_2/\text{SiO}_2$ as a novel bifunctional heterogeneous catalyst and suggested a similar catalytic mechanism (Figure 9D). In the $\text{SO}_4^{2-}/\text{ZrO}_2/\text{SiO}_2$ catalyst, SO_4^{2-} as a Brønsted acid can play the role of proton donor and both ZrO_2 (mainly) and SiO_2 (partially) can act as Lewis acid sites. Therefore, instead of Al metal atoms in HZSM-5, Zr as a metal atom and Si as a semimetal atom of $\text{SO}_4^{2-}/\text{ZrO}_2/\text{SiO}_2$ catalyst can attack the oxygen and nitrogen atoms of carbamate and play the role of active sites for the chemisorption of carbamate. Likewise, a similar Lewis acid role has been suggested for Zr and Ti atoms on the surface of $\text{SO}_4^{2-}/\text{ZrO}_2/\text{SBA-15}$ and $\text{SO}_4^{2-}/\text{TiO}_2$ catalysts, respectively (Figure 9E).^{75,84}

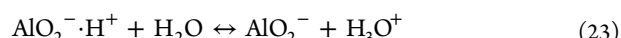
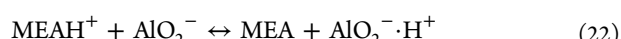
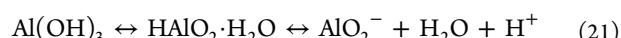
According to the literature, Brønsted acid catalysts display a better regeneration performance than Lewis acid catalysts.^{68,89,90} This can be ascribed to the catalytic mechanism of different acidic groups in which Lewis acids indirectly provide the required number of protons to aid the carbamate breakdown reaction, while Brønsted acids directly supply the required protons with a much lesser amount of energy.⁵³ Thus, by adding Brønsted acid catalysts to the solution as a proton donating solid acid catalyst, protons are directly supplied, take part in the catalytic desorption, and released into the solution. Hence, the carbamate breakdown reaction does not need to wait for the deprotonation reaction to proceed, leading to an appreciable enhancement in CO_2 desorption rate.^{69,70,90,115} Besides the beneficial catalytic role of Brønsted acids in the entire regeneration process of primary amine solutions, they can generate protons in the tertiary amine solution, like MDEA¹⁰⁹ and DEEA,¹¹² and directly attack the HCO_3^- species and accelerate the solvent regeneration process.

The Role of Basic Sites in Amine Deprotonation Reaction. The deprotonation reaction is the key step for initiating the CO_2 desorption process, which releases free protons into the solution and facilitates the subsequent carbamate decomposition reaction.⁶⁹ The deprotonation reaction is simple (unlike the carbamate decomposition reaction) but requires a high amount of energy and is considered as the main reason for the high energy requirement for amine regeneration.^{48,52} With regard to the insignificant proton transfer from MEAH^+ to H_2O and due to the higher basicity of MEA compared to neutral H_2O , the deprotonation of the amine barely occurs at low temperatures ($<100^\circ\text{C}$), resulting in a shortage of available protons for the carbamate decomposition reaction (reaction 4).

The presence of weak basic species like HCO_3^- in the CO_2 -saturated solution can facilitate the CO_2 desorption mechanism, decrease the regeneration temperature, and reduce the amount of required energy. Despite this, the concentration of HCO_3^- in

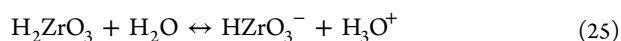
the primary amine solutions like MEA is not significant, especially at CO_2 -lean solutions when all HCO_3^- species have been decomposed. Therefore, using basic catalysts has been one of the main successful strategies to mimic the role of HCO_3^- in the primary amine solutions.

In 2014, Idem and his colleagues investigated the $\gamma\text{-Al}_2\text{O}_3$ catalyst and its inherent capabilities to mimic the role of HCO_3^- at low CO_2 loadings.^{52,53} The $\gamma\text{-Al}_2\text{O}_3$ catalyst is an amphoteric oxide which makes it able to not only play the role of a Lewis acid catalyst but also show basic properties. As is seen from reactions 21–23, Al_2O_3 catalyst can partially turn into AlO_2^- and play the role of an intermediate proton acceptor for MEAH^+ and release it to the water molecules.^{70,75} Therefore, $\gamma\text{-Al}_2\text{O}_3$ catalyst can be utilized as an effective substitute for HCO_3^- to imitate its proton acceptor role in the CO_2 -lean region.^{69,75}



One of the main characteristics of $\gamma\text{-Al}_2\text{O}_3$ catalyst leading to a better solvent regeneration performance at low CO_2 loadings is its surface charge variation at different pH values.¹⁰⁹ Since CO_2 is a weak acid, increased CO_2 absorption in the basic amine solution reduces the pH and increases the accumulation of positive charges on the surface of the $\gamma\text{-Al}_2\text{O}_3$ catalyst. This causes the $\gamma\text{-Al}_2\text{O}_3$ catalyst to barely contribute to the regeneration mechanism. The surface charge of $\gamma\text{-Al}_2\text{O}_3$ is defined based on the point of zero charge (PZC) in which the surface charge is negative for $\text{pH} > \text{pH}_{\text{PZC}}$ and positive for $\text{pH} < \text{pH}_{\text{PZC}}$.⁷⁵ As shown in Figure 9A, the pH_{PZC} of $\gamma\text{-Al}_2\text{O}_3$ has been measured around 9.0–9.7.^{70,75,117} Thus, it is one of the main reasons for the better performance of Brønsted acid catalyst at the beginning of the solvent regeneration process.

Liang et al.⁹⁷ and Gao et al.⁸⁴ reported a similar mechanism for ZrO_2 metal oxide in basic solutions. Based on reactions 24–26, the zirconate ions (HZrO_3^-) that form under the alkaline conditions can act as a catalyst in the amine solution and facilitate proton transfer from MEAH^+ to MEACOO^- .^{118,119} Note that the OH^- ion of ZrO_2 catalyst can partially react with the absorbed CO_2 and form HCO_3^- .



Recently, Idem et al. suggested a dual-site mechanism for the catalytic role of $\gamma\text{-Al}_2\text{O}_3$ which justifies its contribution to both amine deprotonation and carbamate breakdown reactions.¹⁰⁵ The AlO_2^- anion sites of $\gamma\text{-Al}_2\text{O}_3$ withdraw protons from MEAH^+ and carry them to H_2O and then MEACOO^- . Alternatively, the Al^{3+} cation active sites on $\gamma\text{-Al}_2\text{O}_3$ attack the MEACOO^- and weaken the C–N bond. According to the dual-site mechanism of Lewis acids, both MEAH^+ and MEACOO^- are chemically adsorbed to the active surface of the catalyst (reactions 27 and 28), resulting in a proton carry-off from MEAH^+ to MEACOO^- and carbamate decomposition (reaction 29). Thereupon, the MEA molecules chemisorbed on the surface of solid acid catalyst ($\text{AlO}_2\text{-MEA}$) detach from the catalyst and desorb into the solution (reaction 30).

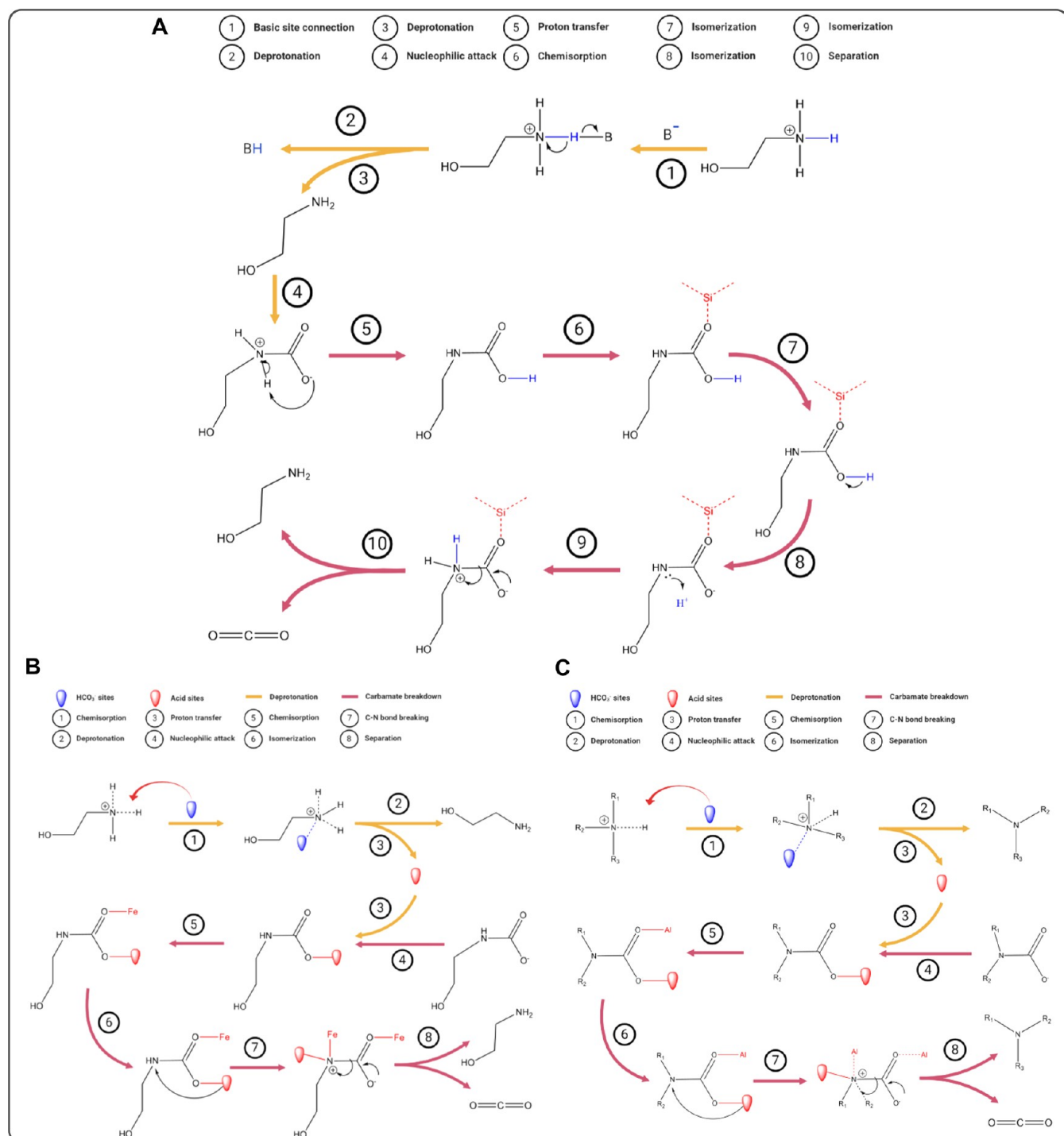
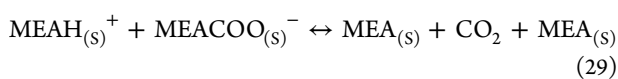
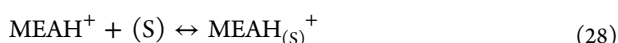


Figure 10. Proposed CO₂ desorption mechanism from (A) MEA solution over SO₄²⁻/ZrO₂/SiO₂ bifunctional catalyst, (B) MEA solution in the presence of metal modified MCM-41, and (C) 3 M MEA–2.5 MDEA–0.5 PZ trisolvant amine mixture over H-mordenite, H-beta, HZSM-5, and Al₂O₃ catalysts.



Based on the reports, a small effect has been observed when using γ-Al₂O₃ catalyst at high CO₂ loadings.^{105,110} This may be due to HCO₃⁻ already existing at high CO₂ concentrations. Generating additional HCO₃⁻ using the γ-Al₂O₃ catalyst may be ineffective until the lean CO₂ region with a low concentration of HCO₃⁻ is reached. Interestingly, the findings of Rosynek¹²⁰ show that γ-Al₂O₃ catalyst not only can mimic the role of HCO₃⁻ in solution but can also generate small amounts of

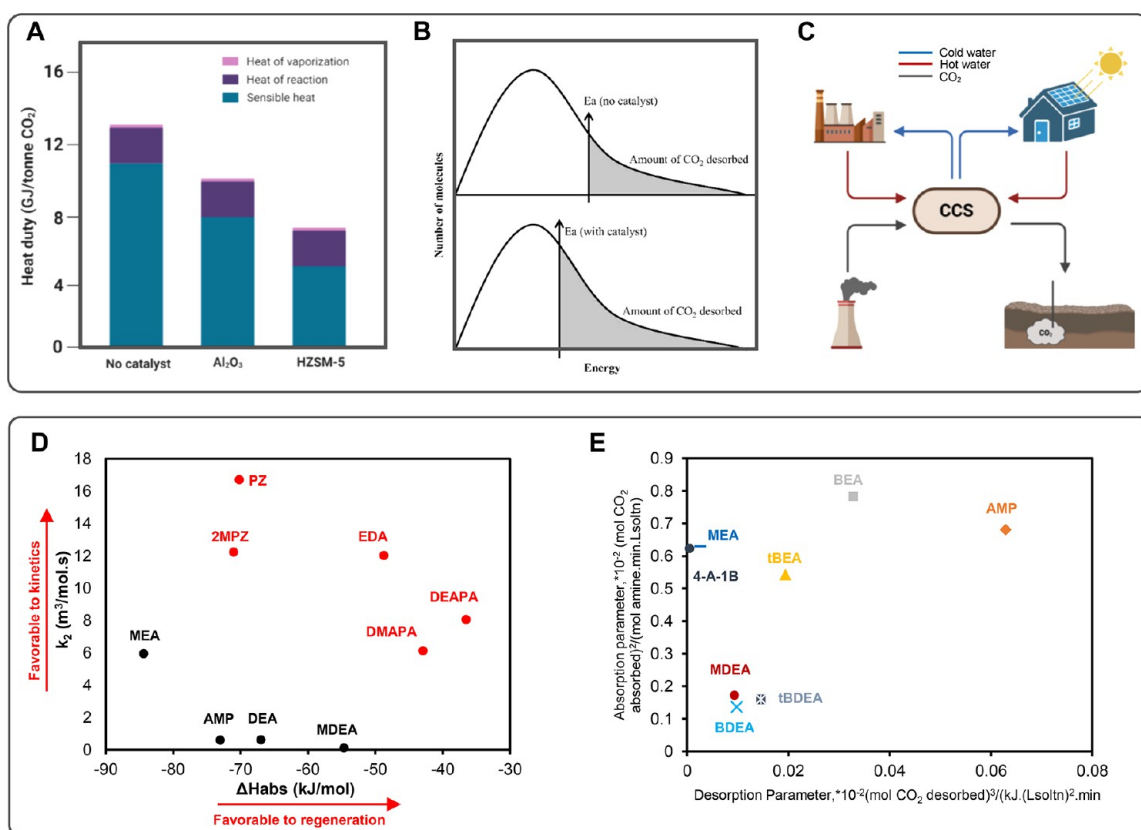


Figure 11. (A) Comparison of heat of vaporization, heat of reaction, and sensible heat for γ -Al₂O₃ and HZSM-5.⁶⁹ (B) Maxwell–Boltzmann distribution describing the relationship between the number and the speed of molecules (or kinetic energy).⁶⁹ Copyright Elsevier 2017. (C) Schematic diagram of using carbon capture and storage (CCS) as a heat sink. Amine selection chart respecting (D) the kinetics of absorption and heat of absorption⁷⁴ and (E) absorption and desorption parameters.¹³¹ Copyright ACS 2018–2019.

HCO₃⁻ through the reaction of CO₂ molecules with the hydroxyl groups of γ -Al₂O₃.

In 2018, Idem et al.⁹⁶ synthesized a hybrid solid acid catalyst by mixing γ -Al₂O₃ and HZSM-5 and, for the first time, studied the effect of basic sites of bifunctional catalysts on the enhanced CO₂ desorption (Figure 10A). Three different basic groups have been detected on the surface of γ -Al₂O₃/HZSM-5 bifunctional catalyst: weak, medium, and strong basic sites. They assigned the weak basicity of catalyst to the isolated O²⁻ anions and their ability to decompose the unidentate carbonate on the surface of bifunctional catalyst.¹²¹ The medium and strong basic sites were ascribed to the Al³⁺–O²⁻ pairs of the bifunctional catalyst and the decomposition of bridged bidentate carbonate. A simple comparison between γ -Al₂O₃, HZSM-5, and γ -Al₂O₃/HZSM-5 revealed that the addition of Al₂O₃ into the HZSM-5 can extend the crystal lattice and improve the medium, strong, and, subsequently, total basic sites of bifunctional catalyst. Consequently, the catalyst can simultaneously contribute to both amine deprotonation (using basic sites) and carbamate breakdown (using acidic sites) reactions with a superior catalytic efficiency in low-temperature solvent regeneration. One year later in 2019, Liang et al.⁹⁹ introduced Fe promoted SO₄²⁻/ZrO₂ supported on MCM-41 (denoted by SZMF) as a new acid–base bifunctional catalyst and investigated its catalytic CO₂ desorption mechanism (Figure 10B). According to the characterizations, all weak, medium, and strong basic sites were detected on the surface of SZMF catalyst. The weak and medium basic sites were mainly attributed to the primary surface OH⁻ groups and the O²⁻ anion in Fe³⁺–O²⁻/Zr⁴⁺–O²⁻ of

metal oxides (either ZrO₂ or Fe₂O₃), respectively.^{122,123} On the other hand, the strong basic sites of SZMF were related to the special position of O²⁻ anion in Zr⁴⁺–Fe³⁺–O²⁻ pairs mainly caused by the electron movement from Fe₂O₃ to ZrO₂.¹²⁴ Evidently, the presence of basic sites in the heterogeneous catalyst, as well as Lewis–Brønsted acid sites, can accelerate the recovery of spent acid catalyst and restore its protons by supplying a reliable proton backup to the spent catalyst from catalytic deprotonation of MEAH⁺. Just recently in 2020, Liang et al.¹⁰⁰ performed a similar study on the acid–base bifunctional role of different metal atoms (i.e., Fe, Al, and Mo) supported on MCM-41 and reported almost the same mechanism for basic sites of different metal atoms. In another study by Liang et al.,⁷⁰ the effects of acidic and basic sites of heterogeneous catalysts into a trisolvant mixture of MEA–MDEA–PZ were investigated (Figure 10C). However, they presented nearly the same reaction mechanism for catalytic CO₂ desorption of trisolvant amine mixtures with minor changes compared to those reported for MEA solution.

■ CO₂ DESORPTION BEHAVIOR OF NANOCATALYSTS

Effect of Amine Type in Single and Blended Solutions. According to the literature, the large quantity of required energy—which can account for up to 70–80% of the total operating cost of the CO₂ capture process—is the main barrier for the implementation of large-scale post-combustion CO₂ capture, especially chemical absorption systems.^{75,125,126} The heat duty of an aqueous amine solution is defined as^{127,128}

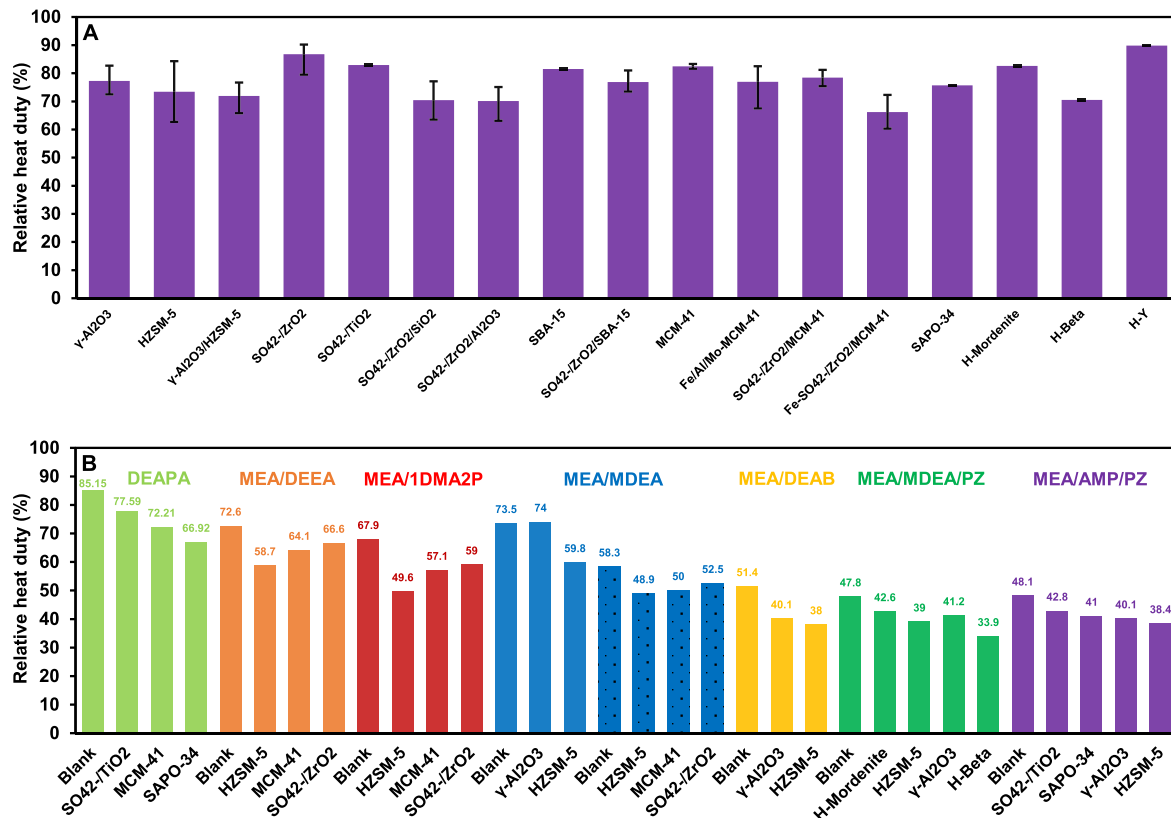


Figure 12. Effect of different heterogeneous catalysts used on the relative heat duty of (A) MEA and (B) tertiary amines and amine mixtures.

$$H = H_{\text{Des}} + H_{\text{Sen}} + H_{\text{Vap}} \quad (31)$$

H_{Des} is the desorption heat (or heat of reaction) and ideally equals the amount of required energy to breakdown amine–CO₂ bonds and release free CO₂ molecules. H_{Sen} is the sensible heat to increase the temperature of aqueous amine solution until its boiling point, and H_{Vap} is the amount of energy required for generating water vapor from liquid solution at its corresponding boiling point. As H_{Des} is used to detach CO₂ from amine molecules, it is primarily determined by amine type and its CO₂ absorption–desorption mechanism. Typically, primary and secondary amines have a high H_{Des} value mainly due to the carbamate formation reaction and difficult proton transfer from protonated amines to the aqueous solution. For 30 wt % MEA solution, as a benchmark for CO₂ absorption, a high H_{Des} value was reported by Oexmann et al.¹²⁹ around 50% of total regeneration heat duty. In contrast, tertiary amines have a low H_{Des} value owing to its bicarbonate production mechanism and the facile availability of protons into the solution. Although it has been widely reported that H_{Vap} is the main energy-intensive component (much higher than H_{Des} and H_{Sen}) for the CO₂ desorption process, the contribution of H_{Vap} is insignificant during low-temperature solvent regeneration (see Figure 11A).^{89,75} This is because the regeneration temperature is kept below the boiling point of aqueous amine solution and there is a negligible amount of solvent evaporation. Hence, many research investigations have been devoted to reducing H_{Sen} to ultimately decrease the total heat duty of the low-temperature solvent regeneration process.

Although tertiary amines have good energy efficiency, low corrosivity, and high CO₂ absorption capacity, the major challenge in CO₂ capture systems is that the tertiary amines typically have a poor kinetics of absorption. On the other hand,

primary amines, like MEA, have a high kinetics of CO₂ absorption but suffer from high corrosivity, medium CO₂ absorption capacity, and high regeneration heat duty.¹¹⁴ Therefore, blending a proper tertiary amine with MEA solution has been considered a method to compromise between the good CO₂ absorption characteristics, low H_{Des} , and regeneration heat duty.¹³⁰ To reach this goal, a wide variety of tertiary amines (e.g., MDEA, DEEA, DEAB, DEAPA, and 1DMA2P) have been blended with MEA to synthesize binary amine solutions. Nonetheless, increasing the temperature of blended amine solution to its boiling point temperature (sensible heat or H_{Sen}) and the necessity of low-pressure stream consumption has substantially limited the effective reduction of regeneration heat duty. This has potentially motivated researchers to adopt the combination of heterogeneous catalysts and blended amines as an innovative energy-efficient strategy for post-combustion CO₂ capture. According to Figure 11A, adding solid acid–base catalyst into the blended amine solutions not only can reduce H_{Sen} and lower the regeneration temperature by changing reaction pathways but also can pave the way to utilize low-grade steams or hot water streams for CO₂ capture. The role of solid acid catalysts in CO₂ desorption and its effect are well described by the Maxwell–Boltzmann distribution scheme (Figure 11B).

The relative heat duty (i.e., compared to the heat duty of blank 30 wt % MEA solution without adding catalyst) of aqueous 30 wt % MEA and blended amine solutions in the presence of 17 different heterogeneous catalysts is demonstrated in Figure 12. As seen, the average relative heat duty of MEA solutions in the presence of solid acid–base catalysts fluctuates from 66.2 to 89.8%, confirming the high efficiency of catalyst-aided solvent regeneration methodology (Figure 12A). On the other hand, a much less relative heat duty was recorded for binary and

Table 1. Surface Area, Total Pore Volume, and Average Pore Diameter of Different Used Heterogeneous Catalysts

catalyst	surface area (m^2/g)			total pore volume (cm^3/g)	average pore diameter (nm)	ref.
	micropore	mesopore	total			
$\gamma\text{-Al}_2\text{O}_3$	0	234.6	234.6	0.37	4.51	70, 96
$\gamma\text{-Al}_2\text{O}_3$	17.13	163.06	180.19	0.47	28.34	97
$\gamma\text{-Al}_2\text{O}_3$	1.3	137.9	139.2	0.83	23.88	133
$\gamma\text{-Al}_2\text{O}_3$			381.9486		4.55	69
$\gamma\text{-Al}_2\text{O}_3$		173.5	173.5		13.67	75
V_2O_5	0.321	2.3999	2.7209	0.3073	22.1	55
MoO_3	0.307	0.0008	0.3073	2.7209	16.2	55
TiO_2	1.9045	8.2287	10.1332	3.0945	14.1	55
TiO_2	102.3	169.3	271.6	0.25	3.7	133
Cr_2O_3	0.7962	2.2983	3.0945	10.1332	15.9	55
WO_3	0.0928	0.0906	0.1834	0.1834	13.4	55
Ag_2O			0.24		9.621	57
Ag_2CO_3			0.51		14.779	57
ZnO	1.020	4.471	5.491	0.0145		56
ZnO_2	0.943	3.477	4.420	0.0136		56
Nb_2O_5	0.5708	2.1662	2.737			48
NiO	0.0533	0.3295	0.3828			48
MnO_2	0.0189	0.0077	0.0266			48
CuO	0.0084	0.1449	0.1533			48
$\text{SO}_4^{2-}/\text{TiO}_2$		45.25	49.13	0.168	4.33	73–75
$\text{SO}_4^{2-}/\text{ZrO}_2$	2.25	72.53	74.78	0.1745	9.3357	82, 83
$\text{SO}_4^{2-}/\text{ZrO}_2$	24.09	34.80	58.89	0.17	7.17	97
$\text{SO}_4^{2-}/\text{ZrO}_2$			10.4	0.04	5.5	99
$\text{SO}_4^{2-}/\text{ZrO}_2$	13.01	52	65.1	0.08	18.23	98
$\text{Ce}(\text{SO}_4)_2/\text{ZrO}_2$	2	25	27	0.15	6.7	89
MCM-41	0	963.19	963.19	0.966	3.8783	74, 82, 83
MCM-41			1058.6	0.998	3.036	99, 100
SAPO-34		146.53	553.70	0.979	5.23	73–75
SBA-15		476.10		1.30	8.45	84
Fe–MCM-41 (5%)			959.8	0.872	2.944	100
Fe–MCM-41 (10%)			892.2	0.788	2.849	100
Fe–MCM-41 (15%)			867.0	0.758	2.836	100
Fe–MCM-41 (50%)			486.6	0.449	3.010	100
Mo–MCM-41 (50%)			36.1	0.011	2.836	100
Al–MCM-41 (50%)			173.6	0.138	2.648	100
$\text{SO}_4^{2-}/\text{ZrO}_2/\gamma\text{-Al}_2\text{O}_3$	12.76	111.49	124.25	0.29	10.60	97
$\text{SO}_4^{2-}/\text{ZrO}_2/\gamma\text{-Al}_2\text{O}_3$	12.34	115.87	128.21	0.33	12.24	97
$\text{SO}_4^{2-}/\text{ZrO}_2/\gamma\text{-Al}_2\text{O}_3$	7.07	158.98	166.05	0.46	14.39	97
Fe– $\text{SO}_4^{2-}/\text{ZrO}_2/\text{MCM-41}$ (5%)			382.5	0.3	5.9	99
Fe– $\text{SO}_4^{2-}/\text{ZrO}_2/\text{MCM-41}$ (10%)			424.9	0.5	5.0	99
Fe– $\text{SO}_4^{2-}/\text{ZrO}_2/\text{MCM-41}$ (15%)			458.7	0.5	5.0	99
$\text{SO}_4^{2-}/\text{ZrO}_2/\text{SBA-15}$		277.11		0.58	8.44	84
$\text{SO}_4^{2-}/\text{ZrO}_2/\text{SBA-15}$		266.45		0.30	3.63	84
$\text{SO}_4^{2-}/\text{ZrO}_2/\text{SBA-15}$		205.3		0.13	3.16	84
$\text{SO}_4^{2-}/\text{ZrO}_2/\text{SiO}_2$	22.39	105.51	127.9	0.17	3.93	98
$\text{SO}_4^{2-}/\text{ZrO}_2/\text{SiO}_2$	21.02	162.08	183.1	0.23	37.77	98
$\text{SO}_4^{2-}/\text{ZrO}_2/\text{SiO}_2$	25.21	364.22	389.43	0.44	23.86	98
$\text{SO}_4^{2-}/\text{ZrO}_2/\text{SiO}_2$	13.01	381.29	394.3	0.62	38.18	98
H-beta	405.1	129.4	534.5	0.413	7.18	70
H-mordenite	381.9	14.5	396.4	0.194	3.66	70
H-Y			615.4914		3.43	69
HZSM-5	128.4	151.56	279.97	0.2921	4.1732	75, 82, 83
HZSM-5	120	170	290	0.16	2.2	89
HZSM-5	101	181	282	0.17	2.2	89
HZSM-5	106	190	296	0.21	2.2	89
HZSM-5	114	188	302	0.22	2.2	89
HZSM-5	162.2	175.5	337.7	0.23	3.75	96
HZSM-5	153.2	16.4	169.6	0.19	4.42	133
HZSM-5			414.1020		3.12	69

Table 1. continued

catalyst	surface area (m^2/g)			total pore volume (cm^3/g)	average pore diameter (nm)	ref.
	micropore	mesopore	total			
HZSM-5	328.7	47.6	376.3		0.24	67
HZSM-5	201.4	163.3	364.7		0.34	67
HZSM-5	154.1	331.2	485.3		0.58	67
HZSM-5	115.7	328.7	444.4		0.91	67
$\gamma\text{-Al}_2\text{O}_3/\text{HZSM-5}$	65.0	235.2	300.2	0.26	4.03	96
$\gamma\text{-Al}_2\text{O}_3/\text{HZSM-5}$	96.1	230.9	327.0	0.39	4.54	96
$\gamma\text{-Al}_2\text{O}_3/\text{HZSM-5}$	44.8	240.8	285.6	0.31	4.46	96
$\gamma\text{-Al}_2\text{O}_3/\text{HZSM-5}$	16.3	265.0	281.3	0.38	4.60	96
$\gamma\text{-Al}_2\text{O}_3\text{-SiO}_2$			613.4463		5.21	69

trisolvent mixtures including primary and tertiary amines (Figure 12B). In the preparation of binary and trisolvent mixtures, choosing an appropriate type of amine blend to complement the properties of MEA amine is imperative. Hu et al.⁷⁴ presented an amine selection chart and displayed that DEAPA is much more favorable than MEA in terms of CO_2 desorption, while both have a nearly similar CO_2 absorption rate (Figure 11D). They reported that the relative heat duty of DEAPA without using any catalyst is 85.15% and further decreases up to 77.59, 72.21, and 66.92% in the presence of $\text{SO}_4^{2-}/\text{TiO}_2$, MCM-41, and SAPO-34 catalysts, respectively. Idem et al.⁸² studied the effect of HZSM-5, MCM-41, and $\text{SO}_4^{2-}/\text{ZrO}_2$ catalysts on the relative heat duty of MEA–DEEA and MEA–1DMA2P binary mixtures and revealed that only the presence of DEEA and 1DMA2P can decrease the relative heat duty of the binary mixture to 72.6 and 67.9%, respectively. As a consequence, adding solid acid catalyst into the solution exhibited a better performance in the MEA–1DMA2P mixture with much less relative heat duty. The best value was recorded for HZSM-5 catalyst with a relative heat duty of 49.6% for MEA–1DMA2P and 58.7% for MEA–DEEA. In two studies, Idem et al. reported 73.5 and 58.3% relative heat duties for blank MEA–MDEA solution (without using catalyst), which is related to the different concentrations of MDEA in the mixture.^{52,53,82} To the best of the authors' knowledge, the minimum relative heat duty among binary amine solutions without using any solid acid–base catalyst belongs to the MEA–DEAB mixture with a 51.4% value.^{52,53} Hereupon, the relative heat duty of blended MEA–DEAB solution decreased as low as 40.1 and 38.0 in the presence of $\gamma\text{-Al}_2\text{O}_3$ and HZSM-5 catalysts, respectively.

Recently, AMP has been investigated as one of the most intriguing amines with a fast kinetics of CO_2 absorption and desorption (see Figure 11E).¹³¹ For the first time in 2018, Liang et al.⁷⁵ investigated the effectiveness of heterogeneous catalysts in a MEA–AMP–PZ trisolvent amine blend. They recorded a 48.1% relative heat duty for the blank MEA–AMP–PZ solution, which confirms its superiority as a potential platform for further energy reduction. Addition measurements showed that adding $\text{SO}_4^{2-}/\text{TiO}_2$, SAPO-34, $\gamma\text{-Al}_2\text{O}_3$, and HZSM-5 catalysts into the MEA–AMP–PZ solution can achieve 42.8, 41.0, 40.1, and 38.4% relative heat duty, respectively. One year later in 2019, Liang et al.⁷⁰ used the positive feedback of their previous research project in 2017¹³² and used MEA–MDEA–PZ tribblend solvent with 47.8% relative heat duty as a base for further catalytic investigations. In this study, they only evaluated the role of three different zeolites and $\gamma\text{-Al}_2\text{O}_3$ catalysts and succeeded to reduce energy consumption in catalyst-aided tribblend solvent regeneration. They measured 42.6% relative heat duty for H-mordenite catalyst, 41.2% for $\gamma\text{-Al}_2\text{O}_3$, 39.0% for

HZSM-5, and 33.9% for H-beta as the minimum recorded relative heat duty to date. Although solid acid–base catalysts have displayed a top performance in tribblend amine solutions, this area is new and there are only two pieces of literature working on these energy-efficient catalyst tribblend amine solutions. Thus, future work needs to focus on the efficient combination of various amine types and its effects on the overall CO_2 desorption rate, the introduction of innovative heterogeneous catalysts with superior physicochemical characteristics, and the synergistic effect between solid acid–base catalysts and tribblend amine solvents.

Effect of Physical Properties. It is widely accepted that both physical and chemical (i.e., physicochemical) characteristics of the solid acid catalyst are likely to impact the CO_2 desorption performance during aqueous solvent regeneration. Hence, it is imperative to investigate the physicochemical properties of catalysts, find the most crucial parameters, and use them in the synthesis of more superior nanocatalysts in the future. According to the literature, three parameters can be highlighted as the most remarkable textural (or physical) properties of nanocatalysts: (i) mesopore surface area, (ii) total surface area, and (iii) average pore diameter. As Liang et al.^{70,73} reported, the micropore surface area of a nanocatalyst, with less than 2 nm pore width, is nearly inaccessible for large amine carbamate molecules. Conversely, the mesopore surface area, related to the pores with 2–50 nm width, has been identified as the best platform to provide active acidic–basic sites of catalysts for CO_2 -containing species (e.g., carbamate, carbonate, and bicarbonate) and protonated amines.¹⁰⁰ Recently, Xu et al.¹³³ found that the micropore surface area of catalysts can also be beneficial for the catalytic regeneration of ammonia solutions and nominated total surface area (micropore + mesopore), rather than the mesopore surface area only, as the influential physical characteristics. This different conclusion can be directly attributed to the small size of ammonia carbamate (NH_2COO^-) compared to the amine carbamates. Therefore, choosing the appropriate physical property of solid acid catalyst can be heavily reliant on the amine type.

In addition to the mesopore surface area of catalysts, it is crucially important to consider the contribution of the average pore diameter. The larger pore size of a solid acid catalyst can not only give better access to the interior surface of heterogeneous catalysts and expose a greater number of active acidic–basic sites to the CO_2 -containing species, but it can also reduce the mass transfer resistance for the diffusion of molecules through the porous structure of catalyst.^{134,135} This increases the reaction kinetics, enabling a faster carbamate breakdown resulting in a substantial energy reduction. Idem et al.⁸⁹ and Xu et al.¹³³ recently found that using solid catalysts with a large

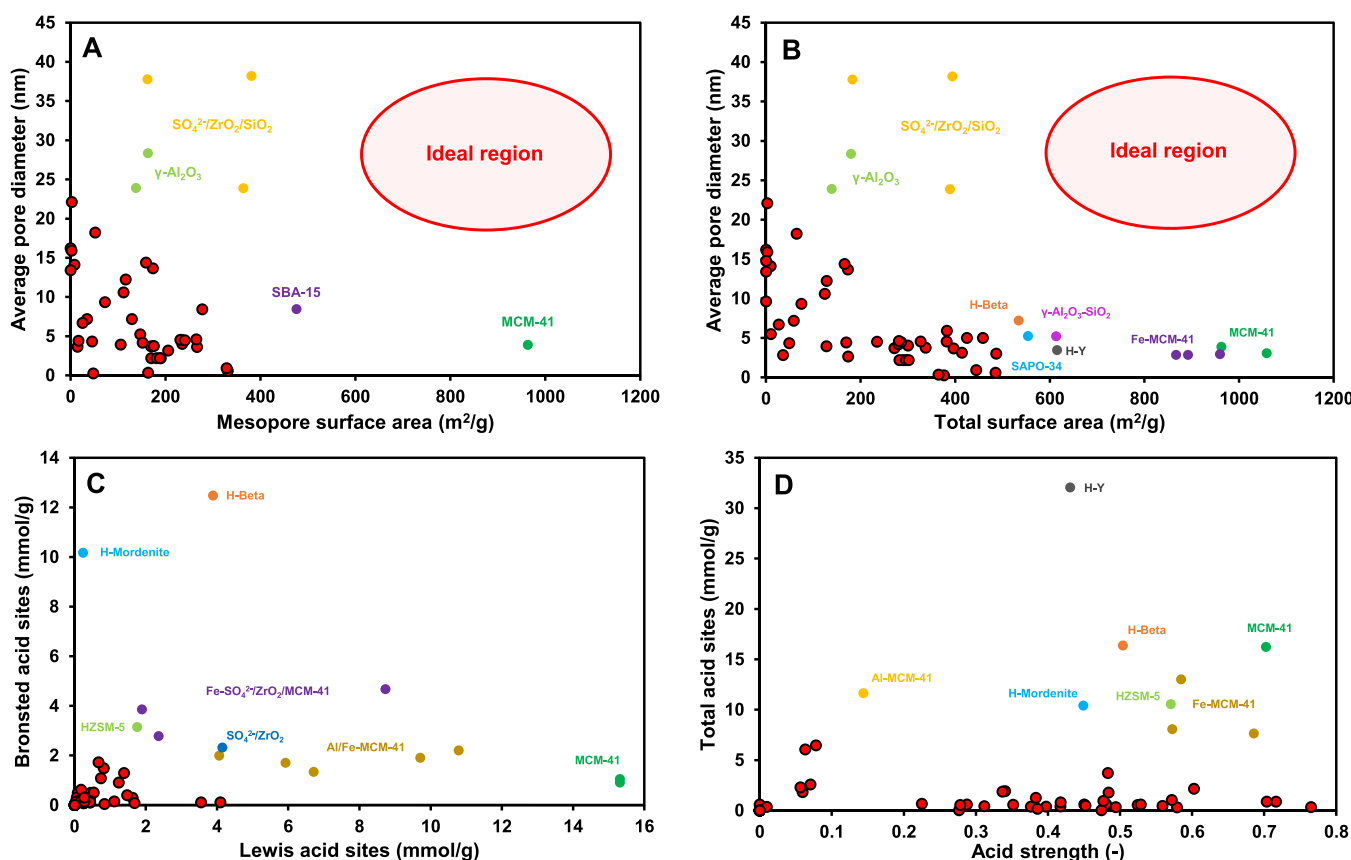


Figure 13. Relationship between (A) mesopore surface area and average pore diameter, (B) total surface area and average pore diameter, (C) Lewis and Bronsted acid sites, and (D) acid strength and total acid sites for different heterogeneous catalysts used for low-temperature CO_2 desorption.

pore diameter can appreciably avoid pore blockage by bulky carbamate molecules and maintain the catalytic efficiency of the catalyst at its initial value after several successive CO_2 absorption–desorption cycles.

The physical properties of all used heterogeneous catalysts are listed in Table 1. For convenience, the relationships between the total surface area, mesopore surface area, and average pore diameter belonging to the different heterogeneous catalysts used are depicted in Figure 13A,B. As is seen, $\gamma\text{-Al}_2\text{O}_3$ has been used for catalytic CO_2 desorption with a wide range of mesopore surface area ($137.9\text{--}234.6\text{ m}^2/\text{g}$), total surface area ($139.2\text{--}381.9\text{ m}^2/\text{g}$), and average pore width ($4.51\text{--}28.34\text{ nm}$). In contrast, all other metal oxides have displayed much inferior textural properties which can markedly diminish the catalytic performance of metal oxides in competition with other structures, like mesoporous silica materials and zeolites. Among different metal oxide nanocatalysts, TiO_2 can be selected as a distinguished catalyst with preferable textural properties. All zeolites have exhibited a high surface area which has made them an attractive material to be used as a solid acid catalyst. HZSM-5, as the most prevalent zeolite for catalytic CO_2 desorption, has $16.4\text{--}331.2\text{ m}^2/\text{g}$ mesopore surface area, $169.6\text{--}485.3\text{ m}^2/\text{g}$ total surface area, and $0.24\text{--}4.42\text{ nm}$ average pore width. As shown in Figure 13A and Table 1, although the mesoporosity of some synthetic HZSM-5 catalysts has been greatly improved by manipulating synthesis variables, typically the low mesoporosity and pore width can be underlined as the main drawback of HZSM-5 zeolites. A similar pattern can be identified for the textural properties of H-beta and H-Y zeolites. Both H-beta and H-Y zeolites take the advantages of having a

high surface area (Figure 13B) while suffering from a high microporosity and low pore diameter, which can seriously hinder the accessibility of CO_2 -containing species (e.g., carbamate molecules) to the active acid–base sites of catalyst and reduce the kinetics of CO_2 desorption.

Due to the critical role of mesopore surface area in the performance of solid acid catalysts during CO_2 regeneration, the mesoporous silica materials, particularly MCM-41 and SBA-15 with hierarchical structures, have gained considerable attention as a new generation of support and have paved the way for the synthesis of eminent heterogeneous catalysts. According to Figure 13A, the best recorded mesoporous surface area ($963.2\text{ m}^2/\text{g}$) and total surface area ($1058.6\text{ m}^2/\text{g}$) of the used catalyst for the catalytic CO_2 desorption process to date belong to MCM-41. Therefore, the metal modified MCM-41 catalysts, like Fe–MCM-41, still have a high mesopore and total surface area which are much greater than those of other solid acid catalysts. Nevertheless, the small pore diameter of mesoporous silica materials can be a limitation of this catalyst family. Contrastingly, a high average pore diameter has been recorded for mesoporous $\gamma\text{-Al}_2\text{O}_3$ and $\text{SO}_4^{2-}/\text{ZrO}_2/\text{SiO}_2$ catalysts up to 28.34 and 38.18 nm , respectively, while having a lower mesopore surface area than mesoporous silica catalysts.

In principle, a heterogeneous catalyst with a high mesopore surface area and large pore diameter is the best catalyst with the ideal physical properties for the regeneration of bulky carbamate molecules of primary and secondary amines. Notwithstanding, as presented in Figure 13A,B, all heterogeneous catalysts in the literature have been far from the ideal region. This apparently shows the necessity of further research in the area of catalyst-

Table 2. Acidic Properties of Different Employed Heterogeneous Catalysts

catalyst	acidity by strength (mmol/g)					acidity by type (mmol/g)				
	weak	medium	strong	total surface acidity	acid strength	LAS	BAS	total acid sites	B/L	ref.
γ -Al ₂ O ₃						3.55	0.11	3.66	0.031	133
γ -Al ₂ O ₃								3.57	0.67	75
γ -Al ₂ O ₃					0.4830			3.7174	0.667	68, 69, 136
γ -Al ₂ O ₃	1.229		0.743	1.972	0.3762	0.287	0.098	0.385	0.34	70, 96
γ -Al ₂ O ₃	0.354		0.894	1.248	0.7163	0.838	0.044	0.882	0.05	97
MoO ₃								0.821	0.32	55
V ₂ O ₅								0.698	0.49	55
Cr ₂ O ₃								0.618	0.013	55
TiO ₂								0.491	0.031	55
TiO ₂						1.39	1.29	2.68	0.93	133
WO ₃								0.423	0.024	55
SO ₄ ²⁻ /TiO ₂	0.712	0.567	1.185	2.464	0.4809	0.2097	0.4033	0.6130	1.92	73-75
SO ₄ ²⁻ /ZrO ₂	1.0008	0.4691	1.3263	2.7961	0.4743	0.0177	0.0103	0.0280	0.5834	82, 83
SO ₄ ²⁻ /ZrO ₂			0.1657			0.4313	0.3068	0.7381	0.71	88
SO ₄ ²⁻ /ZrO ₂			0.1986			0.3026	0.2335	0.5361	0.77	88
SO ₄ ²⁻ /ZrO ₂			0.1399			0.2531	0.0684	0.3215	0.27	88
SO ₄ ²⁻ /ZrO ₂	0.212		0.691	0.903	0.7652	0.091	0.231	0.322	2.53	98
SO ₄ ²⁻ /ZrO ₂	0.582		0.801	1.383	0.5791	0.073	0.228	0.301	3.12	97
SO ₄ ²⁻ /ZrO ₂						4.095	0.109	4.204	0.027	99
Ce(SO ₄) ₂ /ZrO ₂	75		178	253	0.7035	0.4485	0.4269	0.8754	0.952	89
MCM-41	0.3693	0.5772	0.3619	1.3084	0.2765	0.0110	0.0083	0.0193	0.075	74, 82, 83
MCM-41	0.029	0.128	0.369	0.525	0.7028	15.320	0.902	16.222	0.059	100
MCM-41						15.320	1.051	16.371	0.069	99
SAPO-34	0.905	1.072	0.125	2.102	0.059467	0.7406	1.0819	1.8225	1.46	73-75
SBA-15	0.0120	0.0030	0.0000	0.0150	0	0.09	0.49	0.58	5.40	84
Fe-MCM-41 (5%)	0.029	0.119	0.323	0.471	0.6857	5.926	1.699	7.625	0.287	100
Fe-MCM-41 (10%)	0.037	0.141	0.251	0.429	0.5850	10.787	2.205	12.992	0.204	100
Fe-MCM-41 (15%)	0.048	0.149	0.264	0.461	0.5726	6.718	1.338	8.056	0.199	100
Fe-MCM-41 (50%)	0.104		0.007	0.111	0.0630	4.065	1.987	6.052	0.489	100
Mo-MCM-41 (50%)	0.029		0.044	0.073	0.6027	1.241	0.907	2.148	0.731	100
Al-MCM-41 (50%)	0.790		0.133	0.923	0.1440	9.715	1.902	11.617	0.195	100
SO ₄ ²⁻ /ZrO ₂ /Al ₂ O ₃	1.149		0.942	2.091	0.4505	0.292	0.302	0.594	1.04	97
SO ₄ ²⁻ /ZrO ₂ /Al ₂ O ₃	1.441		0.951	2.392	0.3975	0.061	0.316	0.377	5.18	97
SO ₄ ²⁻ /ZrO ₂ /Al ₂ O ₃	1.212		1.105	2.317	0.4769	0.450	0.493	0.943	1.10	97
Fe-SO ₄ ²⁻ /ZrO ₂ /MCM-41 (5%)						2.365	2.781	5.146	1.176	99
Fe-SO ₄ ²⁻ /ZrO ₂ /MCM-41 (10%)						1.898	3.854	5.752	2.031	99
Fe-SO ₄ ²⁻ /ZrO ₂ /MCM-41 (15%)						8.736	4.666	13.402	0.534	99
SO ₄ ²⁻ /ZrO ₂ /SBA-15	1.0600	0.0240	0.0650	1.1490	0.056571	0.82	1.48	2.30	1.80	84
SO ₄ ²⁻ /ZrO ₂ /SBA-15	1.0890	0.0070	0.0830	1.1790	0.070399	0.67	1.72	2.57	2.57	84
SO ₄ ²⁻ /ZrO ₂ /SBA-15	1.1260	0.0680	0.1010	1.2950	0.077992	4.15	2.32	6.47	0.56	84
SO ₄ ²⁻ /ZrO ₂ /SiO ₂	0.572		0.631	1.203	0.5245	0.435	0.102	0.537	0.23	98
SO ₄ ²⁻ /ZrO ₂ /SiO ₂	0.601		0.762	1.363	0.5590	0.223	0.234	0.457	1.04	98
SO ₄ ²⁻ /ZrO ₂ /SiO ₂	0.732		0.821	1.553	0.5286	0.298	0.305	0.603	1.02	98
SO ₄ ²⁻ /ZrO ₂ /SiO ₂	1.04		1.401	2.450	0.5718	0.541	0.502	1.043	0.92	98
H-beta	1.211		1.231	2.442	0.5040	3.890	12.469	16.359	3.20	70
H-mordenite	0.842		0.687	1.529	0.4493	0.238	10.165	10.403	42.69	70
H-Y				0.431				32.0459	2.3	68
HZSM-5	0.80		0.66	1.46	0.4520	0.198	0.268	0.466	1.35	67
HZSM-5	0.89		0.63	1.51	0.4172	0.293	0.099	0.392	0.34	67
HZSM-5	1.1		0.44	1.53	0.2875	0.428	0.163	0.591	0.38	67
HZSM-5	1.53		0.59	2.12	0.2783	0.430	0.118	0.548	0.36	67
HZSM-5	0.4727	0.7082	0.0117	1.1927	0.0098	0.1389	0.2100	0.3489	1.51	82, 83
HZSM-5						1.76	3.14	4.9	1.79	133
HZSM-5								9.5	1.51	75
HZSM-5					0.5707			10.55	1.587	68, 69, 136
HZSM-5	0.346		0.217	0.563	0.3854	0.029	0.125	0.154	4.31	70, 96

Table 2. continued

catalyst	acidity by strength (mmol/g)					acidity by type (mmol/g)				
	weak	medium	strong	total surface acidity	acid strength	LAS	BAS	total acid sites	B/L	ref.
HZSM-5					0.3406	1.6308	0.2903	1.9211	0.178	89
HZSM-5					0.3367	1.4748	0.4007	1.8755	0.272	89
HZSM-5					0.3831	1.1151	0.1459	1.261	0.131	89
HZSM-5					0.4842	1.6850	0.0816	1.7666	0.048	89
γ -Al ₂ O ₃ /HZSM-5	0.664		0.648	1.312	0.4939	0.172	0.158	0.33	0.92	96
γ -Al ₂ O ₃ /HZSM-5	1.249		0.566	1.815	0.3118	0.278	0.137	0.415	0.49	96
γ -Al ₂ O ₃ /HZSM-5	1.159		0.831	1.990	0.4175	0.183	0.615	0.798	3.36	96
γ -Al ₂ O ₃ /HZSM-5	1.166		0.633	1.799	0.3518	0.269	0.302	0.571	1.12	96
SiO ₂ –Al ₂ O ₃					0.2250			0.6653	3.78	69, 136

aided solvent regeneration to introduce advanced nanomaterials and synthesize a heterogeneous catalyst with the maximum possible mesopore surface area and average pore diameter located in the ideal region.

Effect of Chemical Properties. Acidic Sites. As stated in the CO₂ desorption mechanism of aqueous amine solutions, the acid properties of heterogeneous catalysts—including Lewis and Brønsted acid sites—are likely to impact the effectiveness of solid acid catalysts in low-temperature amine solvent regeneration. Importantly, it has been experimentally proven that the role of active acid sites of the heterogeneous catalyst can be even more influential than that of the mesoporous surface area.^{55,56,67} For instance, Xu et al.¹³³ recently displayed that the overall CO₂ desorption rate increases nonlinearly with an increase in the number of Brønsted acid sites, while the physical properties have a lesser impact. Although this finding suggested that Brønsted acid sites have the highest impact on low-temperature solvent regeneration, some studies have also found a good relationship between total acid sites (i.e., the summation of Lewis and Brønsted acid sites) of the catalyst, the CO₂ desorption rate, and the energy reduction.^{48,55,56} In addition to the number of Lewis, Brønsted, and total acid sites, the acid strength of catalysts is another imperative parameter to consider; however, to date, limited attention has been paid to it. Acid strength is defined as the ratio of strong acid sites divided by the total surface acidity (i.e., the summation of weak, medium, and strong acid sites). Liang et al.⁹⁷ reported that by increasing the strong acid sites and acid strength in solid acid catalysts the CO₂ desorption rate increases. However, they also found in another literature work that weak acid sites may also have a positive influence on the performance of solid acid catalysts.⁹⁹

The acidic analysis of different catalysts is presented in Table 2. To better investigate the acidic properties of solid acid catalysts for energy-efficient solvent regeneration, the number of Lewis and Brønsted acid sites, total acid sites, and acid strength of each catalyst are plotted in Figure 13C,D. Figure 13C shows H-beta and H-mordenite zeolite have the best acidic properties with the maximum number of Brønsted acid sites of 12.47 and 10.16 mmol/g, respectively. In the next level, Fe promoted SO₄²⁻/ZrO₂/MCM-41 catalysts can be found with active Brønsted acid sites in the 2.78–4.66 mmol/g range and a high number of Lewis acid sites up to 8.73 mmol/g. This is due to two factors. First, MCM-41 has the highest number of Brønsted acid sites (15.32 mmol/g), which makes it a good candidate as a mesoporous-acidic support for the post-synthesis of solid acid catalysts. Second, metal modification of MCM-41 has substantially increased the number of Brønsted acid sites in Al/Fe–MCM-41 catalysts. Accordingly, the combination of

SO₄²⁻/ZrO₂ (as a predominant strong Brønsted acid catalyst) with Fe–MCM-41 catalyst in Fe–SO₄²⁻/ZrO₂/MCM-41 has resulted in the remarkable acidic properties. To further study the acidic characteristics of solid acid catalysts, the relationship between total acid sites and acid strength of solid acid catalysts is illustrated in Figure 13D. Again, zeolites displayed good acidic properties in H-Y, H-beta, HZSM-5, and H-mordenite order with 32.04, 16.36, 10.55, and 10.40 mmol/g total acid sites, respectively, and a moderate acid strength in the 0.43–0.57 range. Interestingly, MCM-41 possessed one of the highest acid strengths among the utilized solid acid catalysts in the literature. As a consequence, its metal modified derivatives all (except Al–MCM-41) had a high acid strength.

Basic Sites. Since the role of basic sites of catalysts and their drastic effect on the catalytic regeneration of aqueous amine solution was first shown in 2018, there are only a few published papers measuring the basic characteristics of heterogeneous catalysts and its effect on the CO₂ desorption rate and energy consumption (Table 3). The relationship between the number of basic, Brønsted acid, and total acid sites of utilized acidic–basic catalysts is depicted in Figure 14. According to Figure 14,

Table 3. Basic Properties of Different Employed Heterogeneous Catalysts

catalyst	basicity by strength (mmol/g)				ref.
	weak	medium	strong	total	
γ -Al ₂ O ₃	0.129	0.179	0.627	0.935	96
SO ₄ ²⁻ /ZrO ₂				0.533	98
Fe–MCM-41 (5%)	0.127	0.455	0.582	1.164	100
Fe–MCM-41 (10%)	0.056	0.398	0.454	0.908	100
Fe–MCM-41 (15%)	0.040	0.297	0.337	0.674	100
Fe–MCM-41 (50%)	0.046	0.086	0.132	0.264	100
Mo–MCM-41 (50%)	0.010	0.046	0.056	0.112	100
Al–MCM-41 (50%)	0.010	0.515	0.525	1.05	100
SO ₄ ²⁻ /ZrO ₂ /SBA-15	0.4550		0.2490	0.7040	84
SO ₄ ²⁻ /ZrO ₂ /SBA-15	0.5270		0.2490	0.7760	84
SO ₄ ²⁻ /ZrO ₂ /SBA-15	0.5330		0.4610	0.9940	84
SO ₄ ²⁻ /ZrO ₂ /SiO ₂				0.811	98
SO ₄ ²⁻ /ZrO ₂ /SiO ₂				0.873	98
SO ₄ ²⁻ /ZrO ₂ /SiO ₂				0.909	98
SO ₄ ²⁻ /ZrO ₂ /SiO ₂				1.06	98
HZSM-5	0.113	0	0.051	0.164	96
γ -Al ₂ O ₃ /HZSM-5	0.104	0.088	0.241	0.532	96
γ -Al ₂ O ₃ /HZSM-5	0.038	0.143	0.420	0.601	96
γ -Al ₂ O ₃ /HZSM-5	0.078	0.227	0.745	1.050	96
γ -Al ₂ O ₃ /HZSM-5	0.068	0.099	0.497	0.664	96

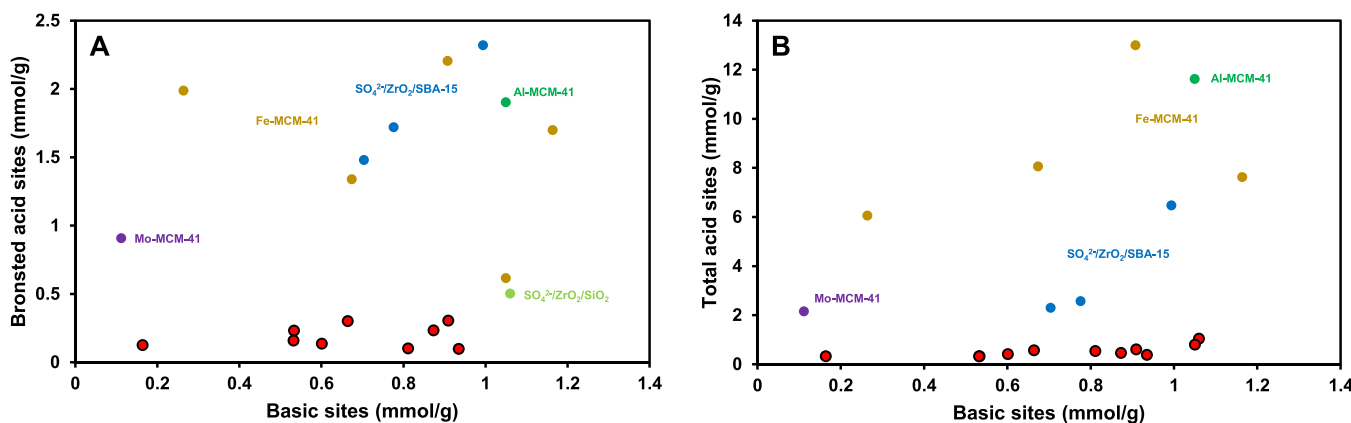


Figure 14. Relationship between (A) basic and Bronsted acid sites and (B) basic and total acid sites for different heterogeneous catalysts used for low-temperature CO₂ desorption.

Al and Fe modified MCM-41 catalysts as well as the hybrid structures of SO₄²⁻/ZrO₂ supported on SiO₂ and SBA-15 have the highest number of basic sites. Nevertheless, SO₄²⁻/ZrO₂/SiO₂ catalysts have a limited number of Brønsted acid sites which can negatively affect their catalytic performance. Regarding the total acid sites (Figure 14B), the same solid acidic–basic catalysts (SO₄²⁻/ZrO₂/SiO₂ and SO₄²⁻/ZrO₂/SBA-15) appeared as the promising catalysts which can disclose the close affinity between basic and Brønsted acid sites in heterogenous catalysts.

Liang et al.^{96,98–100} reported they could not find any linear relationship between the basic sites of catalysts and the kinetics of CO₂ desorption, though it was noticed that the increasing number of basic sites can markedly enhance the catalytic performance. The samples with the best CO₂ desorption performance all had a significant number of basic sites. Based on the results, it can be speculated that basic sites play a dominant role in conjunction with Brønsted acid sites and further explorations are required to determine the role of basic sites and reasonably synthesize better heterogeneous catalysts in the future.

Effect of Physicochemical Properties. Neither physical nor chemical characteristics of a catalyst are independently responsible for the catalyst-aided CO₂ desorption performance. For this reason, the impact of physical and chemical factors is merged in physicochemical dual parameters, like the product of mesopore surface area and Brønsted acid sites (i.e., MSA × BAS), mesopore surface area and total acid sites (i.e., MSA × TAS), mesopore surface area and the ratio of Brønsted to Lewis acid sites (i.e., MSA × B/L), mesopore surface area and total surface acidity (i.e., MSA × TSA), Brønsted acid sites and pore size (i.e., BAS × PS), and mesopore surface area and basic sites (i.e., MSA × BS), to correlate the catalytic CO₂ desorption rate and energy reduction during catalyst-aided solvent regeneration processes.

Bhatti et al.⁶⁷ recently presented a post-treatment methodology to improve the key physicochemical parameters of HZSM-5 and studied the influence of these parameters on the catalytic solvent regeneration performance. In order to comprehend the mechanism of catalytic CO₂ desorption, they evaluated both single (i.e., TSA and TAS) and dual variables (i.e., MSA × TSA, MSA × BAS, and MSA × TAS). They reported that an increase in TSA, MSA × TSA, and MSA × BAS of catalysts can improve the overall kinetics of CO₂ desorption and decrease energy consumption. However, a nonlinear behavior was observed and

some catalysts with a higher TSA, MSA × TSA, and MSA × BAS displayed a lesser CO₂ desorption efficiency. On the other hand, they reported a linear relationship between TAS and the overall CO₂ desorption. In detail, the Brønsted acid sites are useful at high concentrations of CO₂-containing species in the beginning of the solvent regeneration process, while Lewis acid sites are more effective at the end of the solvent regeneration process when low concentrations of CO₂-containing species are remaining in the solution. Thereby, the overall CO₂ desorption in the whole period of the regeneration process can be dependent on LAS and BAS summation (i.e., TAS). In a more comprehensive study, Zhang et al.⁷⁴ expanded this methodology and utilized MSA × TAS as the corresponding influential parameter for the enhancement of catalytic CO₂ desorption rate.

Idem et al.^{69,136} considered TAS × B/L as the influential parameter describing solid acid catalysts for low-temperature CO₂ desorption. They discussed that the B/L ratio is primarily responsible for the catalyzed CO₂ desorption routes, deciding the proportion of Brønsted acid sites in the catalyst and determining the predominant mechanism (i.e., carbamate breakdown or amine deprotonation reaction). However, the acid strength of a catalyst defines the degree of CO₂ desorption, particularly at low temperatures where kinetic mobility of CO₂-containing species is heavily limited and carbamate breakdown and/or amine deprotonation reaction is reliant on the strength of the active sites. In other research studies, they found the effectiveness of MSA × B/L and used it to explain the poor/superior performance of different solid acid catalysts.^{68,82} For instance, MCM-41 and SO₄²⁻/ZrO₂ solid acid catalysts have a relatively low B/L ratio and mesopore surface area, respectively, leading to a poor catalytic performance. Opposingly, the high B/L ratio and mesopore surface area in HZSM-5 catalysts result in a good CO₂ desorption performance in aqueous amine (primary or tertiary) solutions. This methodology was also followed by Liang et al.,^{73,83,99} and MSA × B/L was employed to justify the efficiency of different catalyst samples. They also used MSA × BAS and MSA × acid strength as the predominant factor to anticipate the CO₂ desorption rate and energy reduction of catalyst-aided solvent regeneration in their later publications.^{75,84,97} Recently, Liang et al.⁷⁰ found that MSA, BAS, and the acid strength of the catalyst have a beneficial role in kinetics of CO₂ desorption and applied BAS × MSA × TAS as a more comprehensive variable to explain the superior CO₂ desorption rate of H-beta solid acid catalyst.

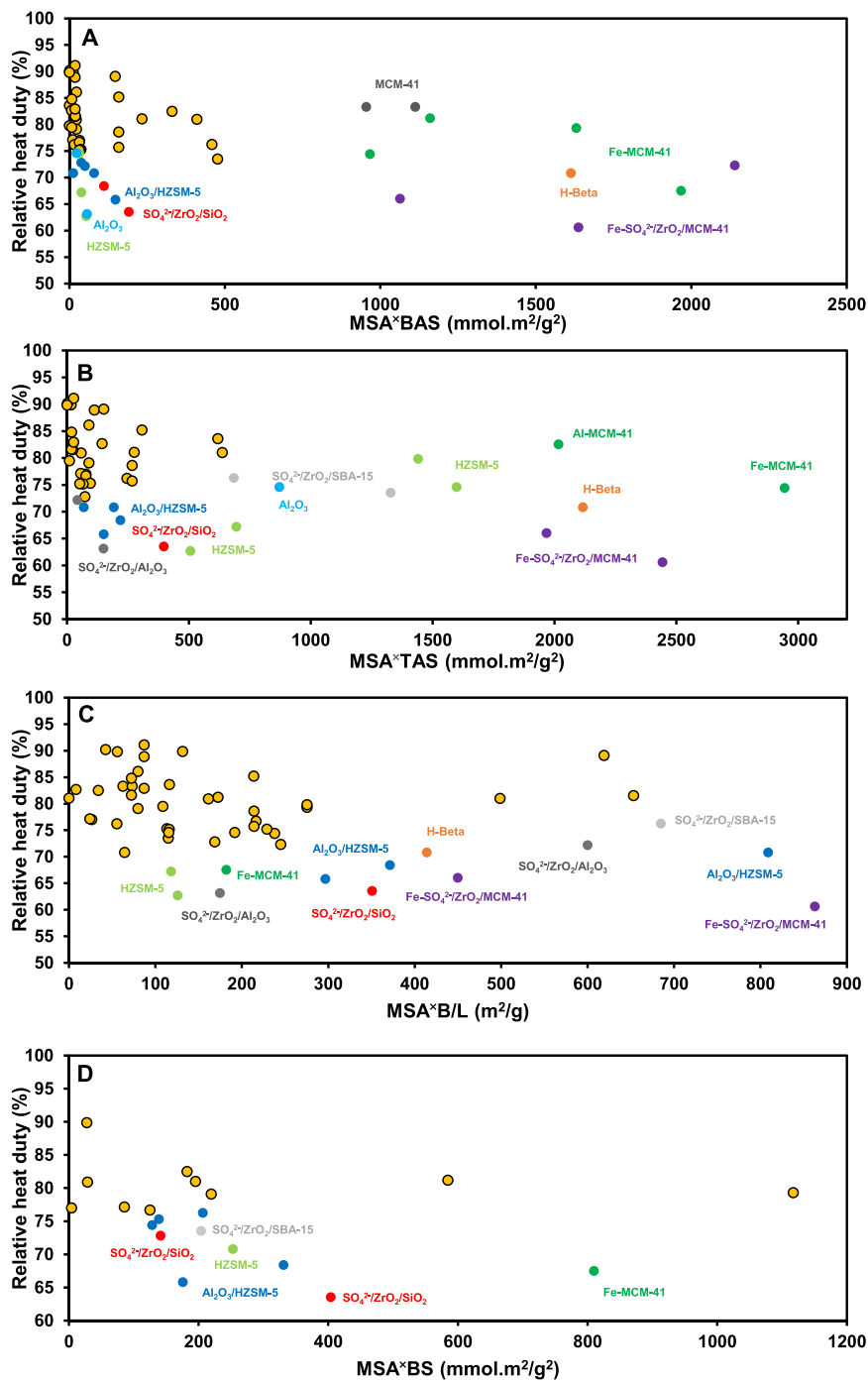


Figure 15. Effect of physicochemical properties of catalysts on the relative heat duty. (A) Mesopore surface area (MSA) and Bronsted acid sites (BAS). (B) Mesopore surface area (MSA) and total acid sites (TAS). (C) Mesopore surface area (MSA) and Bronsted to Lewis acid ratio (B/L). (D) Mesopore surface area (MSA) and Bronsted to basic sites (BS).

In addition to the previous dual physicochemical parameters, Idem et al.^{89,96} declared a good fit and compatibility between the CO₂ desorption rate, BAS × PS, and BAS × BS of heterogeneous catalysts. However, these physicochemical parameters have not been commonly used in the literature. Obviously, using different physicochemical characteristics in various studies implies that solid acid catalysts behave in different ways which are influenced by different physicochemical properties. Thus, a unique parameter has not been found to date predicting the CO₂ desorption performance of all solid acid catalysts from various

material groups and further research investigation is required in the future.

To test the validity of prevalent physicochemical parameters, the relative heat duty of solid acid–base catalysts versus MSA × BAS, MSA × TAS, MSA × B/L, and MSA × BS is presented in Figure 15. As shown, there is a nonlinear trend between various physicochemical parameters and relative energy consumption. The lowest recorded relative heat duty of 60.6% resulted after using Fe–SO₄²⁻/ZrO₂/MCM-41 catalyst with an extra high MSA × BAS, MSA × TAS, and MSA × B/L which justifies its best performance.⁹⁹ In the following, HZSM-5,⁶⁷ SO₄²⁻/ZrO₂/

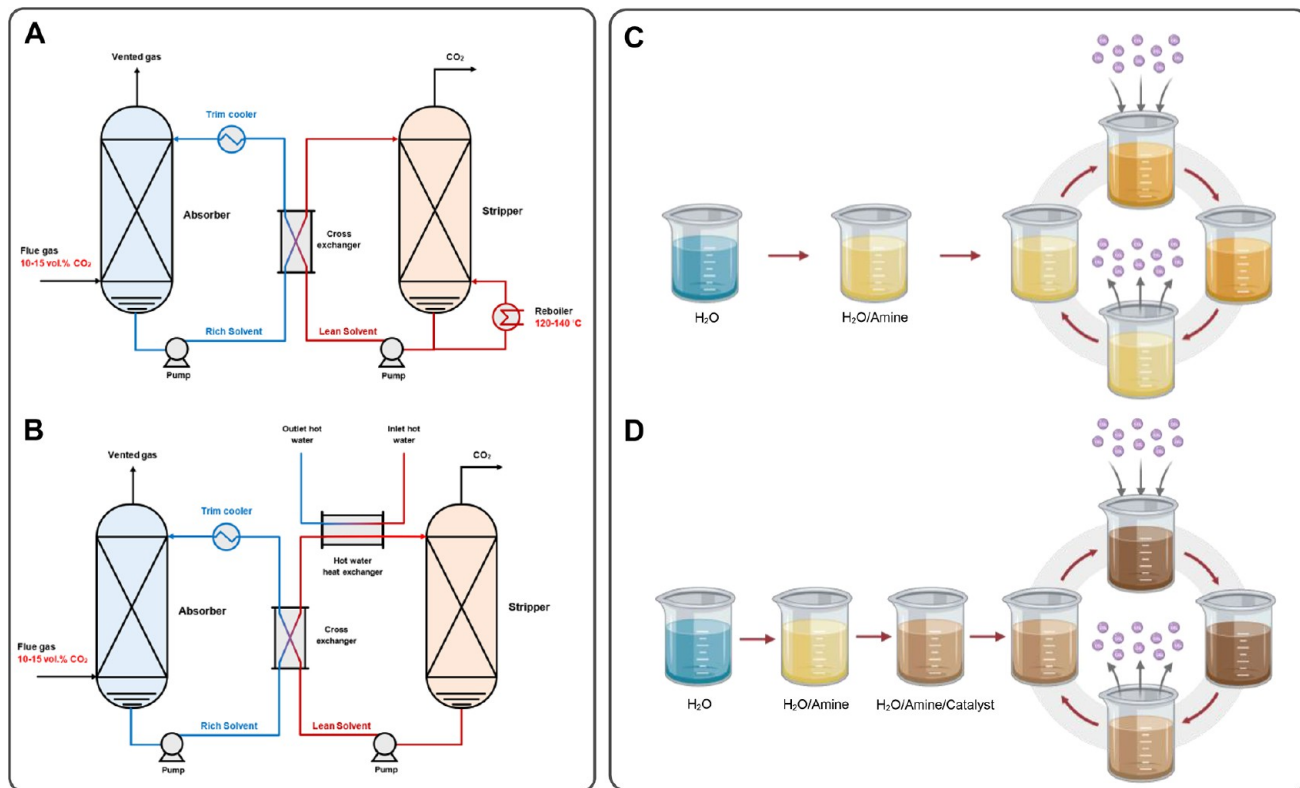


Figure 16. Process flow diagram of the (A) typical bench-scale CO₂ capture process with a reboiler in the bottom of the regeneration column and (B) catalyst-aided bench-scale CO₂ capture process unit with an extra heat exchanger. The schematic diagram of the solvent preparation and cyclic CO₂ absorption–desorption of (C) typical amine solutions and (D) amine solution in the presence of heterogeneous catalysts.

Al₂O₃,⁹⁷ and SO₄²⁻/ZrO₂/SiO₂,⁹⁸ catalysts with 62.7, 63.13, and 63.52% relative heat duty, respectively, exhibited the best catalytic performance after the Fe–SO₄²⁻/ZrO₂/MCM-41 catalyst. Figure 15 shows it is not reasonable to justify the superiority of these catalysts using any of the presented physicochemical characteristics (i.e., MSA × BAS, MSA × TAS, MSA × B/L, and MSA × BS). This inconsistency may be related to the different measurement methods, accuracy of measurement apparatuses, variation of regeneration temperature (i.e., 85–105 °C) and regeneration time (i.e., 60–180 min), nature of catalysts, their particle/crystal size, and concentration. However, all HZSM-5, SO₄²⁻/ZrO₂/Al₂O₃, and SO₄²⁻/ZrO₂/SiO₂ catalysts benefit from a significant number of Brønsted acid sites, acid strength, and basic sites which may make them prominent compared to the others.

CONCLUSION

The intensive energy penalty and high operating cost of amine-based CO₂ capture technologies are unanimously considered as the most crucial obstacle facing its widespread large-scale implementation in various industries. Despite significant efforts to review energy-efficient CO₂ capture technologies (e.g., advanced additives and phase change solvents) and process optimization, a comprehensive review on the recently emerged catalytic CO₂ absorption–desorption technology is lacking and highly needed. The addition of solid acid–base catalyst into aqueous amine solutions can effectively alter reaction pathways, enhance CO₂ desorption rates at low-temperature regeneration operation, and reduce energy consumption. For the first time, this review comprehensively sets out the recent progress on catalyst-aided CO₂ desorption technology and evaluated the

available heterogeneous catalysts, enhancement mechanisms, and effective parameters.

In a typical solvent regeneration process, the CO₂ desorption is undertaken at the boiling point of aqueous amine solvent in the 120–140 °C range (Figure 16A and C). To supply this level of energy, high-quality steam is required, which remarkably increases the operating cost of CO₂ capture processes. In catalyst-aided solvent regeneration, the CO₂ desorption process is performed at a temperature below the boiling temperature of the solvent which is typically around 85–98 °C. The benefit of catalytic solvent regeneration is twofold. First, adding catalyst significantly accelerates the CO₂ desorption mechanism, shortens the regeneration time, and decreases energy consumption. Second, low-temperature regeneration operation markedly reduces both sensible and vaporization heat, resulting in a lower energy consumption and operating cost. However, the heat of reaction remains constant in catalytic solvent regeneration, since the presence of the catalyst does not change the thermodynamics of a system. The low operating temperature can reduce corrosion and solvent degradation rate and mitigate one of the other major challenges of CO₂ absorption processes. This technology aims to replace high-pressure steam with hot water as a reliable source of energy for catalytic post-combustion CO₂ capture (Figure 16B and D). Furthermore, a liquid–liquid heat exchanger can be used instead of a gas–liquid reboiler with a higher efficiency, smaller size, and lower capital cost. More importantly, the low-temperature regeneration operation has raised some promises to utilize solar hot water as the main renewable supply of heat for solvent regeneration or act as the cooling tower to recycle the waste heat streams of energy power plants (Figure 11C).

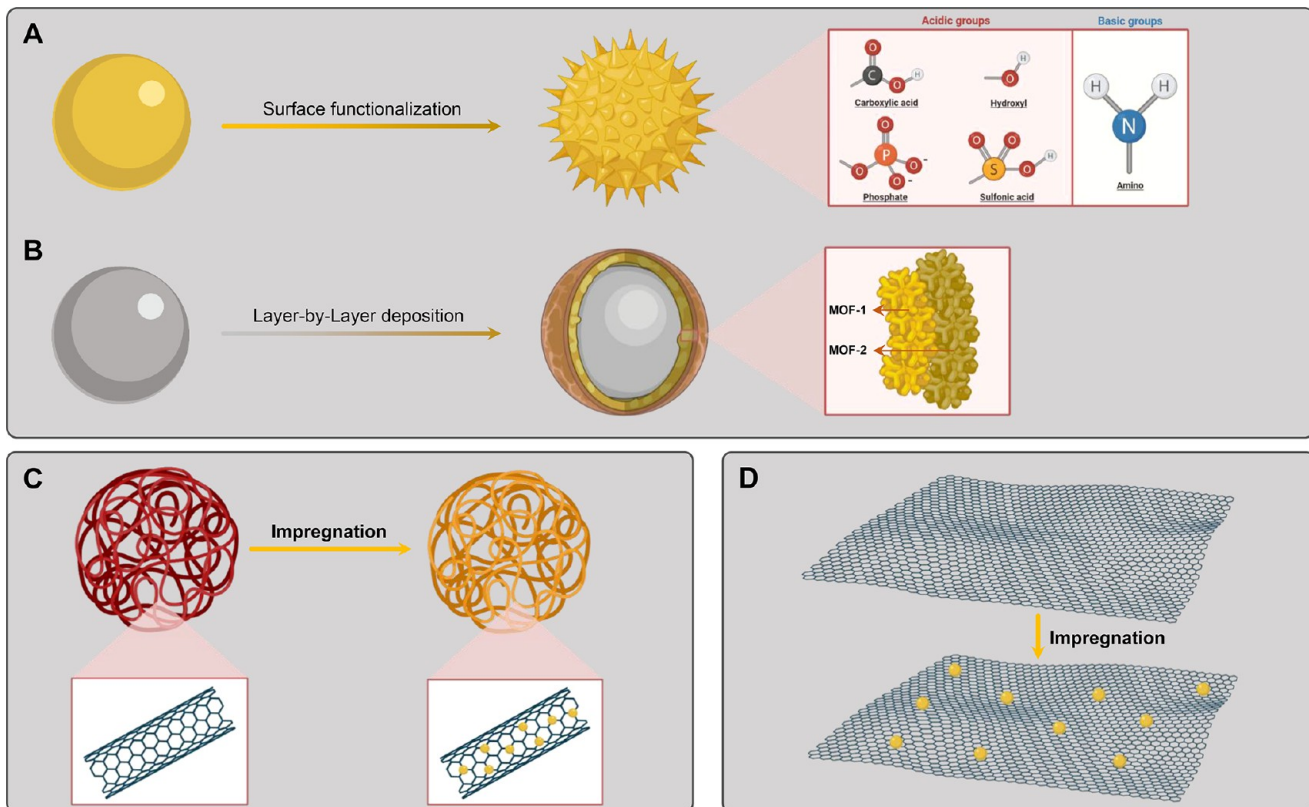


Figure 17. Suggested directions for future research studies to develop highly efficient heterogeneous catalysts for low-temperature CO_2 desorption processes. (A) Surface modification of metal oxide nanocatalysts with different acidic and basic functional groups. (B) Layer-by-layer deposition of metal–organic frameworks (MOFs) on the surface of metal oxide nanocatalysts in order to prepare a core–shell structure with catalytic behavior. Carbon-based structures, like (C) carbon nanotubes (CNTs) and (D) graphene sheets, were used as a superior support for the dispersion of nanocatalysts.

FUTURE PERSPECTIVES

Herein, some practical insights have been provided for developing advanced nanocatalysts to inspire a greater number of research studies in the foreseeable future. Several catalytic enhancement mechanisms have been proposed focusing on physicochemical characteristics of catalysts. However, the current understanding on the role of basic active sites and their reaction mechanism is still under development due to the novelty of this area. There is also no consensus on the most effective physicochemical parameter across the various research studies, and further investigation is required. The acquisition of heat duty information (i.e., heat of reaction and sensible and latent heat) for catalytic solvent regeneration processes has been widely neglected. In addition, the physical properties, especially density and viscosity data, of aqueous amine solution are necessary to be considered in the future along with the physicochemical properties of catalyst. From physical perspectives, solvent viscosity plays an important role in determining mass transfer coefficients and the overall catalytic efficiency. Therefore, the systematic evaluation of viscosity data for different catalyst–amine solutions is indispensable and can further broaden our understanding of catalytic CO_2 desorption performance. A great part of the heterogeneous catalyst family belongs to the old-fashioned commercial catalysts. Research studies working on catalytic solvent regeneration and enhanced low-temperature CO_2 desorption are needed to synthesize and develop new advanced nanomaterials to take this technology one step further toward large-scale utilization. Despite the various solid acid catalysts used for regeneration processes, the

lack of advanced nanomaterials is a challenge for the progress of catalyst-aided solvent regeneration into the future. It is suggested that using novel materials like metal–organic frameworks (MOFs), heteroatom doped carbon-based materials, bimetallic nanoparticles, and single-atom catalysts should greatly improve the kinetics of CO_2 desorption and reduce low-temperature energy consumption.

The technical and economic feasibility of CO_2 absorption technologies with typical aqueous amine solutions has been completely investigated for PCC application in laboratory, bench, and small pilot scales. Nonetheless, there are only two commercialized large-scale CO_2 absorption units using aqueous amine solutions to remove 90% of CO_2 from the flue gas stream: (i) the first one has been located in Boundary Dam coal-fired power plant (Canada, 160 MW) and (ii) another one in Petra Nova power plant (USA, 240 MW).^{14,45} Contrarily, the majority of catalytic solvent regeneration technologies have only been tested at small scales (bench or laboratory scale). Only the Idem group at the University of Regina has succeeded in testing the performance of heterogeneous catalysts at a small pilot scale. This is because catalytic solvent regeneration is a recent research area and further investigations need to be conducted to successfully scale up the application of catalysts in energy-efficient CO_2 absorption units. Hence, future studies need to quantitatively evaluate the techno-economic feasibility of heterogeneous catalysts and their potential for large-scale implementation.

The current procedure for using heterogeneous catalysts in amine solutions is quite straightforward. However, nearly all

utilized heterogeneous catalysts have a short stability in aqueous solution. Future works will likely focus on the use of more efficient metal oxide nanoparticles with a long-term stability and reusable nanocatalyst for the preparation of amine-based nanofluid for energy-efficient CO₂ capture. From the perspective of process design, using stable nanocatalyst-based nanofluids can not only accelerate the CO₂ absorption–desorption rate by promoting both physical and chemical mechanisms, but they are also thoroughly compatible with the current physical infrastructure of CO₂ absorption–desorption columns. On the other hand, the development of heterogeneous catalyst-aided CO₂ capture necessitates the installation of catalyst beds within the regeneration column, which might put a serious question mark on the viability of this technology. Nanocatalyst surface modification by tailoring surface functional group coatings should be another focus area in the future to further tune the stability, dispersibility, surface charge, and reactivity of nanocatalysts (Figure 17A). The layer-by-layer deposition of MOFs on the external surface of metal oxide nanoparticles is another viable option which should be carefully considered in future studies (Figure 17B). The core–shell structure can easily benefit from the catalytic properties of layered MOFs with superior textural properties and active metal sites, as well as the improved heat and mass transfer coefficients due to the presence of nanoparticles in the amine solution.

It is recommended to use carbon-based supports to improve the long-term stability and avoid nanocatalyst aggregation. Recently, carbon nanotube (CNT) and graphene nanosheets have been of great scientific interest as the new generation of support in the area of catalysis. Because of the high dispersibility of carbon-based nanostructures in solution, they can be added into the operating amine solutions without any change or modification in the operating CO₂ regeneration columns. In addition to providing a high dispersibility, carbon-based supports can act in positive synergy with impregnated metal atoms of nanocatalyst and take one step further toward theoretical minimum energy consumption in amine regeneration reactions (Figure 17C,D). Molecular modeling like density functional theory (DFT), molecular dynamics (MD), and Monte Carlo (MC) simulation can be a powerful computational tool revealing valuable information to synthesize a better solid acid catalyst. Generally, simulations can play a key role in the fundamental understanding of reaction pathways and the effect of solid acid–base catalysts on CO₂ desorption mechanisms.

AUTHOR INFORMATION

Corresponding Author

Kathryn A. Mumford — Department of Chemical Engineering and Peter Cook Centre for CCS Research, The University of Melbourne, Parkville, Victoria 3010, Australia;  orcid.org/0000-0002-7056-5600; Email: mumfordk@unimelb.edu.au; Fax: +61 3 83444153

Authors

Masood S. Alivand — Department of Chemical Engineering and Peter Cook Centre for CCS Research, The University of Melbourne, Parkville, Victoria 3010, Australia

Omid Mazaheri — Department of Chemical Engineering and School of Agriculture and Food, Faculty of Veterinary and Agricultural Sciences, The University of Melbourne, Parkville, Victoria 3010, Australia;  orcid.org/0000-0002-9749-9842

Yue Wu — Department of Chemical Engineering and Peter Cook Centre for CCS Research, The University of Melbourne, Parkville, Victoria 3010, Australia

Geoffrey W. Stevens — Department of Chemical Engineering and Peter Cook Centre for CCS Research, The University of Melbourne, Parkville, Victoria 3010, Australia;  orcid.org/0000-0002-5788-4682

Colin A. Scholes — Department of Chemical Engineering and Peter Cook Centre for CCS Research, The University of Melbourne, Parkville, Victoria 3010, Australia;  orcid.org/0000-0002-3810-2251

Complete contact information is available at:
<https://pubs.acs.org/10.1021/acssuschemeng.0c07066>

Notes

The authors declare no competing financial interest.

Biographies

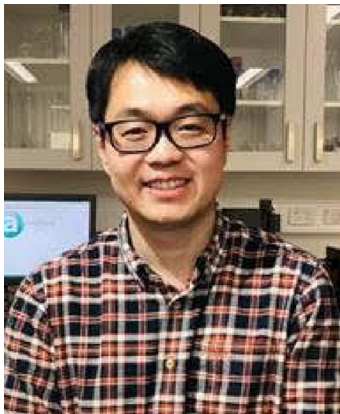


Masood S. Alivand is a Ph.D. student under the supervision of Kathryn A. Mumford at Department of Chemical Engineering, The University of Melbourne, Australia. He has a wide range of research-based experiences regarding advanced nanomaterials and their application for energy-efficient separation and purification technologies. He is currently focused on novel catalytic nanoparticles for energy-efficient CO₂ capture with a low solvent regeneration temperature. The technology that he is developing can pave the way for achieving sustainable energy development and taking a further step toward Paris Climate Accord objectives.



Omid Mazaheri received his B.S. degree in Applied Chemistry from Islamic Azad University (Iran) in 2010 and M.Sc. degree in Organic Chemistry at the same university in 2013 studied on the synthesis of solid acid catalysts (i.e., hierarchical zeolites, functionalized mesoporous silica, and mesoporous carbon and polymers). He then worked as a researcher at different universities and companies where he

specialized in heterogeneous acid-metal bifunctional catalysts and nanocomposites and their applications in organic reactions and heavy metal removal from water and soil. He is currently undertaking his Ph.D. under Assoc. Prof. Helen C. Suter, Assoc. Prof. Kathryn A. Mumford, and Prof. Deli Chen supervisions at the University of Melbourne. His thesis focuses on biocompatible materials development for advanced fertilizer technology to enhance the efficiency of fertilizers by controlling the release rate of nutrients in soil.



Yue Wu is a research fellow at Department of Chemical Engineering, The University of Melbourne, Australia. His research focuses on advanced liquid-based separation process technologies and simulation, including vapor–liquid CO₂ capture processes, liquid–liquid solvent extraction for metal and natural active pharmaceutical ingredients, and liquid–solid crystallization processes for valuable metal compounds manufacture.



Geoffrey W. Stevens is a Laureate Professor in the Department of Chemical and Biomolecular Engineering at The University of Melbourne and is one of Australia's leading Engineers. He has published over 380 peer reviewed publications and is recognized internationally for his work in separations technology in particular solvent extraction and in the development of novel hydrometallurgical processes and equipment and natural product separations for the pharmaceutical industry. He has led the development of solvent technology for CO₂ capture from flue gases from power stations in Australia and in the soil remediation area, particularly in cold regions such as Antarctica.



Colin A. Scholes CChem FRACI CEng MICHEM E is a Senior Lecturer in the Department of Chemical Engineering at the University of Melbourne. He is an expert in clean energy processing and membrane science, particularly developing strategies to assist the transition to a low carbon future. He most recently developed novel membrane-solvent absorption technology for CO₂ capture, which has been commercially demonstrated at the pilot plant level in three different industrial processes, which is currently in the process of being commercialized.



Kathryn A. Mumford is currently an Associate Professor in the Department of Chemical Engineering at the University of Melbourne. Her research interests are in the areas of separations processes, specifically solvent absorption, solvent extraction and ion exchange technologies. These interests range from the manufacture of novel materials to the development of novel thermodynamic models to predict performance and onto large scale implementation in the mining, energy, environmental, and wastewater processing fields.

■ REFERENCES

- (1) Sheikh Alivand, M.; Hosseini Tehrani, N. H. M.; Shafiei-alavijeh, M.; Rashidi, A.; Kooti, M.; Pourreza, A.; Fakhraie, S. Synthesis of a modified HF-free MIL-101(Cr) nanoadsorbent with enhanced H₂S/CH₄, CO₂/CH₄, and CO₂/N₂ selectivity. *J. Environ. Chem. Eng.* **2019**, *7* (2), 102946.
- (2) D'Alessandro, D. M.; Smit, B.; Long, J. R. Carbon Dioxide Capture: Prospects for New Materials. *Angew. Chem., Int. Ed.* **2010**, *49* (35), 6058–6082.
- (3) Sheikh Alivand, M.; Farhadi, F. Multi-objective optimization of a multi-layer PTSA for LNG production. *J. Nat. Gas Sci. Eng.* **2018**, *49*, 435–446.
- (4) Hu, G.; Nicholas, N. J.; Smith, K. H.; Mumford, K. A.; Kentish, S. E.; Stevens, G. W. Carbon dioxide absorption into promoted potassium carbonate solutions: A review. *Int. J. Greenhouse Gas Control* **2016**, *53*, 28–40.

- (5) Saha, D.; Van Bramer, S. E.; Orkoulas, G.; Ho, H.-C.; Chen, J.; Henley, D. K. CO₂ capture in lignin-derived and nitrogen-doped hierarchical porous carbons. *Carbon* **2017**, *121*, 257–266.
- (6) Zhang, P.; Zhong, Y.; Ding, J.; Wang, J.; Xu, M.; Deng, Q.; Zeng, Z.; Deng, S. A new choice of polymer precursor for solvent-free method: Preparation of N-enriched porous carbons for highly selective CO₂ capture. *Chem. Eng. J.* **2019**, *355*, 963–973.
- (7) Singh, G.; Lakhi, K. S.; Sil, S.; Bhosale, S. V.; Kim, I.; Albahily, K.; Vinu, A. Biomass derived porous carbon for CO₂ capture. *Carbon* **2019**, *148*, 164–186.
- (8) Xiang, W.; Zhang, X.; Chen, K.; Fang, J.; He, F.; Hu, X.; Tsang, D. C. W.; Ok, Y. S.; Gao, B. Enhanced adsorption performance and governing mechanisms of ball-milled biochar for the removal of volatile organic compounds (VOCs). *Chem. Eng. J.* **2020**, *385*, 123842.
- (9) Rogelj, J.; den Elzen, M.; Höhne, N.; Fransen, T.; Fekete, H.; Winkler, H.; Schaeffer, R.; Sha, F.; Riahi, K.; Meinshausen, M. Paris Agreement climate proposals need a boost to keep warming well below 2 °C. *Nature* **2016**, *534* (7609), 631–639.
- (10) UNFCCC. *Adoption of the Paris Agreement*; FCCC/CP/2015/L.9/Rev.1; 12/12/2015, 2015.
- (11) Mercure, J. F.; Pollitt, H.; Viñuales, J. E.; Edwards, N. R.; Holden, P. B.; Chewpreecha, U.; Salas, P.; Sognnaes, I.; Lam, A.; Knobloch, F. Macroeconomic impact of stranded fossil fuel assets. *Nat. Clim. Change* **2018**, *8* (7), 588–593.
- (12) Erickson, P.; van Asselt, H.; Koplow, D.; Lazarus, M.; Newell, P.; Oreskes, N.; Supran, G. Why fossil fuel producer subsidies matter. *Nature* **2020**, *578* (7793), E1–E4.
- (13) Wang, M.; Joel, A. S.; Ramshaw, C.; Eimer, D.; Musa, N. M. Process intensification for post-combustion CO₂ capture with chemical absorption: A critical review. *Appl. Energy* **2015**, *158*, 275–291.
- (14) Mumford, K. A.; Wu, Y.; Smith, K. H.; Stevens, G. W. Review of solvent based carbon-dioxide capture technologies. *Front. Chem. Sci. Eng.* **2015**, *9* (2), 125–141.
- (15) Alivand, M. S.; Shafiei-Alavijeh, M.; Tehrani, N. H. M. H.; Ghasemy, E.; Rashidi, A.; Fakhraie, S. Facile and high-yield synthesis of improved MIL-101(Cr) metal-organic framework with exceptional CO₂ and H₂S uptake; the impact of excess ligand-cluster. *Microporous Mesoporous Mater.* **2019**, *279*, 153–164.
- (16) Tehrani, N. H. M. H.; Alivand, M. S.; Maklavany, D. M.; Rashidi, A.; Samipoorgiri, M.; Seif, A.; Yousefian, Z. Novel asphaltene-derived nanoporous carbon with N-S-rich micro-mesoporous structure for superior gas adsorption: Experimental and DFT study. *Chem. Eng. J.* **2019**, *358*, 1126–1138.
- (17) Khalilpour, R.; Mumford, K.; Zhai, H.; Abbas, A.; Stevens, G.; Rubin, E. S. Membrane-based carbon capture from flue gas: a review. *J. Cleaner Prod.* **2015**, *103*, 286–300.
- (18) Scholes, C. A.; Stevens, G. W.; Kentish, S. E. Membrane gas separation applications in natural gas processing. *Fuel* **2012**, *96*, 15–28.
- (19) Yousef, A. M.; El-Maghly, W. M.; Eldrainy, Y. A.; Attia, A. New approach for biogas purification using cryogenic separation and distillation process for CO₂ capture. *Energy* **2018**, *156*, 328–351.
- (20) Yousef, A. M.; Eldrainy, Y. A.; El-Maghly, W. M.; Attia, A. Biogas upgrading process via low-temperature CO₂ liquefaction and separation. *J. Nat. Gas Sci. Eng.* **2017**, *45*, 812–824.
- (21) Afkhamipour, M.; Mofarahi, M. Review on the mass transfer performance of CO₂ absorption by amine-based solvents in low- and high-pressure absorption packed columns. *RSC Adv.* **2017**, *7* (29), 17857–17872.
- (22) Asif, M.; Suleman, M.; Haq, I.; Jamal, S. A. Post-combustion CO₂ capture with chemical absorption and hybrid system: current status and challenges. *Greenhouse Gases: Sci. Technol.* **2018**, *8* (6), 998–1031.
- (23) Wu, Y.; Alivand, M. S.; Hu, G.; Stevens, G. W.; Mumford, K. A. Nucleation kinetics of glycine promoted concentrated potassium carbonate solvents for carbon dioxide absorption. *Chem. Eng. J.* **2020**, *381*, 122712.
- (24) Rahmatmand, B.; Keshavarz, P.; Ayatollahi, S. Study of Absorption Enhancement of CO₂ by SiO₂, Al₂O₃, CNT, and Fe₃O₄ Nanoparticles in Water and Amine Solutions. *J. Chem. Eng. Data* **2016**, *61* (4), 1378–1387.
- (25) Hu, G.; Smith, K. H.; Wu, Y.; Mumford, K. A.; Kentish, S. E.; Stevens, G. W. Carbon dioxide capture by solvent absorption using amino acids: A review. *Chin. J. Chem. Eng.* **2018**, *26* (11), 2229–2237.
- (26) Smith, K. H.; Anderson, C. J.; Tao, W.; Endo, K.; Mumford, K. A.; Kentish, S. E.; Qader, A.; Hooper, B.; Stevens, G. W. Pre-combustion capture of CO₂—Results from solvent absorption pilot plant trials using 30wt% potassium carbonate and boric acid promoted potassium carbonate solvent. *Int. J. Greenhouse Gas Control* **2012**, *10*, 64–73.
- (27) Thee, H.; Suryaputradinata, Y. A.; Mumford, K. A.; Smith, K. H.; Silva, G. d.; Kentish, S. E.; Stevens, G. W. A kinetic and process modeling study of CO₂ capture with MEA-promoted potassium carbonate solutions. *Chem. Eng. J.* **2012**, *210*, 271–279.
- (28) Park, H. M. Reduced-order modeling of carbon dioxide absorption and desorption with potassium carbonate promoted by piperazine. *Int. J. Heat Mass Transfer* **2014**, *73*, 600–615.
- (29) Hafizi, A.; Mokari, M. H.; Khalifeh, R.; Farsi, M.; Rahimpour, M. R. Improving the CO₂ solubility in aqueous mixture of MDEA and different polyamine promoters: The effects of primary and secondary functional groups. *J. Mol. Liq.* **2020**, *297*, 111803.
- (30) Hu, G.; Smith, K. H.; Wu, Y.; Kentish, S. E.; Stevens, G. W. Screening Amino Acid Salts as Rate Promoters in Potassium Carbonate Solvent for Carbon Dioxide Absorption. *Energy Fuels* **2017**, *31* (4), 4280–4286.
- (31) Kelsey, R. A.; Miller, D. A.; Parkin, S. R.; Liu, K.; Remias, J. E.; Yang, Y.; Lightstone, F. C.; Liu, K.; Lippert, C. A.; Odom, S. A. Carbonic anhydrase mimics for enhanced CO₂ absorption in an amine-based capture solvent. *Dalton Trans.* **2016**, *45* (1), 324–333.
- (32) Hu, G.; Smith, K. H.; Nicholas, N. J.; Yong, J.; Kentish, S. E.; Stevens, G. W. Enzymatic carbon dioxide capture using a thermally stable carbonic anhydrase as a promoter in potassium carbonate solvents. *Chem. Eng. J.* **2017**, *307*, 49–55.
- (33) Dharmalingam, S.; Park, K. T.; Lee, J.-Y.; Park, I.-G.; Jeong, S. K. Catalytic effect of metal oxides on CO₂ absorption in an aqueous potassium salt of lysine. *J. Ind. Eng. Chem.* **2018**, *68*, 335–341.
- (34) Taheri, M.; Mohebbi, A.; Hashemipour, H.; Rashidi, A. M. Simultaneous absorption of carbon dioxide (CO₂) and hydrogen sulfide (H₂S) from CO₂–H₂S–CH₄ gas mixture using amine-based nanofluids in a wetted wall column. *J. Nat. Gas Sci. Eng.* **2016**, *28*, 410–417.
- (35) Song, Y.; Cao, L.; Yu, J.; Zhang, S.; Chen, S.; Jiang, Y. Amino-functionalized graphene oxide blend with monoethanolamine for efficient carbon dioxide capture. *J. Alloys Compd.* **2017**, *704*, 245–253.
- (36) Lin, Y.-J.; Rochelle, G. T. Approaching a reversible stripping process for CO₂ capture. *Chem. Eng. J.* **2016**, *283*, 1033–1043.
- (37) James, R. E.; Kearins, D.; Marc, T.; Woods, M.; Kuehn, N.; Zoelle, A. Cost and Performance Baseline for Fossil Energy Plants Volume 1: Bituminous Coal and Natural Gas to Electricity. 2013, DOI: 10.2172/1569246.
- (38) Liu, F.; Fang, M.; Dong, W.; Wang, T.; Xia, Z.; Wang, Q.; Luo, Z. Carbon dioxide absorption in aqueous alkanolamine blends for biphasic solvents screening and evaluation. *Appl. Energy* **2019**, *233–234*, 468–477.
- (39) Huang, Q.; Jing, G.; Zhou, X.; Lv, B.; Zhou, Z. A novel biphasic solvent of amino-functionalized ionic liquid for CO₂ capture: High efficiency and regenerability. *J. CO₂ Util.* **2018**, *25*, 22–30.
- (40) Mohsin, H. M.; Johari, K.; Shariff, A. M. Virgin coconut oil (VCO) and potassium glycinate (PG) mixture as absorbent for carbon dioxide capture. *Fuel* **2018**, *232*, 454–462.
- (41) Li, Y.; Cheng, J.; Hu, L.; Liu, J.; Zhou, J.; Cen, K. Phase-changing solution PZ/DMF for efficient CO₂ capture and low corrosiveness to carbon steel. *Fuel* **2018**, *216*, 418–426.
- (42) Kang, M.-K.; Jeon, S.-B.; Cho, J.-H.; Kim, J.-S.; Oh, K.-J. Characterization and comparison of the CO₂ absorption performance into aqueous, quasi-aqueous and non-aqueous MEA solutions. *Int. J. Greenhouse Gas Control* **2017**, *63*, 281–288.
- (43) Zhang, W.; Jin, X.; Tu, W.; Ma, Q.; Mao, M.; Cui, C. Development of MEA-based CO₂ phase change absorbent. *Appl. Energy* **2017**, *195*, 316–323.

- (44) Wang, X.; Akhmedov, N. G.; Hopkinson, D.; Hoffman, J.; Duan, Y.; Egbebi, A.; Resnik, K.; Li, B. Phase change amino acid salt separates into CO₂-rich and CO₂-lean phases upon interacting with CO₂. *Appl. Energy* **2016**, *161*, 41–47.
- (45) Zhang, S.; Shen, Y.; Wang, L.; Chen, J.; Lu, Y. Phase change solvents for post-combustion CO₂ capture: Principle, advances, and challenges. *Appl. Energy* **2019**, *239*, 876–897.
- (46) Alivand, M. S.; Mazaheri, O.; Wu, Y.; Stevens, G. W.; Scholes, C. A.; Mumford, K. A. Development of aqueous-based phase change amino acid solvents for energy-efficient CO₂ capture: The role of antisolvent. *Appl. Energy* **2019**, *256*, 113911.
- (47) Decardi-Nelson, B.; Akachuku, A.; Osei, P.; Srisang, W.; Pouryousefi, F.; Idem, R. A flexible and robust model for low temperature catalytic desorption of CO₂ from CO₂-loaded amines over solid acid catalysts. *Chem. Eng. Sci.* **2017**, *170*, 518–529.
- (48) Bhatti, U. H.; Sivanesan, D.; Lim, D. H.; Nam, S. C.; Park, S.; Baek, I. H. Metal oxide catalyst-aided solvent regeneration: A promising method to economize post-combustion CO₂ capture process. *J. Taiwan Inst. Chem. Eng.* **2018**, *93*, 150–157.
- (49) Wang, X.; Li, B. Chapter 1 - Phase-Change Solvents for CO₂ Capture. In *Novel Materials for Carbon Dioxide Mitigation Technology*; Shi, F., Morreale, B., Eds.; Elsevier: Amsterdam, The Netherlands, 2015; pp 3–22.
- (50) Zhuang, Q.; Clements, B.; Dai, J.; Carrigan, L. Ten years of research on phase separation absorbents for carbon capture: Achievements and next steps. *Int. J. Greenhouse Gas Control* **2016**, *52*, 449–460.
- (51) Idem, R.; Shi, H.; Gelowitz, D.; Tontiwachwuthikul, P. Catalytic method and apparatus for separating a gaseous component from an incoming gas stream. WO2011120138A1, 2011.
- (52) Shi, H.; Naami, A.; Idem, R.; Tontiwachwuthikul, P. Catalytic and non catalytic solvent regeneration during absorption-based CO₂ capture with single and blended reactive amine solvents. *Int. J. Greenhouse Gas Control* **2014**, *26*, 39–50.
- (53) Shi, H.; Idem, R.; Naami, A.; Gelowitz, D.; Tontiwachwuthikul, P. Catalytic Solvent Regeneration Using Hot Water During Amine Based CO₂ Capture Process. *Energy Procedia* **2014**, *63*, 273–278.
- (54) Wang, T.; Yu, W.; Liu, F.; Fang, M.; Farooq, M.; Luo, Z. Enhanced CO₂ Absorption and Desorption by Monoethanolamine (MEA)-Based Nanoparticle Suspensions. *Ind. Eng. Chem. Res.* **2016**, *55* (28), 7830–7838.
- (55) Bhatti, U. H.; Shah, A. K.; Kim, J. N.; You, J. K.; Choi, S. H.; Lim, D. H.; Nam, S.; Park, Y. H.; Baek, I. H. Effects of Transition Metal Oxide Catalysts on MEA Solvent Regeneration for the Post-Combustion Carbon Capture Process. *ACS Sustainable Chem. Eng.* **2017**, *5* (7), 5862–5868.
- (56) Bhatti, U. H.; Nam, S.; Park, S.; Baek, I. H. Performance and Mechanism of Metal Oxide Catalyst-Aided Amine Solvent Regeneration. *ACS Sustainable Chem. Eng.* **2018**, *6* (9), 12079–12087.
- (57) Bhatti, U. H.; Sivanesan, D.; Nam, S.; Park, S. Y.; Baek, I. H. Efficient Ag₂O–Ag₂CO₃ Catalytic Cycle and Its Role in Minimizing the Energy Requirement of Amine Solvent Regeneration for CO₂ Capture. *ACS Sustainable Chem. Eng.* **2019**, *7* (12), 10234–10240.
- (58) Lai, Q.; Toan, S.; Assiri, M. A.; Cheng, H.; Russell, A. G.; Adidharma, H.; Radosz, M.; Fan, M. Catalyst-TiO(OH)₂ could drastically reduce the energy consumption of CO₂ capture. *Nat. Commun.* **2018**, *9* (1), 2672.
- (59) Wei, Y.; Parmentier, T. E.; de Jong, K. P.; Zečević, J. Tailoring and visualizing the pore architecture of hierarchical zeolites. *Chem. Soc. Rev.* **2015**, *44* (20), 7234–7261.
- (60) Javad Kalbasi, R.; Mansouri, S.; Mazaheri, O. In situ polymerization of poly(vinylimidazole) into the pores of hierarchical MFI zeolite as an acid–base bifunctional catalyst for one-pot C–C bond cascade reactions. *Res. Chem. Intermed.* **2018**, *44* (5), 3279–3291.
- (61) Li, J.; Corma, A.; Yu, J. Synthesis of new zeolite structures. *Chem. Soc. Rev.* **2015**, *44* (20), 7112–7127.
- (62) Möller, K.; Bein, T. Mesoporosity – a new dimension for zeolites. *Chem. Soc. Rev.* **2013**, *42* (9), 3689–3707.
- (63) Zhang, K.; Ostreaat, M. L. Innovations in hierarchical zeolite synthesis. *Catal. Today* **2016**, *264*, 3–15.
- (64) Schreiber, M. W.; Plaisance, C. P.; Baumgärtl, M.; Reuter, K.; Jentys, A.; Bermejo-Deval, R.; Lercher, J. A. Lewis–Brønsted Acid Pairs in Ga/H-ZSM-5 To Catalyze Dehydrogenation of Light Alkanes. *J. Am. Chem. Soc.* **2018**, *140* (14), 4849–4859.
- (65) Yu, Z.; Li, S.; Wang, Q.; Zheng, A.; Jun, X.; Chen, L.; Deng, F. Brønsted/Lewis Acid Synergy in H-ZSM-5 and H-MOR Zeolites Studied by ¹H and ²⁷Al DQ-MAS Solid-State NMR Spectroscopy. *J. Phys. Chem. C* **2011**, *115* (45), 22320–22327.
- (66) Wang, C.; Zhang, L.; Huang, X.; Zhu, Y.; Li, G.; Gu, Q.; Chen, J.; Ma, L.; Li, X.; He, Q.; Xu, J.; Sun, Q.; Song, C.; Peng, M.; Sun, J.; Ma, D. Maximizing sinusoidal channels of HZSM-5 for high shape-selectivity to p-xylene. *Nat. Commun.* **2019**, *10* (1), 4348.
- (67) Bhatti, U. H.; Shah, A. K.; Hussain, A.; Khan, H. A.; Park, C. Y.; Nam, S. C.; Baek, I. H. Catalytic activity of facilely synthesized mesoporous HZSM-5 catalysts for optimizing the CO₂ desorption rate from CO₂-rich amine solutions. *Chem. Eng. J.* **2020**, *389*, 123439.
- (68) Liang, Z.; Idem, R.; Tontiwachwuthikul, P.; Yu, F.; Liu, H.; Rongwong, W. Experimental study on the solvent regeneration of a CO₂-loaded MEA solution using single and hybrid solid acid catalysts. *AIChE J.* **2016**, *62* (3), 753–765.
- (69) Srisang, W.; Pouryousefi, F.; Osei, P. A.; Decardi-Nelson, B.; Akachuku, A.; Tontiwachwuthikul, P.; Idem, R. Evaluation of the heat duty of catalyst-aided amine-based post combustion CO₂ capture. *Chem. Eng. Sci.* **2017**, *170*, 48–57.
- (70) Zhang, X.; Huang, Y.; Gao, H.; Luo, X.; Liang, Z.; Tontiwachwuthikul, P. Zeolite catalyst-aided tri-solvent blend amine regeneration: An alternative pathway to reduce the energy consumption in amine-based CO₂ capture process. *Appl. Energy* **2019**, *240*, 827–841.
- (71) Moliner, M.; Martínez, C.; Corma, A. Synthesis Strategies for Preparing Useful Small Pore Zeolites and Zeotypes for Gas Separations and Catalysis. *Chem. Mater.* **2014**, *26* (1), 246–258.
- (72) Chen, J.; Li, J.; Wei, Y.; Yuan, C.; Li, B.; Xu, S.; Zhou, Y.; Wang, J.; Zhang, M.; Liu, Z. Spatial confinement effects of cage-type SAPO molecular sieves on product distribution and coke formation in methanol-to-olefin reaction. *Catal. Commun.* **2014**, *46*, 36–40.
- (73) Zhang, X.; Zhang, X.; Liu, H.; Li, W.; Xiao, M.; Gao, H.; Liang, Z. Reduction of energy requirement of CO₂ desorption from a rich CO₂-loaded MEA solution by using solid acid catalysts. *Appl. Energy* **2017**, *202*, 673–684.
- (74) Hu, X.; Yu, Q.; Cui, Y.; Huang, J.; Shiko, E.; Zhou, Y.; Zeng, Z.; Liu, Y.; Zhang, R. Toward Solvent Development for Industrial CO₂ Capture by Optimizing the Catalyst–Amine Formulation for Lower Energy Consumption in the Solvent Regeneration Process. *Energy Fuels* **2019**, *33* (11), 11507–11515.
- (75) Zhang, X.; Zhang, R.; Liu, H.; Gao, H.; Liang, Z. Evaluating CO₂ desorption performance in CO₂-loaded aqueous tri-solvent blend amines with and without solid acid catalysts. *Appl. Energy* **2018**, *218*, 417–429.
- (76) Ordomsky, V. V.; Ivanova, I. I.; Knyazeva, E. E.; Yuschenko, V. V.; Zaikovskii, V. I. Cumene disproportionation over micro/mesoporous catalysts obtained by recrystallization of mordenite. *J. Catal.* **2012**, *295*, 207–216.
- (77) Chu, W.; Li, X.; Zhu, X.; Xie, S.; Guo, C.; Liu, S.; Chen, F.; Xu, L. Size-controlled synthesis of hierarchical ferrierite zeolite and its catalytic application in 1-butene skeletal isomerization. *Microporous Mesoporous Mater.* **2017**, *240*, 189–196.
- (78) Kustovskaya, A. D.; Kosenko, E. I. Catalytic activity of natural zeolites in the conversion of methanol to dimethyl ether. *Pet. Chem.* **2014**, *S4* (2), 137–141.
- (79) Shahbazi, A.; Gonzalez-Olmos, R.; Kopinke, F.-D.; Zarabadi-Poor, P.; Georgi, A. Natural and synthetic zeolites in adsorption/oxidation processes to remove surfactant molecules from water. *Sep. Purif. Technol.* **2014**, *127*, 1–9.
- (80) Yang, Y.; Yu, C. Advances in silica based nanoparticles for targeted cancer therapy. *Nanomedicine* **2016**, *12* (2), 317–332.
- (81) Giraldo, L. F.; López, B. L.; Pérez, L.; Urrego, S.; Sierra, L.; Mesa, M. Mesoporous Silica Applications. *Macromol. Symp.* **2007**, *258* (1), 129–141.

- (82) Liu, H.; Zhang, X.; Gao, H.; Liang, Z.; Idem, R.; Tontiwachwuthikul, P. Investigation of CO₂ Regeneration in Single and Blended Amine Solvents with and without Catalyst. *Ind. Eng. Chem. Res.* **2017**, *56* (27), 7656–7664.
- (83) Zhang, X.; Liu, H.; Liang, Z. CO₂ Desorption in Single and Blended Amine Solvents with and without Catalyst. *Energy Procedia* **2017**, *114*, 1862–1868.
- (84) Gao, H.; Huang, Y.; Zhang, X.; Bairq, Z. A. S.; Huang, Y.; Tontiwachwuthikul, P.; Liang, Z. Catalytic performance and mechanism of SO₄²⁻/ZrO₂/SBA-15 catalyst for CO₂ desorption in CO₂-loaded monoethanolamine solution. *Appl. Energy* **2020**, *259*, 114179.
- (85) Hino, M.; Kobayashi, S.; Arata, K. Solid catalyst treated with anion. 2. Reactions of butane and isobutane catalyzed by zirconium oxide treated with sulfate ion. Solid superacid catalyst. *J. Am. Chem. Soc.* **1979**, *101* (21), 6439–6441.
- (86) López, T.; Bosch, P.; Tzompantzi, F.; Gómez, R.; Navarrete, J.; López-Salinas, E.; Llanos, M. E. Effect of sulfation methods on TiO₂–SiO₂ sol–gel catalyst acidity. *Appl. Catal., A* **2000**, *197* (1), 107–117.
- (87) de Almeida, R. M.; Noda, L. K.; Gonçalves, N. S.; Meneghetti, S. M. P.; Meneghetti, M. R. Transesterification reaction of vegetable oils, using superacid sulfated TiO₂–base catalysts. *Appl. Catal., A* **2008**, *347* (1), 100–105.
- (88) Li, L.; Liu, Y.; Wu, K.; Liu, C.; Tang, S.; Yue, H.; Lu, H.; Liang, B. Catalytic solvent regeneration of a CO₂-loaded MEA solution using an acidic catalyst from industrial rough metatitanic acid. *Greenhouse Gases: Sci. Technol.* **2020**, *10* (2), 449–460.
- (89) Prasongthum, N.; Natewong, P.; Reubroycharoen, P.; Idem, R. Solvent Regeneration of a CO₂-Loaded BEA–AMP Bi-Blend Amine Solvent with the Aid of a Solid Brønsted Ce(SO₄)₂/ZrO₂ Superacid Catalyst. *Energy Fuels* **2019**, *33* (2), 1334–1343.
- (90) Natewong, P.; Prasongthum, N.; Reubroycharoen, P.; Idem, R. Evaluating the CO₂ Capture Performance Using a BEA-AMP Biblend Amine Solvent with Novel High-Performing Absorber and Desorber Catalysts in a Bench-Scale CO₂ Capture Pilot Plant. *Energy Fuels* **2019**, *33* (4), 3390–3402.
- (91) Zhang, Q.; Wang, T.; Li, B.; Jiang, T.; Ma, L.; Zhang, X.; Liu, Q. Aqueous phase reforming of sorbitol to bio-gasoline over Ni/HZSM-5 catalysts. *Appl. Energy* **2012**, *97*, 509–513.
- (92) Wei, J.; Ge, Q.; Yao, R.; Wen, Z.; Fang, C.; Guo, L.; Xu, H.; Sun, J. Directly converting CO₂ into a gasoline fuel. *Nat. Commun.* **2017**, *8* (1), 15174.
- (93) Gao, P.; Li, S.; Bu, X.; Dang, S.; Liu, Z.; Wang, H.; Zhong, L.; Qiu, M.; Yang, C.; Cai, J.; Wei, W.; Sun, Y. Direct conversion of CO₂ into liquid fuels with high selectivity over a bifunctional catalyst. *Nat. Chem.* **2017**, *9* (10), 1019–1024.
- (94) Chen, Z.; Lin, F.; He, D.; Jiang, H.; Zhang, J.; Wang, X.; Huang, M. A hybrid composite catalyst of Fe₃O₄ nanoparticles-based carbon for electrochemical reduction of oxygen. *New J. Chem.* **2017**, *41* (12), 4959–4965.
- (95) Li, C.; Ni, W.; Zang, X.; Wang, H.; Zhou, Y.; Yang, Z.; Yan, Y.-M. Magnesium oxide anchored into a hollow carbon sphere realizes synergistic adsorption and activation of CO₂ for electrochemical reduction. *Chem. Commun.* **2020**, *56*, 6062–6065.
- (96) Zhang, X.; Liu, H.; Liang, Z.; Idem, R.; Tontiwachwuthikul, P.; Jaber Al-Marri, M.; Benamor, A. Reducing energy consumption of CO₂ desorption in CO₂-loaded aqueous amine solution using Al₂O₃/HZSM-5 bifunctional catalysts. *Appl. Energy* **2018**, *229*, 562–576.
- (97) Zhang, X.; Hong, J.; Liu, H.; Luo, X.; Olson, W.; Tontiwachwuthikul, P.; Liang, Z. SO₄²⁻/ZrO₂ supported on γ-Al₂O₃ as a catalyst for CO₂ desorption from CO₂-loaded monoethanolamine solutions. *AIChE J.* **2018**, *64* (11), 3988–4001.
- (98) Ali Saleh Bairq, Z.; Gao, H.; Huang, Y.; Zhang, H.; Liang, Z. Enhancing CO₂ desorption performance in rich MEA solution by addition of SO₄²⁻/ZrO₂/SiO₂ bifunctional catalyst. *Appl. Energy* **2019**, *252*, 113440.
- (99) Zhang, X.; Zhu, Z.; Sun, X.; Yang, J.; Gao, H.; Huang, Y.; Luo, X.; Liang, Z.; Tontiwachwuthikul, P. Reducing Energy Penalty of CO₂ Capture Using Fe Promoted SO₄²⁻/ZrO₂/MCM-41 Catalyst. *Environ. Sci. Technol.* **2019**, *53* (10), 6094–6102.
- (100) Zhang, X.; Huang, Y.; Yang, J.; Gao, H.; Huang, Y.; Luo, X.; Liang, Z.; Tontiwachwuthikul, P. Amine-based CO₂ capture aided by acid-basic bifunctional catalyst: Advancement of amine regeneration using metal modified MCM-41. *Chem. Eng. J.* **2020**, *383*, 123077.
- (101) Bairq, Z. A. S.; Gao, H.; Murshed, F. A. M.; Tontiwachwuthikul, P.; Liang, Z. Modified Heterogeneous Catalyst-Aided Regeneration of CO₂ Capture Amines: A Promising Perspective for a Drastic Reduction in Energy Consumption. *ACS Sustainable Chem. Eng.* **2020**, *8* (25), 9526–9536.
- (102) Caplow, M. Kinetics of carbamate formation and breakdown. *J. Am. Chem. Soc.* **1968**, *90* (24), 6795–6803.
- (103) Danckwerts, P. V. The reaction of CO₂ with ethanolamines. *Chem. Eng. Sci.* **1979**, *34* (4), 443–446.
- (104) Lv, B.; Guo, B.; Zhou, Z.; Jing, G. Mechanisms of CO₂ Capture into Monoethanolamine Solution with Different CO₂ Loading during the Absorption/Desorption Processes. *Environ. Sci. Technol.* **2015**, *49* (17), 10728–10735.
- (105) Akachuku, A.; Osei, P. A.; Decardi-Nelson, B.; Srisang, W.; Pouryousefi, F.; Ibrahim, H.; Idem, R. Experimental and kinetic study of the catalytic desorption of CO₂ from CO₂-loaded monoethanolamine (MEA) and blended monoethanolamine – Methyl-diethanolamine (MEA-MDEA) solutions. *Energy* **2019**, *179*, 475–489.
- (106) Shi, H.; Zheng, L.; Huang, M.; Zuo, Y.; Kang, S.; Huang, Y.; Idem, R.; Tontiwachwuthikul, P. Catalytic-CO₂-Desorption Studies of DEA and DEA-MEA Blended Solutions with the Aid of Lewis and Brønsted Acids. *Ind. Eng. Chem. Res.* **2018**, *57* (34), 11505–11516.
- (107) Akachuku, A.; Osei, A.; Decardi-Nelson, B.; Srisang, W.; Pouryousefi, F.; Ibrahim, H.; Idem, R. Kinetics of the Catalytic Desorption of CO₂ from Monoethanolamine (MEA) and Monoethanolamine and Methyldiethanolamine (MEA-MDEA). *Energy Procedia* **2017**, *114*, 1495–1505.
- (108) Barzaghi, F.; Mani, F.; Peruzzini, M. Continuous cycles of CO₂ absorption and amine regeneration with aqueous alkanolamines: a comparison of the efficiency between pure and blended DEA, MDEA and AMP solutions by ¹³C NMR spectroscopy. *Energy Environ. Sci.* **2010**, *3* (6), 772–779.
- (109) Srisang, W.; Pouryousefi, F.; Osei, P. A.; Decardi-Nelson, B.; Akachuku, A.; Tontiwachwuthikul, P.; Idem, R. CO₂ capture efficiency and heat duty of solid acid catalyst-aided CO₂ desorption using blends of primary-tertiary amines. *Int. J. Greenhouse Gas Control* **2018**, *69*, 52–59.
- (110) Decardi-Nelson, B.; Akachuku, A.; Osei, P.; Srisang, W.; Pouryousefi, F.; Idem, R. Catalyst performance and experimental validation of a rigorous desorber model for low temperature catalyst-aided desorption of CO₂ in single and blended amine solutions. *J. Environ. Chem. Eng.* **2017**, *5* (4), 3865–3872.
- (111) Sinfelt, J. H. Chemistry of catalytic processes, by Bruce C. Gates, James R. Katzer, and G. C. A. Schuit. McGraw-Hill, 1979, 464 pp. *AIChE J.* **1979**, *25* (4), 734..
- (112) Shi, H.; Huang, M.; Wu, Q.; Zheng, L.; Cui, L.; Zhang, S.; Tontiwachwuthikul, P. Study of Catalytic CO₂ Absorption and Desorption with Tertiary Amine DEEA and 1DMA-2P with the Aid of Solid Acid and Solid Alkaline Chemicals. *Molecules* **2019**, *24* (6), 1009.
- (113) Xie, H.-B.; Zhou, Y.; Zhang, Y.; Johnson, J. K. Reaction Mechanism of Monoethanolamine with CO₂ in Aqueous Solution from Molecular Modeling. *J. Phys. Chem. A* **2010**, *114* (43), 11844–11852.
- (114) Shi, H.; Fu, J.; Wu, Q.; Huang, M.; Jiang, L.; Cui, M.; Idem, R.; Tontiwachwuthikul, P. Studies of the coordination effect of DEA-MEA blended amines (within 1 + 4 to 2 + 3 M) under heterogeneous catalysis by means of absorption and desorption parameters. *Sep. Purif. Technol.* **2020**, *236*, 116179.
- (115) Narku-Tetteh, J.; Afari, D. B.; Coker, J.; Idem, R. Evaluation of the Roles of Absorber and Desorber Catalysts in the Heat Duty and Heat of CO₂ Desorption from Butylethanolamine–2-Amino-2-methyl-1-propanol and Monoethanolamine–Methyldiethanolamine Solvent Blends in a Bench-Scale CO₂ Capture Pilot Plant. *Energy Fuels* **2018**, *32* (9), 9711–9726.

- (116) Gao, H.; Liang, Z.; Liao, H.; Idem, R. O. Thermal degradation of aqueous DEEA solution at stripper conditions for post-combustion CO₂ capture. *Chem. Eng. Sci.* **2015**, *135*, 330–342.
- (117) Kasprzyk-Hordern, B. Chemistry of alumina, reactions in aqueous solution and its application in water treatment. *Adv. Colloid Interface Sci.* **2004**, *110* (1), 19–48.
- (118) Ryu, H. S.; Lim, T. S.; Ryu, J.; Hong, S.-H. Corrosion Protection Performance of YSZ Coating on AA7075 Aluminum Alloy Prepared by Aerosol Deposition. *J. Electrochem. Soc.* **2013**, *160* (1), C42–C47.
- (119) Yurdakul, A.; Gunkaya, G.; Dolekcekic, E.; Kavas, T.; Karasu, B. Novel glass compositions for fiber drawing. *Ceram. Int.* **2015**, *41* (10), 13105–13114.
- (120) Rosynek, M. P. Isotherms and energetics of carbon dioxide adsorption on gamma-alumina at 100–300 deg. *J. Phys. Chem.* **1975**, *79* (13), 1280–1284.
- (121) Liu, N.; Wu, Z.; Li, M.; Li, S.; Li, Y.; Yu, R.; Pan, L.; Liu, Y. A novel strategy for constructing mesoporous solid superbases catalysts: bimetallic Al–La oxides supported on SBA-15 modified with KF. *Catal. Sci. Technol.* **2017**, *7* (3), 725–733.
- (122) Fellenz, N. A.; Bengoa, J. F.; Marchetti, S. G.; Gervasini, A. Influence of the Brønsted and Lewis acid sites on the catalytic activity and selectivity of Fe/MCM-41 system. *Appl. Catal., A* **2012**, *435*–436, 187–196.
- (123) Magnacca, G.; Cerrato, G.; Morterra, C.; Signoretto, M.; Somma, F.; Pinna, F. Structural and Surface Characterization of Pure and Sulfated Iron Oxides. *Chem. Mater.* **2003**, *15* (3), 675–687.
- (124) Jung, H.; Park, H.; Kim, J.; Lee, J.-H.; Hur, H.-G.; Myung, N. V.; Choi, H. Preparation of Biotic and Abiotic Iron Oxide Nanoparticles (IONPs) and Their Properties and Applications in Heterogeneous Catalytic Oxidation. *Environ. Sci. Technol.* **2007**, *41* (13), 4741–4747.
- (125) Liang, Z.; Fu, K.; Idem, R.; Tontiwachwuthikul, P. Review on current advances, future challenges and consideration issues for post-combustion CO₂ capture using amine-based absorbents. *Chin. J. Chem. Eng.* **2016**, *24* (2), 278–288.
- (126) Idem, R.; Wilson, M.; Tontiwachwuthikul, P.; Chakma, A.; Veawab, A.; Aroonwilas, A.; Gelowitz, D. Pilot Plant Studies of the CO₂ Capture Performance of Aqueous MEA and Mixed MEA/MDEA Solvents at the University of Regina CO₂ Capture Technology Development Plant and the Boundary Dam CO₂ Capture Demonstration Plant. *Ind. Eng. Chem. Res.* **2006**, *45* (8), 2414–2420.
- (127) El Hadri, N.; Quang, D. V.; Goetheer, E. L. V.; Abu Zahra, M. R. M. Aqueous amine solution characterization for post-combustion CO₂ capture process. *Appl. Energy* **2017**, *185*, 1433–1449.
- (128) Leimbrink, M.; Sandkämper, S.; Wardhaugh, L.; Maher, D.; Green, P.; Puxty, G.; Conway, W.; Bennett, R.; Botma, H.; Feron, P.; Górkak, A.; Skiborowski, M. Energy-efficient solvent regeneration in enzymatic reactive absorption for carbon dioxide capture. *Appl. Energy* **2017**, *208*, 263–276.
- (129) Oexmann, J.; Kather, A. Minimising the regeneration heat duty of post-combustion CO₂ capture by wet chemical absorption: The misguided focus on low heat of absorption solvents. *Int. J. Greenhouse Gas Control* **2010**, *4* (1), 36–43.
- (130) Liang, Z.; Rongwong, W.; Liu, H.; Fu, K.; Gao, H.; Cao, F.; Zhang, R.; Sema, T.; Henni, A.; Sumon, K.; Nath, D.; Gelowitz, D.; Srisang, W.; Saiwan, C.; Benamor, A.; Al-Marri, M.; Shi, H.; Supap, T.; Chan, C.; Zhou, Q.; Abu-Zahra, M.; Wilson, M.; Olson, W.; Idem, R.; Tontiwachwuthikul, P. Recent progress and new developments in post-combustion carbon-capture technology with amine based solvents. *Int. J. Greenhouse Gas Control* **2015**, *40*, 26–54.
- (131) Afari, D. B.; Coker, J.; Narku-Tetteh, J.; Idem, R. Comparative Kinetic Studies of Solid Absorber Catalyst (K/MgO) and Solid Desorber Catalyst (HZSM-5)-Aided CO₂ Absorption and Desorption from Aqueous Solutions of MEA and Blended Solutions of BEA-AMP and MEA-MDEA. *Ind. Eng. Chem. Res.* **2018**, *57* (46), 15824–15839.
- (132) Zhang, R.; Zhang, X.; Yang, Q.; Yu, H.; Liang, Z.; Luo, X. Analysis of the reduction of energy cost by using MEA-MDEA-PZ solvent for post-combustion carbon dioxide capture (PCC). *Appl. Energy* **2017**, *205*, 1002–1011.
- (133) Xu, Y.; Jin, B.; Jiang, H.; Li, L.; Wei, J. Investigation of the regeneration of a CO₂-loaded ammonia solution with solid acid catalysts: A promising alternative for reducing regeneration energy. *Fuel Process. Technol.* **2020**, *205*, 106452.
- (134) Ko, Y. G.; Shin, S. S.; Choi, U. S. Primary, secondary, and tertiary amines for CO₂ capture: Designing for mesoporous CO₂ adsorbents. *J. Colloid Interface Sci.* **2011**, *361* (2), 594–602.
- (135) Alivand, M. S.; Mazaheri, O.; Wu, Y.; Stevens, G. W.; Scholes, C. A.; Mumford, K. A. Preparation of nanoporous carbonaceous promoters for enhanced CO₂ absorption in tertiary amines. *Engineering* **2020**, DOI: 10.1016/j.eng.2020.05.004.
- (136) Osei, P. A.; Akachuku, A.; Decardi-Nelson, B.; Srisang, W.; Pouryousefi, F.; Tontiwachwuthikul, P.; Idem, R. Mass transfer studies on catalyst-aided CO₂ desorption from CO₂-loaded amine solution in a post-combustion CO₂ capture plant. *Chem. Eng. Sci.* **2017**, *170*, 508–517.